

# **Function and Regulation of Rat Na<sup>+</sup>/H<sup>+</sup> Exchanger Isoforms**

by

**Frank Hong Yu**

Department of Physiology  
Faculty of Medicine  
McGill University  
Montréal, Québec  
Canada

April 1997

A thesis submitted to the Faculty of Graduate Studies and Research in partial fulfilment  
of the requirements for the degree of Doctor of Philosophy.

© Frank H. Yu 1997



National Library  
of Canada

Acquisitions and  
Bibliographic Services

395 Wellington Street  
Ottawa ON K1A 0N4  
Canada

Bibliothèque nationale  
du Canada

Acquisitions et  
services bibliographiques

395, rue Wellington  
Ottawa ON K1A 0N4  
Canada

*Your file Votre référence*

*Our file Notre référence*

The author has granted a non-exclusive licence allowing the National Library of Canada to reproduce, loan, distribute or sell copies of this thesis in microform, paper or electronic formats.

The author retains ownership of the copyright in this thesis. Neither the thesis nor substantial extracts from it may be printed or otherwise reproduced without the author's permission.

L'auteur a accordé une licence non exclusive permettant à la Bibliothèque nationale du Canada de reproduire, prêter, distribuer ou vendre des copies de cette thèse sous la forme de microfiche/film, de reproduction sur papier ou sur format électronique.

L'auteur conserve la propriété du droit d'auteur qui protège cette thèse. Ni la thèse ni des extraits substantiels de celle-ci ne doivent être imprimés ou autrement reproduits sans son autorisation.

0-612-30423-X

## ABSTRACT

Recent molecular cloning studies have identified multiple isoforms of the  $\text{Na}^+/\text{H}^+$  exchanger. The objective of my research was to characterize and compare some of the functional and regulatory properties of individual members of this gene family. To facilitate comparison of properties, a mutant Chinese hamster ovary cell line devoid of endogenous  $\text{Na}^+/\text{H}^+$  exchanger activity (AP-1 cells) was utilized.

1. Functional characterization of the rat NHE2 isoform revealed differences in its pharmacological and kinetic properties compared to two other isoforms, NHE1 and NHE3. Half-maximal inhibition of NHE2 activity by amiloride and some of its analogues occurred at intermediate concentrations compared to NHE1 and NHE3, although the rank order of potency of the compounds was similar. Analyses of its kinetic behaviour also showed that while the transport dynamics of NHE2 were similar to those of the other isoforms, it had quite different affinities for its cation substrates. Therefore, these differences provide a biochemical and a pharmacological basis for discriminating NHE2 from NHE1 and NHE3.

2. Structural analysis of the NHE3 isoform was conducted in two studies by generating deletion and chimeric mutants. The first study examined the structural domains involved in its regulation by cAMP and ATP. Chimeras of NHE1 and NHE3 that were constructed by the homologous exchange of their C-terminal cytosolic tail regions demonstrated that the cytosolic tail of NHE3 is sufficient to confer sensitivity to inhibition by cAMP. Additional analysis of NHE3 deletion mutants revealed a region between amino acids 579 and 684 that is essential for this inhibitory effect. In contrast, comparable ATP dependence was observed in wild type and all mutant exchangers examined, suggesting that a region of the molecule in or adjacent to the transmembrane

domain is involved in this response. It is concluded that different sites, suggesting of different mechanisms, underlie inhibition of NHE3 by cAMP and by depletion of ATP.

3. In the final study, NHE3 inhibition by hyperosmolarity was examined using the same mutational approach. The cytoplasmic tail of NHE3 was insufficient to confer the hyperosmotic inhibitory effect to a chimeric exchanger that contained the *N*-terminal transmembrane region of NHE1, suggesting that an interaction between the *N* and *C* termini of NHE3 may be required for this inhibition. Deletion analysis revealed two hyperosmolarity sensitive domains in the NHE3 cytosolic tail region: a hyperosmotically activatable region between amino acids 579 and 638 and an inhibitory region between amino acids 649 and 684, the latter acting in a dominant manner in the presence of the former domain. These data are consistent with the conclusion that hyperosmotic inhibition of NHE3 is mediated by mechanisms that appear to be distinct from those that underlie cAMP-sensitivity and ATP dependence.

## RÉSUMÉ

De récentes études de clonage moléculaire ont permis d'identifier plusieurs isoformes de l'échangeur  $\text{Na}^+/\text{H}^+$  (NHE). Le but de ma recherche était de caractériser et comparer certaines propriétés ayant trait à la fonction de même qu'à la régulation de divers membres de cette famille de gènes. Pour faciliter la comparaison des différentes propriétés, une lignée cellulaire mutante d'ovaires de hamsters chinois (cellules AP-1), déficiente en activité endogène d'échange  $\text{Na}^+/\text{H}^+$ , a été utilisée.

1. La caractérisation fonctionnelle de l'isoforme NHE2 du rat révèle des différences distinctes au niveau de ses propriétés pharmacologiques et kinétiques par rapport à deux autres isoformes, NHE1 et NHE3. L'inhibition à demi maximale de l'activité de NHE2 par l'amiloride et ses analogues s'est produite à des concentrations intermédiaires en comparaison à NHE1 et NHE3, même si le potentiel des composés était similaire. Les analyses du comportement kinétique ont montré que même si les dynamiques de transport de NHE2 sont semblables à celles des autres isoformes, il a des affinités très différentes pour ses substrats cationiques. En somme, ces différences fournissent des bases biochimiques et pharmacologiques distinguant NHE2 de NHE1 et de NHE3.

2. L'analyse de la structure de l'isoforme NHE3 a été conduite de deux façons en générant des mutants, par délétions ou par chimères. La première étude examine la structure des domaines impliqués dans la régulation de NHE3 via l'AMPc, et l'ATP. Les chimères, qui échangent réciproquement le domaine C-terminal cytosolique, démontrent que cette région de NHE3 est suffisante pour conférer une sensibilité à l'inhibition par AMPc. Une analyse additionnelle des mutants par délétions de NHE3 révèle que la région entre les acides aminés 579 et 684 est essentielle pour cet effet inhibiteur. Par

contre, une dépendance à l'ATP comparable a été observée chez tous les échangeurs mutants, suggérant qu'une région de la molécule, adjacente ou dans le domaine transmembranaire, est impliquée dans la réponse. On en déduit que différents sites, donc différents mécanismes déterminent l'inhibition de NHE3 par l'AMPc et par la réduction d'ATP.

3. Dans la dernière étude, l'inhibition de NHE3 par hyperosmolarité a été examinée en utilisant la même approche mutationnelle. La région cytoplasmique de NHE3 seule étant insuffisante pour conférer un effet inhibiteur hypertonique chez un échangeur chimérique contenant la région transmembranaire de NHE1, ceci suppose qu'une interaction entre *N* et *C* terminals puisse être requise pour cette inhibition. L'analyse par délétions révèlent deux domaines sensibles à l'hyperosmolarité dans la région cytosolique de NHE3. Une région de stimulation hypertonique est située entre les acides aminés 579 et 638, et une région inhibitrice entre les acides aminés 649 et 684, qui elle, agit de façon dominante en présence du domaine antérieur. Ces résultats correspondent à la conclusion que l'inhibition hyperosmotique de NHE3 est transmise par des domaines distincts de ceux responsables de la sensibilité à l'AMPc et de la dépendance à l'ATP.

## ACKNOWLEDGMENTS

I would like to express my sincere gratitude to my supervisor, Dr. John Orlowski, for his invaluable advise, support, encouragement, and precious time in the formation of this thesis. I am very happy to have had the opportunity to contribute my two-cents worth in his obsessive quest of characterizing the NHE physiology. The time that I have spent in the Orlowski lab was the most productive as well as enjoyable. I have learned much under his tutelage: the dedication, the boundless enthusiasm for research, the importance of life outside McIntyre as well as the respect, friendship, and the genuine concern he had for me and the rest of the Orlowski lab family. I know that I leave the Orlowski lab as a better scientist than I had started, and I believe that the main reason for this lies in my unashamed plagiarism of John Orlowski. I have even picked up the game of squash! I thank John for his efforts in the shaping of this scientist.

My deep appreciation is also extended to my Olab family: Annie Boucher, my French teacher, whose serene smile and delightful work habits made my "home" brighter, enjoyable and friendly; Dr. Elöd Szabo and doctor-to-be Amole Khadilkar whose company these last few months would not have been as productive, nor as tortuously satisfying or enjoyable; and Mohammed Basil Adul-sharif whose youthful enthusiasm and timely humor chased away the dullness of monotony and injected periodic bursts of sanity to each lab day that he joined us. I must also acknowledge the former members of my lab family: my tutor of molecular biology and longtime bench-mate, Ramani Kandasamy – her excellent guidance and supportive encouragement was instrumental to the project getting-off to a running start and staying that way; and Jonathan D. Wasserman whose drive for excellence was quite inspirational and helped to renew the excitement of discovery during latter portion of my tenure at the Orlowski Lab. Dr. Norma Lake, my co-conspirator in "Macintosh: Alive and well in Olab Movement". I

appreciate her enormous capacity to provide the patient guidance, encouragement, and generous assistance.

Two other comrades-in-arms that I must also acknowledge are Andrew Fraser for the coffee and other well-timed distractions, and John Ferrara for the friendship that was and still is refreshingly energetic, inexplicably baffling, and surprisingly true.

I also wish to thank Drs. John White and John Hanrahan for their concern and interest in my research as well as the helpful advice. I am particularly fortunate to have had help from so many generous members of the McGill Physiology. I apologize for not being able to name each one of you whose contributions are also reflected in this work.

Most importantly, I would like to thank my wife, parents and the rest of my family without whose support this thesis would not have been possible.



## **PREFACE**

Candidates have the option of including, as part of their thesis, the text of one or more papers submitted or to be submitted for publication, or the clearly-duplicated text of one or more published papers. These texts must be bound as an integral part of the thesis.

If this option is chosen, connecting texts that provide logical bridges between the different papers are mandatory. The thesis must be written in such a way that it is more than a mere collection of manuscripts; in other words, results of a series of papers must be integrated.

The thesis must still conform to all other requirements of the "Guidelines for Thesis Preparation". The thesis must include: A Table of Contents, an abstract in English and French, an introduction which clearly states the rationale and objectives of the study, a comprehensive review of the literature, a final conclusion and summary and a thorough bibliography or reference list.

Additional material must be provided where appropriate (*e.g.*, in appendices) and in sufficient detail to allow a clear and precise judgment to be made of the importance and originality of the research reported in the thesis.

In the case of manuscripts co-authored by the candidate and others, the candidate is required to make an explicit statement in the thesis as to who contributed to such work and to what extent. Supervisor must attest to the accuracy of such statements at the doctoral oral defense. Since the task of the examiners is made more difficult in these cases, it is in the candidate's interest to make perfectly clear the responsibilities of all the authors of the co-authored papers.

## ABBREVIATIONS

AP-1	Na <sup>+</sup> /H <sup>+</sup> exchanger-deficient Chinese hamster ovary cell line
BCECF	2',7'-bis(carboxyethyl)-5(6)-carboxyfluorescein
BCECF-AM	BCECF-acetoxymethyl ester
CMV	Cytomegalovirus
DMA	5-( <i>N,N</i> -dimethyl)amiloride
DMSO	Dimethylsulfoxide
EIPA	5-( <i>N</i> -ethyl- <i>N</i> -isopropyl)amiloride
FOR	Forskolin
HOE694	(3-methylsulfonyl-4-piperidinobenzoyl) guanidine methanesulfonate
IMCD	Mouse inner medullary collecting duct cell line
LLC-PK	Piglet kidney cell line
MCT	Mouse proximal cortical tubule cell line
MDCK	Madin-Darby canine kidney cell line
NHE	Na <sup>+</sup> /H <sup>+</sup> exchanger
OK	Opossum kidney cell line
PKA	Adenosine 3',5'-cyclic monophosphate-dependent protein kinase A
PKC	Diacylglycerol-dependent protein kinase C
PMA	Phorbol 12-myristate 13-acetate
PS120	Na <sup>+</sup> /H <sup>+</sup> exchanger-deficient Chinese hamster lung fibroblast cell line
RKPC	Rabbit kidney S <sub>2</sub> proximal tubule cell line
TBE	Tris Boric Acid EDTA

## TABLE OF CONTENTS

ABSTRACT .....	ii
RÉSUMÉ.....	iii
ACKNOWLEDGEMENTS .....	vi
PREFACE .....	ivi
ABBREVIATIONS .....	ix
TABLE OF CONTENTS.....	x
STATEMENT OF CONTRIBUTION TO ORIGINAL KNOWLEDGE .....	xii
 CHAPTER I. Introduction.....	 1
1.1. Evidence of Multiple Classes of Na <sup>+</sup> /H <sup>+</sup> Exchangers.....	3
1.2. Molecular Diversity .....	4
1.2.1. Na <sup>+</sup> /H <sup>+</sup> Exchanger Isoforms and Tissue Expression .....	5
1.2.1.1. NHE1 .....	5
1.2.1.2. NHE2 .....	6
1.2.1.3. NHE3 .....	8
1.2.1.4. NHE4 .....	8
1.2.1.5. NHE5 .....	9
1.2.2. Chromosomal Mapping and Genomic Organization.....	9
1.2.3. Primary and Secondary Structures.....	10
1.2.4. Quaternary Structure.....	13
1.2.5. Glycosylation Sites.....	13
1.3. Functional Characteristics and Kinetics.....	14
1.3.1. Selectivity and Kinetics.....	14
1.3.2. Sensitivity to Inhibitors .....	16
1.4. Physiological Roles of Na <sup>+</sup> /H <sup>+</sup> Exchangers .....	19
1.4.1. Regulation of Intracellular pH.....	19
1.4.2. Regulation of Cell Volume.....	19
1.4.3. Transepithelial Transport .....	21
1.4.4. Facilitation of Cellular Proliferation.....	21
1.5. Regulation of Na <sup>+</sup> /H <sup>+</sup> Exchanger .....	23
1.5.1. Acute Regulation.....	23
1.5.1.1. Protein Kinases A and C.....	23
1.5.1.2. ATP Dependence.....	28
1.5.1.3. Hyperosmolarity.....	28

1.5.2. Chronic Regulation.....	29
1.6. Rationale and Objectives.....	30
CHAPTER II. Functional Properties of the Rat Na <sup>+</sup> /H <sup>+</sup> Exchanger NHE2 Isoform Expressed in Na <sup>+</sup> /H <sup>+</sup> Exchanger-Deficient Chinese Hamster Ovary Cells.....	33
SUMMARY .....	34
INTRODUCTION .....	35
EXPERIMENTAL PROCEDURES .....	37
RESULTS.....	40
DISCUSSION .....	44
CHAPTER III. Distinct Structural Domains Confer cAMP Sensitivity and ATP Dependence to the Na <sup>+</sup> /H <sup>+</sup> Exchanger NHE3 Isoform.....	58
SUMMARY .....	59
INTRODUCTION .....	60
EXPERIMENTAL PROCEDURES .....	63
RESULTS.....	70
DISCUSSION .....	77
CHAPTER IV. Localization of an Osmoresponsive Inhibitory Domain of the Na <sup>+</sup> /H <sup>+</sup> Exchanger NHE3 Isoform.....	92
SUMMARY .....	93
INTRODUCTION .....	94
EXPERIMENTAL PROCEDURES .....	96
RESULTS.....	100
DISCUSSION .....	105
CHAPTER V. General Discussion and Conclusion.....	114
Concluding Remarks.....	121
BIBLIOGRAPHY.....	122

## STATEMENT OF CONTRIBUTION TO ORIGINAL KNOWLEDGE

1. Rat NHE2 isoform cDNA encodes a functional  $\text{Na}^+/\text{H}^+$  exchanger when stably expressed in exchanger-deficient Chinese hamster ovary AP-1 cells.
2. Distinctive pharmacological properties are displayed by NHE2 that distinguish this isoform from others. Inhibitory potencies by amiloride and other drugs are generally intermediate compared to those of NHE1 (amiloride-sensitive isoform) and NHE3 (amiloride-insensitive isoform).
3. NHE2 possesses similar cation transport dynamics as NHE1 and NHE3: first order dependence on extracellular  $\text{Na}^+$  and allosteric activation of transport activity by intracellular  $\text{H}^+$ .
4. NHE2 activity is competitively inhibited by extracellular  $\text{Li}^+$  and  $\text{H}^+$ , but not  $\text{K}^+$ .
5. Sensitivity of NHE3 to inhibition by cAMP involves a region between amino acid residues 579 and 684 of the cytoplasmic domain.
6. Sensitivity of NHE3 to inhibition by cellular depletion of ATP is conferred by a region in or adjacent to the transmembrane domain.
7. Hyperosmotic inhibition of NHE3 involves a region between amino acid residues 649 and 684.
8. The NHE3 cytoplasmic domain spanned by amino acid residues 455 to 638 harbours a cryptic site that can confer a stimulatory response to hyperosmolarity and PKC in the absence of downstream C-terminal residues.

# **Chapter I.**

## **Introduction**

Donnan equilibrium and the large interior-negative potential of typical mammalian cells predicts an intracellular pH ( $\text{pH}_i$ ) of 6.3 to 6.5. Even more acidic  $\text{pH}_i$  is anticipated when one considers the continuous production of metabolic acids by various cellular homeostatic processes. Confounding these predictions are measurements of intracellular pH values that are near neutrality in numerous mammalian cell types, clearly implying the presence of regulatory mechanisms that must involve energy-requiring, net  $\text{H}^+$  elimination (1). Not surprisingly, built into most cells are seemingly redundant mechanisms that mount a coordinated defense of the cytosolic pH in face of the relentless pressure to acidify. A major component of this defense is the cellular buffering systems such as intracellular proteins, metabolites (*e.g.*, phosphates) and bicarbonates. The other mechanisms comprise the activities of various ion transporters that precisely modulate cytosolic pH. These proteins include the  $\text{Na}^+/\text{H}^+$  exchanger (NHE) and the  $\text{Na}^+$ -dependent  $\text{Cl}^-/\text{HCO}_3^-$  exchanger that both extrude acid equivalents, and the  $\text{Na}^+$ -independent  $\text{Cl}^-/\text{HCO}_3^-$  exchanger which promotes entry of base equivalents. In more specialized cells, transport proteins such as the  $\text{H}^+$ -ATPase and the  $\text{H}^+/\text{K}^+$ -ATPase can also influence  $\text{pH}_i$ . However, in most cells  $\text{Na}^+/\text{H}^+$  exchanger is the primary mechanism of  $\text{H}^+$  efflux and thus regulates the intracellular pH in the acidic range (2,3).

In its normal transport mode, the  $\text{Na}^+/\text{H}^+$  exchanger catalyzes an electroneutral extrusion of protons that is coupled in a 1:1 stoichiometry to  $\text{Na}^+$  influx. The inwardly directed  $\text{Na}^+$  gradient that is generated and maintained by the  $\text{Na}^+/\text{K}^+$ -ATPase provides the driving force for the proton extrusion mediated by the exchanger. The  $\text{Na}^+/\text{H}^+$  exchanger is present in most mammalian cells and participates in many vital homeostatic processes, such as the maintenance of intracellular pH in the neutral range, control of cell volume in response to osmotic stress, transepithelial reabsorption of  $\text{Na}^+$  and  $\text{HCO}_3^-$ , and facilitation of cell proliferation in response to various mitogenic signals (reviewed in 2-5).

The diverse physiological functions of the  $\text{Na}^+/\text{H}^+$  exchanger can be attributed in part to the existence of multiple  $\text{Na}^+/\text{H}^+$  exchanger isoforms.

### **1.1. Evidence of Multiple Classes of $\text{Na}^+/\text{H}^+$ Exchangers**

The initial evidence of  $\text{Na}^+/\text{H}^+$  exchange dates back to 1976 when Murer and co-workers demonstrated  $^{22}\text{Na}^+$  accumulation in inside-acidified membrane vesicles prepared from the brush borders of rat small intestine and kidney (6). Since then, many investigators have documented the existence of  $\text{Na}^+/\text{H}^+$  exchange in a multitude of different cell types (reviewed in 7).

The most compelling evidence in support of multiple  $\text{Na}^+/\text{H}^+$  exchanger types originates from pharmacological studies using agents which specifically inhibit  $\text{Na}^+/\text{H}^+$  exchanger activity (8-12). The diuretic drug amiloride and its more potent derivatives (see section 1.3.2.) have been employed as experimental probes to discriminate  $\text{Na}^+/\text{H}^+$  exchange activity. The  $\text{Na}^+/\text{H}^+$  exchanger in most cell types is inhibited by amiloride in the range of 1-10  $\mu\text{M}$  ( $IC_{50}$ ). This amiloride-sensitive form of the  $\text{Na}^+/\text{H}^+$  exchange activity is associated with the basolateral membranes of most polarized epithelial cells, such as those of the intestine and kidney (8,9,13). However, in polarized epithelia of human placenta (10,14,15) and rat colon epithelium (16), an amiloride-sensitive  $\text{Na}^+/\text{H}^+$  exchanger activity has been found on the apical surface. Based on its ubiquitous distribution, this amiloride-sensitive exchanger has been suggested to fulfill "house-keeping" functions such as the defense of cells against intracellular acidification and cell shrinkage (17).

In contrast to the amiloride-sensitive  $\text{Na}^+/\text{H}^+$  exchanger, the low affinity or amiloride-insensitive form of the  $\text{Na}^+/\text{H}^+$  exchanger has been found exclusively at the apical membranes of polarized intestinal and renal epithelia and has been implicated in the



vectorial transport of  $\text{Na}^+$  and  $\text{HCO}_3^-$  from the lumen to interstitial space. This form of the  $\text{Na}^+/\text{H}^+$  exchanger is generally 20- to 200-fold less susceptible to inhibition by amiloride analogues than its basolateral counterpart (8,9 and reviewed in 7).

Differences in regulation by agents that modulate various second messenger pathways also support the existence of more than one type of  $\text{Na}^+/\text{H}^+$  exchanger. Growth factors and peptide hormones have been reported to activate the amiloride-sensitive form of the exchanger in numerous target cells (11,18-22), although exceptions have been reported (23,24). In contrast, many of these agents inhibit the apical  $\text{Na}^+/\text{H}^+$  exchanger (amiloride-insensitive form) present in pig LLC-PK<sub>1</sub> (11) and opossum OK proximal tubule kidney cell lines (25,26). Overall, the data support the existence of at least two distinct forms of the  $\text{Na}^+/\text{H}^+$  exchanger that are distinguished by their pharmacology, regulation, and physiological functions.

## **1.2. Molecular Diversity**

Recent molecular cloning studies have identified five isoforms of the  $\text{Na}^+/\text{H}^+$  exchanger, termed NHE1 to NHE5 in the order of their identification. They exhibit similar predicted secondary structure and are under separate genetic control, originating from distinct but related genes. The overall aim of this thesis was to delineate some of the functional differences among the isoforms utilizing a heterologous mammalian cell expression system. As shall be presented, the  $\text{Na}^+/\text{H}^+$  exchanger isoforms display differences in their pharmacological sensitivities, cation affinities, and regulation by various molecular signals.

### **1.2.1. $\text{Na}^+/\text{H}^+$ Exchanger Isoforms and Tissue Expression**

#### **1.2.1.1. NHE1**

The first molecular isolation and characterization of the  $\text{Na}^+/\text{H}^+$  exchanger was performed by Sardet *et al.* (27) who cloned the amiloride-sensitive form (*i.e.*, NHE1 isoform) using an elegant genetic complementation strategy. As a first step, Sardet and colleagues isolated chemically mutagenized Chinese hamster lung fibroblast cells (PS120) that were devoid of endogenous  $\text{Na}^+/\text{H}^+$  exchanger activity (28) using a functional selection scheme. This innovative technique of “ $\text{H}^+$  suicide” takes advantage of the reversibility of the  $\text{Na}^+/\text{H}^+$  exchanger and its ability to transport other monovalent cations. When mutagen-pretreated,  $\text{Li}^+$ -loaded fibroblast cells are exposed to an acidic  $\text{Na}^+$ - and  $\text{Li}^+$ -free solution (pH 5.5), a massive, cytotoxic influx of protons occurs in exchange for intracellular  $\text{Li}^+$  only in cells still expressing functional  $\text{Na}^+/\text{H}^+$  exchangers. Repeated selection using this scheme permits isolation of mutant cells that lack functional exchangers (28,29). Next, total human genomic DNA was transfected into these mutant cells, and the cells overexpressing the human  $\text{Na}^+/\text{H}^+$  exchanger were selected by “reverse  $\text{H}^+$  suicide” for their ability to survive an  $\text{NH}_4^+$ -induced intracellular acidification in a manner that was dependent on extracellular  $\text{Na}^+$  (30). Human repetitive DNA that cosegregated with  $\text{Na}^+/\text{H}^+$  exchanger expressing cells was used as a probe to clone human genomic and cDNA fragments corresponding to the  $\text{Na}^+/\text{H}^+$  exchanger NHE1 isoform (27).

Since this initial cloning, many investigators have successfully used portions of the human NHE1 cDNA as probes to isolate this clone from other human tissues and NHE1 homologues from other species. To date, the same NHE1 isoform has been cloned from the human kidney and heart (31,32). In addition, its homologue has been identified

in rat (33), rabbit (34,35), pig (36), hamster (37), trout (38), crab (Genbank accession number U09274), nematode (39) and yeast (40).

Northern blot analyses indicate that NHE1 mRNA is present in most mammalian tissues and cells (33-35). However, some exceptions have been reported in the literature: 1) the opossum kidney proximal tubule OK cell line (41,42) and 2) epithelium isolated from rat proximal tubule cortical segments S<sub>1</sub> and S<sub>3</sub> (42). Although this evidence is consistent with the lack of measurable basolateral Na<sup>+</sup>/H<sup>+</sup> exchanger activity in these cells, limitations in the detection sensitivity of the assays employed cannot be ruled out. Immunohistochemical analyses have localized NHE1 to the basolateral surface of several polarized epithelia, including the villus and crypt cells of rabbit (34) and rat (43) ileal epithelia, the human intestinal Caco-2 cell line (44), the porcine renal epithelial LLC-PK<sub>1</sub> cell line, (36) and various tubular epithelial segments of the rabbit kidney (45). The generally ubiquitous nature of NHE1 expression is again consistent with this isoform fulfilling essential functions in cell homeostasis such as the maintenance of intracellular pH and cellular volume.

Further screening of cDNA libraries using the NHE1 probe under low stringency hybridization conditions has lead to the identification of additional members of the Na<sup>+</sup>/H<sup>+</sup> exchanger gene family, named consecutively as NHE2, NHE3, NHE4, and NHE5 (reviewed in 46).

#### 1.2.1.2. NHE2

The Na<sup>+</sup>/H<sup>+</sup> exchanger NHE2 isoform has so far been cloned from rat (47) and rabbit (48) gastrointestinal cDNA libraries. Recently, another rat NHE2 clone that lacks the coding sequence for the N-terminal 116 amino acids has also been reported by Collins *et al.* (49) This variant clone shows no homology in the 5' untranslated region to other

Na<sup>+</sup>/H<sup>+</sup> exchanger isoforms except for the distal most 56 nucleotides which are identical to a coding segment of the full-length NHE2 cDNA. Despite the absence of the first two putative transmembrane  $\alpha$ -helical segments, this variant NHE2 clone mediates Na<sup>+</sup>-H<sup>+</sup> exchange, *albeit* with minimal activity compared to the full-length rat NHE2 (47). Although this variant NHE2 is postulated to be alternatively spliced, evidence suggests it may be a cloning artifact derived from a processing intermediate RNA: 1) the sequence divergence occurs at a region that resembles a consensus intron-exon boundary acceptor sequence, (*i.e.*, (T/C)<sub>n</sub>N(C/T)AG/G where  $n > 11$ ) (50); 2) the position of this potential splice-site junction is analogous to the published intron-exon boundary between the first and second exons of the human NHE1 gene. Additional studies are required to elucidate the physiological relevance, if any, of this variant clone.

The NHE2 mRNA is also expressed in a wide range of tissues. In adult rat, high levels of the transcript are expressed throughout the gastrointestinal tract, with substantially reduced levels in skeletal muscle, brain, kidney, testis, uterus, heart, and lung (47). The tissue distribution in rabbit reveals a similar pattern of mRNA expression (48); however, differences in relative tissue abundance of mRNA exist between the two species. Immunohistochemical characterization of NHE2 in gastrointestinal tissues or kidney has not been studied. However, in cultured polarized renal epithelial cells, NHE2 has been reported to target to either the basolateral membrane of mouse inner medullary collecting duct cells (IMCD-3) (51) or the apical membrane of SV-40 transformed rabbit S<sub>2</sub> proximal tubule cells (RKPC-2) (52). Although the physiological roles of NHE2 are not well understood, Soleimani *et al.* (51) have suggested that NHE2 may be involved in volume regulation of IMCD cells, based on an increase in NHE2 mRNA levels in response to chronic high osmolarity. Additionally, NHE2 expressed in Chinese hamster ovary cells regulates cell pH, volume, and proliferation in a manner similar to NHE1 (53), suggesting that it may also fulfill these roles *in vivo*.

#### 1.2.1.3. NHE3

The NHE3 isoform has been identified from rat (33), rabbit (54), opossum (55), and human (56) tissues. Unlike the two previous  $\text{Na}^+/\text{H}^+$  exchanger isoforms, NHE3 shows a more restricted pattern of tissue distribution. In adult rat and rabbit, NHE3 mRNA is predominantly expressed in kidney and gastrointestinal tract (33,54). In addition to the high abundance in these tissues, the human NHE3 is also present in lower levels in testis, ovary, prostate, thymus, leukocytes, brain, spleen, and placenta (56). Subcellular localization studies in polarized renal proximal tubule (57,58) and intestinal (43) cells have demonstrated that NHE3 is exclusively localized to the apical or luminal membrane of polarized epithelia. As such, the NHE3 isoform is most likely involved in  $\text{Na}^+$  absorption in these tissues. In kidney proximal tubule epithelium, the luminal secretion of  $\text{H}^+$  necessary for  $\text{HCO}_3^-$  reabsorption (59) is also an important task fulfilled by this isoform.

#### 1.2.1.4. NHE4

To date, NHE4 has only been cloned from a rat stomach cDNA library (33). The NHE4 mRNA is most abundant in stomach with the greatest expression localized to the antrum, followed by the corpus, the gastric mucosa, and the forestomach. Considerably lower levels of the transcript were also detected in uterus, brain, kidney, and skeletal muscle (33). In kidney, the NHE4 mRNA is specifically expressed in the collecting tubule of the inner medulla (60). Based on the high osmolarity of this region, Bookstein and coworkers have suggested that this isoform may have a specialized role in cell volume homeostasis (60). Furthermore, they reported that the heterologous expression of rat NHE4 in fibroblastic PS120 cells is only active under conditions of both low intracellular pH ( $\text{pH}_i \sim 6.0$ ) and high extracellular osmolarity ( $\sim 500$  mosM). Such extreme experimental conditions to activate the transporter complicate the interpretation of the true

physiological role of this isoform. In fact, in our hands, the same PSCN4-4 cells that express the rat NHE4 isoform exhibit at most 0.1% of the activity of the full-length rat NHE1, and moreover fail to survive the standard  $\text{NH}_4^+$ -induced acid-recovery functional selection protocol that discriminates  $\text{Na}^+/\text{H}^+$  exchanger positive and negative stable transfectants (unpublished observation, F.H. Yu and J. Orlowski).

#### 1.2.1.5. NHE5

The fifth  $\text{Na}^+/\text{H}^+$  exchanger isoform is the latest to be cloned. This human NHE5 has been identified by partial genomic cloning and polymerase chain reaction (PCR) analysis (61). In sharp contrast to other isoforms, NHE5 is predominantly localized to a subset of nonepithelial tissues, such as brain, and spleen with lower expression in testis and skeletal muscle (61). There is no information regarding the functional role of this novel isoform.

#### **1.2.2. Chromosomal Mapping and Genomic Organization**

Recent studies have localized  $\text{Na}^+/\text{H}^+$  exchanger genes to distinct regions of the mammalian genome. The NHE1 isoform has been mapped to human chromosome 1p35-p36.1 by *in situ* hybridization (62), and rat chromosome 5 using rat-mouse somatic cell hybrids (63). Szpirer *et al.* (63) have used rat cDNAs probes on human-rat somatic cell hybrids to assign the general location of both NHE2 and NHE4 to rat chromosome 9 and human chromosome 2. Together with the higher amino acid similarity between these two isoforms, these data suggest that NHE2 and NHE4 may have arisen from a recent gene duplication event. Independent studies by Szpirer *et al.* (63) and Brant *et al.* (64) have mapped the NHE3 gene to distal portions of human chromosome 5. In addition, both groups have reported the presence of a NHE3-related pseudogene that maps to human chromosome 10 (63,64). The rat homologue of NHE3 has been assigned to chromosome 1 (63). Finally, fluorescence *in situ* hybridization (FISH) analysis of human metaphase

chromosomes and analysis of high-resolution human-mouse somatic cell hybrids have localized the human NHE5 to the cytogenetic subband 16q22.1 (61).

Limited information is available regarding the genomic organization of  $\text{Na}^+/\text{H}^+$  exchanger genes. The human NHE1 gene consists of 12 exons spanning approximately 70 kilobases of nucleotide sequence (65). The 5'-flanking promoter/enhancer regions of human (65), mouse (66) and rabbit (67) NHE1 genes have been characterized. All of them share similar consensus sequences for a variety of potentially *cis*-acting regulatory transcription factors, including CCAAT-box binding protein (C/EBP), AP-1, Sp-1, cAMP responsive element-binding protein (CREB), and the glucocorticoid receptor. In mouse, transcriptional regulation of the *Nhe1* gene by AP-2 transcription factor has been demonstrated (66) and appears to be critically involved in retinoic acid-induced neuronal differentiation of mouse P19 embryonic carcinoma cells (68).

Preliminary genomic characterization of mouse *Nhe2*, *Nhe3*, *Nhe4* and human NHE5 reveal that *Nhe2* and *Nhe4* share similar intron/exon boundaries in exon 2 to human NHE1 (61), again consistent with these genes originating from a closely related ancestral gene. In contrast, the second exon of the rat *Nhe3* and human NHE5 is split at the same position by an intron that is not present in other genes, suggesting that these two isoforms comprise a distinct sub-branch of the  $\text{Na}^+/\text{H}^+$  exchanger gene family.

### 1.2.3. Primary and Secondary Structures

The mammalian members of the  $\text{Na}^+/\text{H}^+$  exchanger gene family share ~40-70% amino acid identity and range from 717 to 835 residues in length ( $M_r$  ranging from ~81-93 kDa). Computer-aided analysis using the algorithms of Kite and Doolittle (69) and Engleman (70) predicts a hydropathy profile with two distinct structural domains: a *N*-terminal hydrophobic region with 10-12 putative membrane-spanning  $\alpha$ -helices (M) and a

large C-terminal hydrophilic region that is predicted to be cytoplasmic (27,33,34). Indeed, this putative cytoplasmic region of the exchanger can be antibody-labeled only following permeabilization of the membrane (71), confirming that this domain is directed intracellularly. The putative topological model of NHE is illustrated in Fig.1.1.

The topology of the N-terminal putative transmembrane region of  $\text{Na}^+/\text{H}^+$  exchangers has yet to be defined experimentally. However, the close sequence similarity of the membrane-spanning segments M6 and M7 where 95% identity exists amongst the isoforms of different species, suggests that this region may play a critical role in the cation selective transport of  $\text{Na}^+$  and  $\text{H}^+$  across the membrane. The different isoforms exhibit no appreciable homology in the region surrounding the first membrane-spanning segment. This region is believed to constitute a peptide leader sequence that gets cleaved following post-translational processing (17).

Sequence similarity of the C-terminal domain of the  $\text{Na}^+/\text{H}^+$  exchanger isoforms is low, ranging from 24-31% amino acid identity, with the exception of NHE2 and NHE4 which show ~56% identity. This region contains several consensus sequences for potential phosphorylation by different protein kinases known to modulate  $\text{Na}^+/\text{H}^+$  exchanger activity (reviewed in 72).



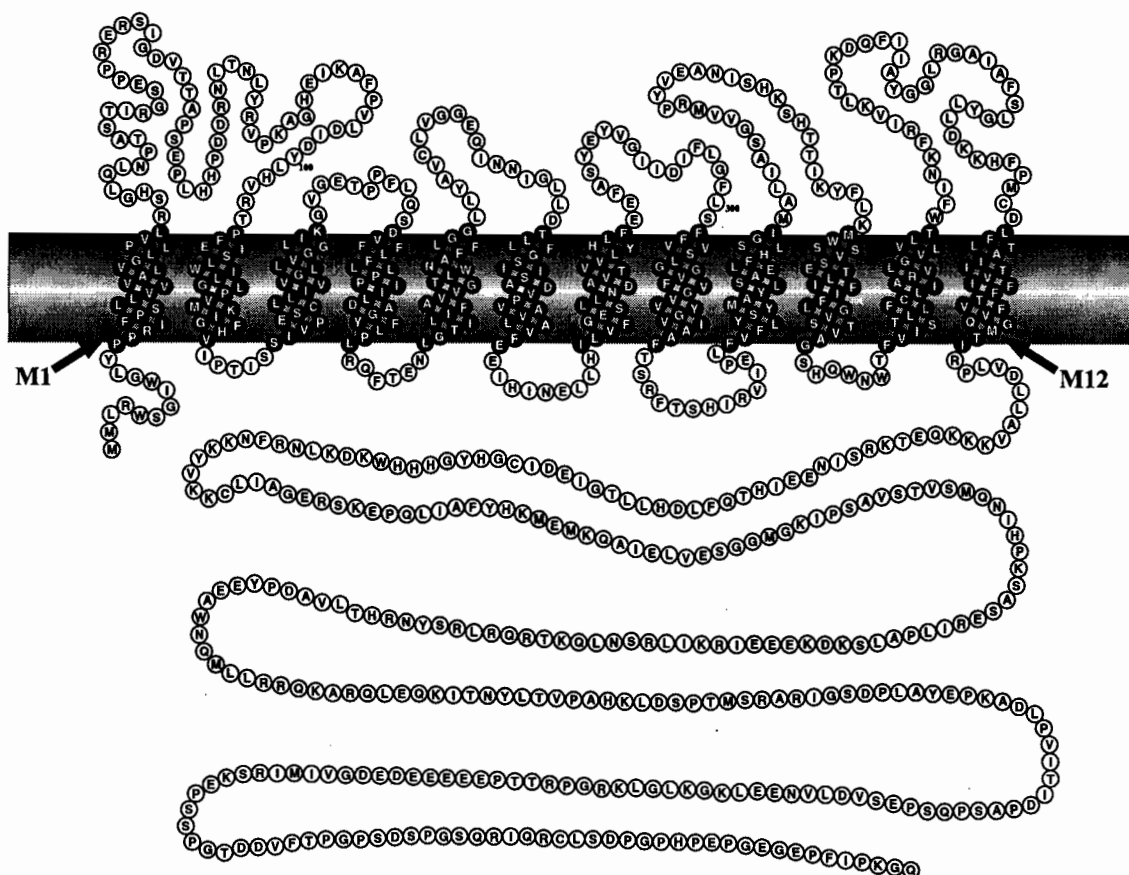


Fig. 1.1. Putative topological model of rat NHE1. Single letter amino acid code used. Residues that are believed to comprise the membrane-spanning  $\alpha$ -helical segments (M1 to M12) are highlighted as darkened circles.

#### 1.2.4. Quaternary Structure

Many membrane transport proteins are oligomeric (203). Similarly, it has recently been demonstrated that  $\text{Na}^+/\text{H}^+$  exchangers form homodimers in fibroblasts (73,74), at least in the case of NHE1 and NHE3, and do not form heterodimers. The intrinsic dimerization sequences of each isoform appear to reside in the *N*-terminal transmembranous domain (73,74). Whether the functional units of  $\text{Na}^+/\text{H}^+$  exchangers are homodimers *in vivo* remains to be proven experimentally. Of note is some evidence from pre-steady state kinetic analyses (75) and radiation inactivation (76) studies that support a tetrameric organization as the functional unit.

#### 1.2.5. Glycosylation Sites

The primary sequence of  $\text{Na}^+/\text{H}^+$  exchangers contains several potential glycosylation sites. A recent study of fibroblasts stably expressing NHE1 demonstrated that glycosylation of this isoform results in a high-mannose complex (*N*-glycosylation) at Asn<sup>75</sup>; two other potential glycosylation sites (Asn<sup>370</sup>, Asn<sup>410</sup>) present in this molecule apparently were not utilized (34,71). Further analysis of these cells showed *O*-linked glycosylation in the vicinity of Asn<sup>75</sup> of the first extracellular loop (77). The absence of glycosylation at Asn<sup>370</sup> is noteworthy considering that this particular site is highly conserved throughout the phylogeny (27,33); conceivably, this sequence, which is postulated to be within an extracellular loop, may in fact be directed intracellularly.

Unlike NHE1, NHE2 is restricted to *O*-linked glycosylation (78). Interestingly, NHE3 does not appear to be glycosylated as it is resistant to *N*-glycosidase F, neuraminidase, and *O*-glycanase (57,77). The state of glycosylation of NHE4 and NHE5 is presently not known.

The functional significance of glycosylation of heterologously expressed  $\text{Na}^+/\text{H}^+$  exchangers is not clear. Deglycosylation of NHE1 and NHE2 in exchanger-deficient fibroblastic cells (PS120) resulted in no appreciable change in transport characteristics (77-79). In contrast, a similar treatment of rat renal brush border membranes reduced the  $V_{\max}$  of the  $\text{Na}^+/\text{H}^+$  exchange (80). It is conceivable that the post-translational processing and membrane targeting mechanisms in mutant fibroblast cell lines are not the same as in renal epithelial cells.

### **1.3. Functional Characteristics and Kinetics**

#### **1.3.1. Selectivity and Kinetics**

The  $\text{Na}^+/\text{H}^+$  exchanger activity is driven solely by the electrochemical gradients of both ions and does not require metabolic energy. In mammalian cells, the inward  $\text{Na}^+$  gradient established by the  $\text{Na}^+/\text{K}^+$ -ATPase is utilized by the  $\text{Na}^+/\text{H}^+$  exchanger to power the extrusion of protons out of the cell. In addition to  $\text{Na}^+$  and  $\text{H}^+$ , the exchanger can function in multiple exchange modes involving other monovalent cations (*e.g.*,  $\text{Na}^+/\text{H}^+$ ,  $\text{Li}^+/\text{H}^+$ ,  $\text{Na}^+/\text{Na}^+$ ,  $\text{Na}^+/\text{NH}_4^+$  exchanges; reviewed in 81). The apparent affinities for external  $\text{H}^+$ ,  $\text{Li}^+$ , and  $\text{NH}_4^+$  are greater than that for  $\text{Na}^+$ , and all are competitive inhibitors of  $\text{Na}^+$  influx. Interestingly, the relative rates of transport of these cations differ from their affinities for the protein. For instance, although the apparent affinity for binding of  $\text{Na}^+$  is lower than  $\text{Li}^+$ , the  $V_{\max}$  for exchange of internal  $\text{H}^+$  with external  $\text{Na}^+$  is several-fold greater than the  $V_{\max}$  for exchange of external  $\text{Li}^+$  (82). This implies that the physical translocation of ions is the rate-limiting step in  $\text{Na}^+/\text{H}^+$  exchanger proteins and the order of selectivity for the monovalent cations favour the entry of  $\text{Na}^+$  over  $\text{Li}^+$  and other cations (81). In contrast to the aforementioned cations, the larger monovalent cations,  $\text{K}^+$ ,  $\text{Cs}^+$ , and  $\text{Rb}^+$  demonstrate no appreciable affinity for the  $\text{Na}^+/\text{H}^+$  exchanger and are transported very poorly, if at all (83-86).

The ion transport mediated by the mammalian exchangers is electroneutral. Indeed, stimulation or inhibition of  $\text{Na}^+/\text{H}^+$  exchangers has no direct effect on the transmembrane electrical potential difference (83,87,88). Moreover, when the  $\text{Na}^+$  gradient is thermodynamically balanced by an identical  $\text{H}^+$  gradient, no net flux of  $\text{Na}^+$  and  $\text{H}^+$  occurs, implying that the exchange is an electroneutral process with a stoichiometry of 1:1 ( $\text{Na}^+:\text{H}^+$ ) (89). This is unlike the bacterial  $\text{Na}^+/\text{H}^+$  exchangers which are characteristically electrogenic with a stoichiometry of 1:2 ( $\text{Na}^+:\text{H}^+$ ) (90). Under physiological conditions, the uptake of  $\text{Na}^+$  through the mammalian  $\text{Na}^+/\text{H}^+$  exchangers conforms to simple saturating Michaelis-Menten kinetics (82-84,91,92). This conclusion is most consistent with the presence of a single extracellular binding site for  $\text{Na}^+$  and hence the translocation of one  $\text{Na}^+$  for one  $\text{H}^+$  per transport cycle.

One of the most prominent features of  $\text{Na}^+/\text{H}^+$  exchangers is the allosteric activation by intracellular protons. In contrast to the simple Michaelis-Menten kinetics of the exchanger with respect to external  $\text{Na}^+$ , the transport rate has greater than first-order dependence on the internal  $\text{H}^+$  concentration (83,93,94). Taking into account the one-to-one stoichiometry of the exchanger, this behaviour is most inconsistent with simple saturating kinetics. Aronson and colleagues (93) first proposed that a second cytoplasmic  $\text{H}^+$  binding site, independent of the translocation site, may allosterically activate the exchanger. Evidence in support of this hypothesis comes from the observation that in cells preloaded with  $^{22}\text{Na}^+$ , raising  $\text{H}^+$ , can actually *stimulate* the  $\text{Na}^+$  efflux (93), an effect opposite to that expected if  $\text{H}^+$  were only competing for the internal transport site. Although the mechanism of this allosteric activation has yet to be delineated, the simplest interpretation is the presence of one or more titratable groups that upon protonation lead to a change in protein conformation that causes activation of the transporter.

This allosteric activation of  $\text{Na}^+/\text{H}^+$  exchangers by internal protons is a critical regulatory feature that is important in controlling  $\text{pH}_i$ . If allowed to approach thermodynamic equilibrium under a symmetrical exchange process, the inwardly directed  $\text{Na}^+$  gradient would be predicted to drive the  $\text{pH}_i$  to very alkaline levels ( $\text{pH}_i \approx 8.3$ ). However, the asymmetric properties of the  $\text{Na}^+/\text{H}^+$  exchanger exert kinetic control of the transport process through an activity threshold or a  $\text{pH}_i$  set point, and thus permit the regulation of  $\text{pH}_i$  within narrowly defined limits for optimal cell homeostasis. Above this  $\text{pH}_i$  set point, the exchanger becomes virtually quiescent, thereby protecting the cell against intracellular alkalosis. In unstimulated cells,  $\text{Na}^+/\text{H}^+$  exchange is indeed nearly undetectable at normal  $\text{pH}_i$  (8.3, 9.2, 9.5). On the other hand, below this set point, the protonation of the modifier site greatly enhances the transport activity of the exchanger, allowing for a prompt response against intracellular acidification.

### 1.3.2. Sensitivity to Inhibitors

One of the best known inhibitors of the  $\text{Na}^+/\text{H}^+$  exchanger is amiloride, a potassium-sparing diuretic drug. This pharmacological agent inhibits mammalian exchangers with a  $K_i$  that ranges between 1 and 100  $\mu\text{M}$ , depending on the isoform/cell type (7). Amiloride's chemical structure consists of a substituted pyrazine ring with two amino groups attached at ring positions 3 and 5, a chloride moiety at ring position 6, and an acylguanidium group at ring position 2 (see Fig. 1.2). Since amiloride is a weak base with a  $\text{pK}_a$  of 8.7, it exists essentially as a monovalent cation within the physiological pH range. The positive charge of the guanidium group may partly account for the competitive behaviour of amiloride with  $\text{Na}^+$ ,  $\text{Li}^+$ , and  $\text{H}^+$ , and for the fact that amiloride inhibits other  $\text{Na}^+$  transporters such as  $\text{Na}^+$  channels,  $\text{Na}^+/\text{Ca}^{2+}$  exchangers and  $\text{Na}^+$ -dependent amino acid transporters (96).

Many structural analogues of amiloride that display greater inhibitory potency for the  $\text{Na}^+/\text{H}^+$  exchanger have been synthesized from the parent molecule (reviewed in 96-98). Briefly, alkylations at ring position 5 produce more potent inhibitors, with some analogues being 100-times more efficacious than amiloride itself. In contrast, modifications at the terminal guanidino nitrogen yield very poor inhibitors. Finally, replacement of the  $-\text{Cl}$  moiety at ring position 6 with  $-\text{I}$  only slightly enhances the inhibitory potency.

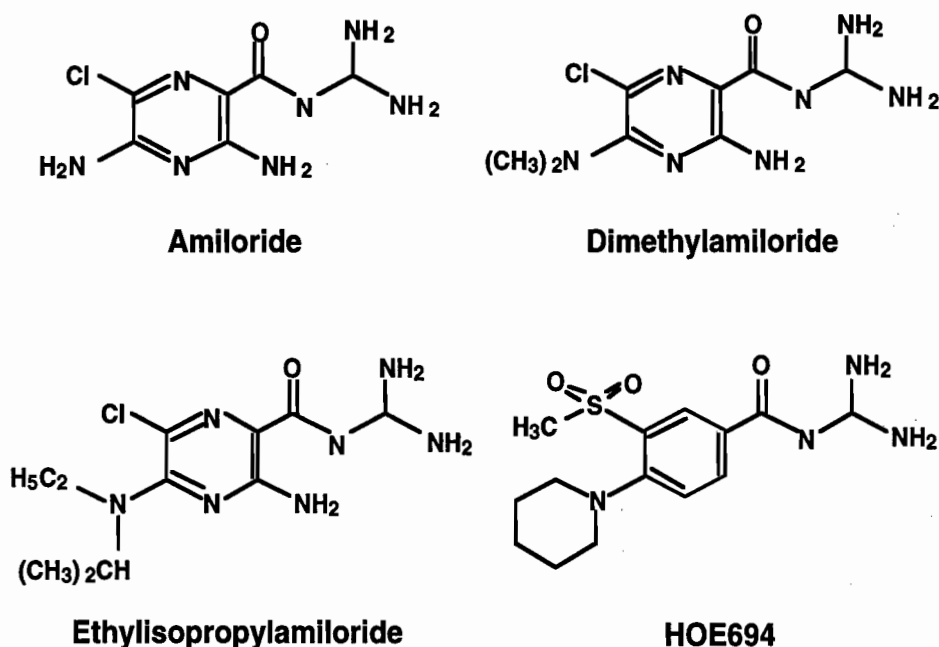


Fig. 1.2. Molecular structures of pharmacological agents amiloride, two 5-amino-substituted analogues, and HOE694

Available evidence indicates that it is the positively charged form of amiloride that is active as a blocker of the  $\text{Na}^+/\text{H}^+$  exchanger and that there may be two distinct attachment sites for amiloride: (1) alkyl substitutions of the 5-amino group of amiloride greatly increases the inhibitory potency (97), suggesting that a hydrophobic moiety on the  $\text{Na}^+/\text{H}^+$  exchanger provides an attachment site in addition to the  $\text{Na}^+$  site where the

charged guanidinium group is believed to bind and produce an inhibitory effect; (2) mutant cell lines have been isolated which have reduced sensitivity to amiloride, yet exhibit increased affinity for  $\text{Na}^+$ , suggesting an involvement of distinct sites (99). In many studies, amiloride acts as a purely competitive inhibitor of  $\text{Na}^+/\text{H}^+$  exchanger with respect to external  $\text{Na}^+$  (92,100-102), although an exception has been noted (82). Substantial amount of evidence is consistent with amiloride and its derivatives binding to the exchanger from the extracellular side; indeed, amiloride entrapped within dog red cell ghosts is ineffective at concentrations which completely eliminate the  $\text{Na}^+/\text{H}^+$  exchange when the drug is added externally (103).

Recently, HOE694 was demonstrated to be a potent and specific inhibitor of  $\text{Na}^+/\text{H}^+$  exchangers. While not derived from amiloride, it has a similar chemical structure and inhibits the  $\text{Na}^+/\text{H}^+$  exchangers with an identical order of sensitivity, but over a larger concentration range (three orders of magnitude) (104). The potent inhibition of NHE1 by HOE694 (nM concentrations) compared to the other isoforms has potential clinical applications in the treatments of cardiac ischemia and reperfusion injuries, without the complications of the diuretic side effects (105).

Other pharmacological agents exist that block  $\text{Na}^+/\text{H}^+$  exchanger activity. These compounds include, clonidine, an  $\alpha_2$ -adrenergic receptor agonist (10,14), cimetidine, a histamine  $\text{H}_2$ -receptor antagonist (10,106), harmaline, a hallucinogenic drug known to antagonize amine oxidase and some  $\text{Na}^+$ -dependent transporters (10,86,107), loperamide, an opiate receptor antagonist (23), and other guanidinium derivatives (98). The inhibitory effects of some of these compounds have been demonstrated in the presence of specific antagonists for each receptor, suggesting a direct inhibitory effect on the  $\text{Na}^+/\text{H}^+$  exchangers (23,106). The common feature in the chemical structures of these compounds with amiloride and HOE derivatives is the presence of either an imidazoline or guanidino

moiety, and this suggests similar mechanisms of inhibition as a  $\text{Na}^+$  competitor (98,104). The few studies which have employed these compounds generally show that the different isoforms display a similar order of drug sensitivity compared to amiloride (*i.e.*,  $\text{NHE1} > \text{NHE2} > \text{NHE3}$ ) (10,14,106,108).

#### **1.4. Physiological Roles of $\text{Na}^+/\text{H}^+$ Exchangers**

##### **1.4.1. Regulation of Intracellular pH**

Through proton efflux, the  $\text{Na}^+/\text{H}^+$  exchanger attains its primary function – intracellular pH regulation. As discussed above, this prominent role is likely fulfilled by the “housekeeping” NHE1 isoform, although the contributions of other isoforms cannot be ruled out (53). The exchanger is remarkably efficient in its regulation of cytosolic pH due to the  $\text{pH}_i$  dependence of its transport rate. In most cells, the  $\text{Na}^+/\text{H}^+$  exchanger is virtually quiescent at or around physiological  $\text{pH}_i$  ( $\text{pH} \sim 7.0\text{--}7.2$ ), but it becomes dramatically stimulated when the cell interior is acidified even slightly (83,93,95,109, 110). In general, the  $\text{Na}^+/\text{H}^+$  exchanger facilitates recovery only to the baseline  $\text{pH}_i$  at which point, its transport activity is sharply curtailed. This phenomenon is most consistent with a role in  $\text{pH}_i$  homeostasis and is a function of the apparent  $\text{H}^+_{i-}$ -sensitivity or  $\text{pH}_i$  set-point of the exchanger, dictated primarily by the  $\text{H}^+_{i-}$ -sensitive modifier site. Despite this tight regulation, the  $\text{pH}_i$  set-point of the  $\text{Na}^+/\text{H}^+$  exchangers can be modified by various stimuli. For instance, an acidic shift of the NHE1  $\text{pH}_i$  set-point can be induced by a metabolic depletion of cellular ATP while an alkaline shift occurs when the exchanger is stimulated by growth factors or osmotic cell shrinkage (reviewed in 5).

##### **1.4.2. Regulation of Cell Volume**

Another pivotal role of the  $\text{Na}^+/\text{H}^+$  exchanger is in cell volume regulation. Because most cell membranes are more permeable to water than solutes, cell volume is determined



primarily by the total osmotic content of the cell, and thus the regulation of volume is achieved through the control of cellular osmolytes. The major osmolytes are the ions  $\text{Na}^+$ ,  $\text{K}^+$ , and  $\text{Cl}^-$ . If these ions were allowed to equilibrate unchecked across the plasma membrane, cells would tend to swell due to the Donnan osmotic component of nondiffusible intracellular macromolecules. In steady state, most cells maintain their volume primarily by controlling electrolyte levels via  $\text{Na}^+/\text{K}^+$ -ATPase (111,112). In conditions that produce acute alterations in cell volume, other ion transporters play larger roles;  $\text{K}^+$  and  $\text{Cl}^-$  channels mediate regulatory volume decrease when cells are osmotically swollen, and parallel operation of the  $\text{Na}^+/\text{H}^+$  exchanger and the  $\text{Na}^+$ -independent  $\text{Cl}^-/\text{HCO}_3^-$  exchanger promotes regulatory volume increase in osmotically shrunken cells. It should be noted that these transport mechanisms are not the exclusive regulators of cell volume (113).

In principle, the ion transport through the  $\text{Na}^+/\text{H}^+$  exchanger appear osmotically ineffective since the electroneutral exchange of monovalent cations by itself does not alter the total concentrations of monovalent cations on either side of the cell membrane. However, since the extruded  $\text{H}^+$  are readily replaced from the intracellular buffers, a net cellular accumulation of  $\text{Na}^+$ , and therefore cell swelling occurs, even in experimental manipulations that exclude  $\text{HCO}_3^-$  from the media. When  $\text{HCO}_3^-/\text{CO}_2$  buffer is available, the alkalization resulting from the osmotically-stimulated  $\text{Na}^+/\text{H}^+$  exchange leads to accumulation of cytosolic  $\text{HCO}_3^-$  that in turn drives  $\text{Cl}^-$  into the cytoplasm through an exchange mediated by the  $\text{Na}^+$ -independent  $\text{Cl}^-/\text{HCO}_3^-$  exchanger (87,114). Thus, cells possessing this latter transporter will swell even further than those without. Although an alkaline-shift in  $\text{pH}_i$ , sensitivity of the  $\text{Na}^+/\text{H}^+$  exchanger is known to occur when osmotically stimulated (114), the precise molecular mechanisms of osmosensing and the transduction of this signal to the transporter remain largely unresolved. This is a focus of this thesis.

### 1.4.3. Transepithelial Transport

The  $\text{Na}^+/\text{H}^+$  exchangers of polarized epithelia play a key role in the net transport of solutes and water across this barrier. In mammalian renal proximal tubules, the apical  $\text{Na}^+/\text{H}^+$  exchanger (*i.e.*, NHE3) plays an important role in the reabsorption of over 90% of the filtered  $\text{HCO}_3^-$  load (91). The secondary-active secretion of  $\text{H}^+$  by NHE3 promotes the following series of steps: 1) luminal bicarbonate capture, 2) its hydration and dissociation of  $\text{CO}_2$  catalyzed by the luminal carbonic anhydrase, 3)  $\text{CO}_2$  diffusion and intracellular accumulation of  $\text{HCO}_3^-$  catalyzed by a cellular form of the carbonic anhydrase, and finally 4) exit of  $\text{HCO}_3^-$  via the basolateral  $\text{Na}^+/\text{HCO}_3^-$ -cotransporter, down its electrochemical gradient (see Fig. 1.3). In epithelia that possess both an apical  $\text{Na}^+/\text{H}^+$  exchanger and an apical  $\text{Na}^+$ -independent  $\text{Cl}^-/\text{HCO}_3^-$  exchanger, a similar sequence of events that involve  $\text{HCO}_3^-/\text{CO}_2$  shuttling across the apical membrane promotes active transepithelial  $\text{Cl}^-$  transport (3,86). Furthermore, the cumulative gain of  $\text{NaCl}$  from the luminal space and the osmotically obliged water also influence the water balance across epithelial tissues. In addition, the luminal acidification mediated by the  $\text{Na}^+/\text{H}^+$  exchanger can also drive net absorption of weak organic acids by a non-ionic diffusion of lipid-soluble, protonated species. Once inside the apical membrane, the charged organic anions become trapped by the alkaline pH of the cytosol and accumulate. This mechanism is believed to be involved in the renal handling of organic anions such as butyrate, propionate, and acetate (115).

### 1.4.4. Facilitation of Cellular Proliferation

A controversial role ascribed to  $\text{Na}^+/\text{H}^+$  exchangers is their participation in cellular proliferation. This notion began with the identification of  $\text{Na}^+/\text{H}^+$  exchange-mediated alkalization as one of the early events in the genesis of the growth response. Although thought to be non-essential, several lines of evidence (comprehensively reviewed by

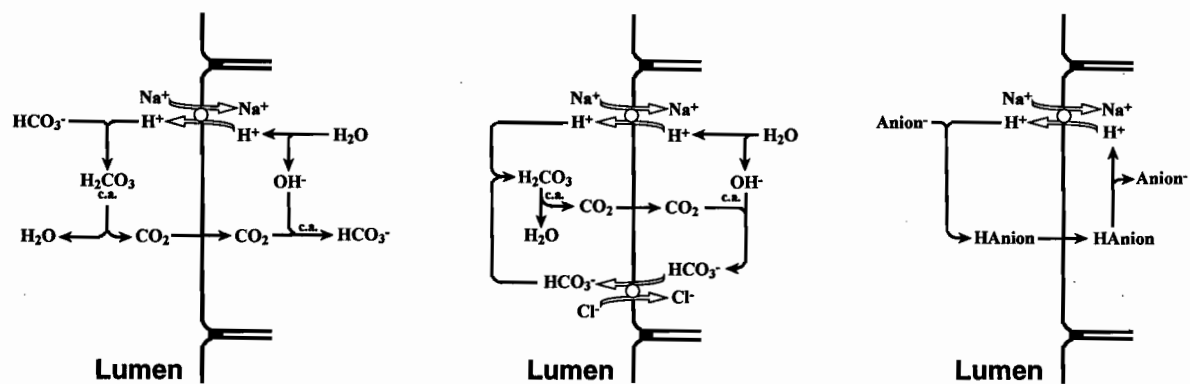


Fig. 1.3. Involvement of  $\text{Na}^+/\text{H}^+$  exchangers in facilitation of transepithelial transport of  $\text{HCO}_3^-$ ,  $\text{Cl}^-$ , and organic anions

Grinstein *et al.* (5)) support the notion that  $\text{Na}^+/\text{H}^+$  exchange activation is at least facilitative to cell proliferation: 1) virtually all mitogenic agents acutely activate  $\text{Na}^+/\text{H}^+$  exchange; 2) manipulations that induce cellular alkalization can promote cell proliferation in the absence of mitogens in some systems; 3) cell proliferation is dependent on extracellular  $\text{Na}^+$ ; and 4) amiloride and amiloride analogues can inhibit the proliferative responses. Definitive evidence that links the  $\text{Na}^+/\text{H}^+$  exchanger to cell proliferation has been elusive; however, the consequent cytosolic alkalization following  $\text{Na}^+/\text{H}^+$  exchanger activation may facilitate some of the processes of the mitogenic cascade.

### **1.5. Regulation of $\text{Na}^+/\text{H}^+$ Exchanger**

A wide variety of molecular signals are known to modulate  $\text{Na}^+/\text{H}^+$  exchanger activity. These agonists of the  $\text{Na}^+/\text{H}^+$  exchanger can be grouped into two categories: 1) acute regulators that influence the transport rate within minutes, such as growth factors, neurotransmitters, peptide hormones, phorbol esters, chemotactic factors, mitogenic lectins, and osmotic shrinkage; 2) chronic signals that manifest their effects after several hours, such as acidosis, thyroid and steroid hormones (2,5). The complexity of  $\text{Na}^+/\text{H}^+$  exchanger regulation by these diverse signals is a reflection of the existence of multiple  $\text{Na}^+/\text{H}^+$  exchanger isoforms, the diversity of signaling pathways, and the differences in the subcellular *milieu* or localization of the exchangers.

#### **1.5.1. Acute Regulation**

##### **1.5.1.1. Protein Kinases A and C**

It has been speculated repeatedly that growth factor regulation of  $\text{Na}^+/\text{H}^+$  exchanger activity could be most simply accounted for by a direct phosphorylation of the transporter. Moolenaar *et al.*(95) suggested that the mechanism of growth factor

activation of the  $\text{Na}^+/\text{H}^+$  exchanger involved increased affinity of  $\text{H}^+_i$  (an alkaline shift in  $\text{pH}_i$  set point) of the exchanger, perhaps caused by protein kinase C (PKC)-mediated phosphorylation. Indeed, phorbol ester derivatives that increase PKC activity have been found to activate the  $\text{Na}^+/\text{H}^+$  exchanger with the same rank order of sensitivity (116). This notion of control via phosphorylation is also consistent with studies which showed that phorbol esters no longer stimulate  $\text{Na}^+/\text{H}^+$  exchangers in lymphocytes previously depleted of PKC (18) and intracellular ATP (117). Data from Pouyssegur and co-workers demonstrated that  $\text{Na}^+/\text{H}^+$  exchange in fibroblasts is activated by  $\alpha$ -thrombin and epidermal growth factor (EGF) (118-120). Furthermore, they showed that both of these mitogenic agents induce phosphorylation of the exchanger (NHE1) exclusively on serine residues of five common tryptic peptide fragments in parallel with increases in  $\text{Na}^+/\text{H}^+$  exchanger activity (71,121). Considering the different signaling routes of  $\alpha$ -thrombin (phosphoinositide turnover) and EGF (tyrosine kinase activation), these findings suggest an integration of various signal transduction pathways through a common protein kinase that activates the exchanger through phosphorylation. However, whether phosphorylation of the exchanger directly causes the activation of the exchanger has yet to be conclusively demonstrated.

The presence of several consensus phosphorylation sites for serine/threonine protein kinases in the C-terminal cytoplasmic domain of the  $\text{Na}^+/\text{H}^+$  exchanger isoforms suggests that this region may be involved in regulation. Evidence in support of this hypothesis was provided by Winkel *et al.* (122) who showed that a microinjection of a polyclonal antibody raised against amino acids 658-815 of human NHE1 into the cytoplasm of mammalian cells results in a loss of  $\alpha$ -thrombin and EGF stimulation of NHE1, but not phorbol ester or hyperosmotic stress-induced stimulation. Furthermore, deletion studies that removed most of the C-terminal domain of NHE1 resulted in a total loss of growth-factor regulation (123,124). Interestingly, the deletion of amino acids 635-

815 that contain the potential serine-phosphorylation sites only partially impairs the activation by 50%, while the removal of an upstream segment spanned by amino acids 567-635 that does not contain any of the phosphorylation sites completely abolishes activation by several growth-promoting agents (123). Therefore, these results suggest that a direct phosphorylation may not be an essential requirement for activation of the exchanger and provide support for the existence of a mechanism of activation that does not require a direct phosphorylation. Conceivably, such mode of activation could involve an ancillary protein(s) (possibly regulated by phosphorylation) that interact with the proximal portions of the C-terminal domain (amino acid residues 567-635).

Although these factors have yet to be identified, several recent studies indicate that NHE1 has at least the capacity for intermolecular protein-protein interactions: 1) the  $\text{Na}^+/\text{H}^+$  exchanger forms a dimer in plasma membranes (73,74); 2) rabbit NHE1 binds the 70 kDa heat shock protein (hsp70) *in vitro* (125); 3) NHE1 can be activated following  $\text{Ca}^{2+}$ /calmodulin (CaM) (126,127) binding to its C-terminal domain; and 4) a calcineurin homologous protein (CHP) binds and inhibits serum-stimulated NHE1 (202). In addition, an unidentified 24 kDa protein has been found to associate with NHE1 *in situ* (128). However, at present, the functional relevance of this protein in the regulation of NHE1 activity remains hypothetical.

Unlike the role of PKC in regulating NHE1, cAMP modulation of NHE1 activity has not been studied as extensively. The cAMP-dependent stimulation of  $\text{Na}^+/\text{H}^+$  exchanger activity has been demonstrated in murine macrophages (129), primary rat hepatocytes (130) and rat osteoblastic UMR-106 cells (131) that express only the NHE1 isoform (33,47,132). Rat NHE1 is also stimulated by increasing  $\text{cAMP}_i$  when stably expressed in Chinese hamster ovary AP-1 cells (141). An interesting exception is when human NHE1 is transfected into opossum kidney (OK) cells, cAMP inhibits NHE1 in a

similar fashion to the endogenous NHE3 isoform (133). In contrast, human (38) and rabbit (134) homologues of NHE1 when stably expressed in PS120 mouse fibroblasts are insensitive to maneuvers that increase cAMP even though the protein kinase A (PKA) pathway is intact in these cells. Taken together, these conflicting results are suggestive of possible cell-specific regulatory effects.

However, support for species differences also exists. For example, trout  $\beta$ NHE isoform which displays the strongest homology to NHE1, is stimulated by cAMP and other activators of PKA in PS120 cells (38). Furthermore, a substitution of human NHE1 C-terminal cytoplasmic region with that of  $\beta$ NHE produced a chimeric exchanger that was sensitive to increases in cAMP levels (135), indicating that the cytoplasmic region contained necessary elements to dictate hormonal regulation of the exchanger. Examination of the amino acid sequence of  $\beta$ NHE in the cytoplasmic region revealed two optimal consensus sites (Ser<sup>641</sup> and Ser<sup>648</sup>) for phosphorylation by PKA which are not present in human, rabbit nor rat homologues (135). In the same study, elimination of these serine residues by site-directed mutagenesis only partially abrogated the cAMP stimulation, indicating that other regions of C-terminal cytoplasmic domain may be involved in cAMP-dependent regulation of this trout  $\beta$ NHE. This interaction could be mediated by additional cryptic PKA sites or cAMP/PKA-dependent accessory factors that have yet to be identified.

Unlike NHE1, the C-terminal cytoplasmic domains of rat and rabbit NHE2 contain several classical consensus sites for phosphorylation by PKA as well as PKC. However, similar to NHE1, rat NHE2 activity can be stimulated in response to activators of the PKA and PKC pathways when stably expressed in AP-1 cells (141). In contrast, a recent study by Levine *et al.* (134) demonstrated that rabbit NHE2 when heterologously expressed in PS120 fibroblasts, is unresponsive to cell permeant cAMP analogues

although it retained its stimulatory response to phorbol esters and serum. It has yet to be determined whether the regulation of NHE2 is mediated through direct phosphorylation of the exchanger.

Compared to NHE2, much more is known about the regulation of the NHE3 isoform. There is a convincing body of evidence that demonstrates that maneuvers which acutely increase  $\text{cAMP}_i$  content inhibit  $\text{Na}^+/\text{H}^+$  exchanger activity in the rabbit renal brush border membrane vesicles (136,137), and in the opossum kidney proximal tubule cell line (OK) (25,26,138). In addition, pharmacological activation of the PKC pathway also inhibits the NHE3 activity in OK cells (139). Rat NHE3 heterologously expressed in AP-1 mutant Chinese hamster ovary cells devoid of endogenous  $\text{Na}^+/\text{H}^+$  exchanger activity retains its capacity to be inhibited by cAMP (140,141) as well as phorbol esters (141). In fact, it has been demonstrated recently that this amiloride-sensitive rat isoform is a phosphoprotein and that phosphorylation content increases following cAMP treatment (140). In contrast, when the rabbit NHE3 cDNA was stably expressed in PS120 cells, only activation of PKC, but not PKA, produced inhibition of exchanger activity (134), suggesting once again that cAMP-dependent regulation may depend on the cellular *milieu*.

Structural analyses by Levine and colleagues (142) reveal that a region flanked by amino acid residues 585 and 689 is critical for PKC regulation of rabbit NHE3. Although this region contains several consensus sites for potential phosphorylation by PKA and PKC in both rabbit and rat NHE3 isoforms, it is not known whether the phosphorylation actually occurs at these sites. Alternatively, one cannot rule out the possibility of phosphorylation-dependent ancillary protein factors which may effect their regulatory influences through this cytoplasmic region of NHE3. Consistent with this postulation, Weinman *et al.* (143-145) have isolated and cloned a 42-55 kDa phosphoprotein which is



thought to be a cofactor for PKA regulation of rabbit kidney brush border membrane  $\text{Na}^+/\text{H}^+$  exchanger activity. Additional studies are needed to delineate the exact molecular mechanism of NHE3 regulation and is a focus of this thesis.

#### 1.5.1.2. ATP Dependence

The  $\text{Na}^+/\text{H}^+$  exchanger does not directly require the hydrolysis of ATP during the transport cycle. Nevertheless, the metabolic depletion of ATP drastically depresses  $\text{Na}^+/\text{H}^+$  exchanger activity in a variety of cell types (18,146-148), through a mechanism that does not involve  $\text{Na}^+/\text{K}^+$ -ATPase. In NHE1-transfected fibroblasts, growth factor and PKC regulation of the exchanger was eliminated by ATP depletion (124), possibly via a dephosphorylation mediated reduction in  $\text{H}^+$  affinity (124). However, Goss and co-workers demonstrated that the phosphorylation state of NHE1 is not appreciably altered following metabolic depletion of cellular ATP (140). In stably transfected AP-1 (53) and PS120 (134) cells expressing NHE1, NHE2 or NHE3, an acidic shift in  $\text{pH}_i$  dependence and/or a decreased  $V_{\text{max}}$  have been reported to contribute to the inhibition of exchanger activity following cellular depletion of ATP.

#### 1.5.1.3. Hyperosmolarity

$\text{Na}^+/\text{H}^+$  exchange activity is also known to be modulated by changes in cellular osmolarity. In most cells, the activation of  $\text{Na}^+/\text{H}^+$  exchange (presumably NHE1) that is coupled to cation-independent  $\text{Cl}^-/\text{HCO}_3^-$  exchange plays a crucial role in cell volume recovery following hyperosmotic challenge (18,149). This shrinkage-dependent activation of the exchanger is largely due to a shift in the  $\text{pH}_i$  sensitivity of the rate of transport (114). In transfected AP-1 cells, both rat NHE1 and NHE2 are activated following exposure to an acute hyperosmotic stress (53). In contrast, rat NHE3 is inhibited (53). This shrinkage-induced inhibition of NHE3 precisely mimics that observed for the endogenous, apical NHE3 isoform in renal proximal tubule OK cells

(150) and rat medullary thick ascending limb (151). Little is known about the molecular mechanism involved in the osmotic regulation of the exchangers, although it appears to differ from growth factor regulation. Unlike the latter, activation of NHE1 following exposure to hyperosmotic media does not appear to involve changes in phosphorylation of the exchanger (152). Nevertheless, G proteins independent of the PKC and PKA pathways (153,154) and protein kinases such as myosin light-chain kinase (155), tyrosine kinase (156), p38 protein kinase (157), and Jun kinase/stress-activated protein kinase (158) have been implicated in this osmosensing cascade.

### **1.5.2. Chronic Regulation**

Long-term regulation of  $\text{Na}^+/\text{H}^+$  exchangers by hormones and other stimuli also occurs. Thyroid hormone has been shown to affect rat renal brush border membrane  $\text{Na}^+/\text{H}^+$  exchange. Hypothyroid rats exhibit reduced  $\text{Na}^+/\text{H}^+$  exchange activity, while the opposite occurs in hyperthyroid rats (159,160). Moreover, thyroid hormone also stimulates  $\text{Na}^+/\text{H}^+$  exchange activity in cultured OK cells (161). Removal of glucocorticoid by adrenalectomy in rats can also diminish  $\text{Na}^+/\text{H}^+$  exchanger activity measured in renal microvillus membrane vesicles (162). In this study, administration of exogenous dexamethasone, but not aldosterone (a mineralocorticoid), restored the renal brush border  $\text{Na}^+/\text{H}^+$  exchanger activity. These results implicate glucocorticoids in stimulating the  $\text{Na}^+/\text{H}^+$  exchangers. To identify the  $\text{Na}^+/\text{H}^+$  exchanger isoform involved in glucocorticoid stimulation of the exchanger activity, Yun and colleagues demonstrated that NHE3 mRNA, but not NHE1 or NHE2, became elevated in rabbit ileal brush border membranes upon methylprednisolone treatment. This increase correlated temporally with the increase in  $\text{Na}^+/\text{H}^+$  exchanger activity (163). Recent studies have shown that the control of NHE3 mRNA levels by glucocorticoid occurs largely at the level of transcription (164). Similarly, an increase in NHE1 transcription also appears to be the

underlying mechanism by which mouse P19 embryonic carcinoma cells and HL60 cells respond to retinoic acid treatment (68,165).

Adaptive regulation of  $\text{Na}^+/\text{H}^+$  exchangers under conditions of high osmolarity and acidosis has also been described in several systems. For example, incubation of IMCD cells in hyperosmotic media for 72 h stimulates  $\text{Na}^+/\text{H}^+$  exchange activity in association with increased NHE2 and reduced NHE1 mRNA levels (51). Interestingly, in these same cells, chronic exposure to acidic medium reduces NHE2 mRNA abundance and activity while it elevates those of NHE1 (51). Increased NHE1 activity and mRNA abundance have also been observed in other renal cells chronically exposed to acidosis, including LLC-PK<sub>1</sub> (166) and mouse renal cortical tubule (MCT) cells (167). Likewise, elevated renal cortical NHE1 levels have been found in animals fed  $\text{NH}_4\text{Cl}$  to induce metabolic acidosis (167,168). In addition, acid incubation also increases NHE3 mRNA abundance in OK cells (55). In contrast, a prolonged exposure to acidic media reduces NHE1 mRNA and activity in NIH3T3 fibroblasts (167). Although the exact mechanism of acid-induced activation of renal NHE1 has not been delineated, recent data have implicated PKC and the transcription factor AP-1 in this process (169,170). Likewise, the *c-src* family of nonreceptor protein-tyrosine kinases has been implicated in acid-induced activation of NHE3 (171). Furthermore, the complex, isoform-specific and cell-type-dependent regulation of  $\text{Na}^+/\text{H}^+$  exchanger activity by acid is further complicated by evidence suggesting that acute regulation by acid can occur through the recruitment of pre-existing  $\text{Na}^+/\text{H}^+$  exchangers from intracellular stores (172).

## **1.6. Rationale and Objectives**

The presence of  $\text{Na}^+/\text{H}^+$  exchanger activity in all mammalian cells studied thus far is indicative of its crucial importance to cell homeostasis. The principal role of this exchanger in most cells is to defend the cell against intracellular acidification by

maintaining the  $\text{pH}_i$  slightly above neutral as well as to participate in the cell volume recovery response to osmotic stress and in the proliferative response to mitogenic signals.

Despite the essential nature of these functions, cells can be deprived of  $\text{Na}^+/\text{H}^+$  exchanger activity by experimental manipulations; these mutant cells are able to survive and proliferate provided the medium contains bicarbonate and is maintained at an alkaline pH (29,173). A mutant Chinese hamster ovary cell line, AP-1, is one such model system that very much simplifies the comparison of the functional properties of the recently identified isoforms of the  $\text{Na}^+/\text{H}^+$  exchanger gene family.

In native tissues, the measurements of the  $\text{Na}^+/\text{H}^+$  exchanger activity are complicated by the coexistence of multiple isoforms in individual cell types. Heterologous expression of  $\text{Na}^+/\text{H}^+$  exchanger isoforms into AP-1 cells overcomes these confounding factors and permits the analysis of the functional characteristics of each isoform in isolation. Furthermore, the common cellular background of this heterologous expression system facilitates comparisons of the functional and regulatory properties of the different isoforms. An important caveat to consider in such experiments is that the endogenous *milieu* of the native cell types is not entirely simulated in these heterologous systems and may complicate interpretation of the data. Nevertheless, useful information can be obtained using transfected cell lines such as AP-1 cells. Previous studies have shown that intact regulatory signaling pathways and overall cell responses of wild type Chinese hamster ovary AP-1 cells (NHE1) are precisely mimicked when transfected with the full-length rat NHE1 isoform (53,108).

The focus of this thesis was to use this heterologous expression system to characterize some of the functional and regulatory properties of the more specialized rat NHE isoforms (*i.e.*, NHE2 and NHE3). These exchangers appeared to be present in great abundance in renal and gastrointestinal tissues and were therefore postulated to have

specialized functions in these tissues. The results that define some of the unique functional properties of NHE2 are presented in Chapter II.

Comparison of the regulatory properties of NHE2 with those of NHE1 and NHE3 revealed that the NHE2 responses were qualitatively similar to NHE1, but opposite to those of NHE3 (141). The fact that NHE3 is consistently inhibited by a divergent array of regulatory stimuli suggests a mechanism whereby different intracellular signaling pathways are integrated at a common point to modulate transporter activity. The results presented in Chapters III and IV test this hypothesis using deletion and chimeric mutants of NHE1 and NHE3. Chapter III examined the inhibitory effects of cAMP and ATP-depletion while Chapter IV studied the hyperosmotic inhibition of NHE3.

## **Chapter II.**

### **Functional Properties of the Rat Na<sup>+</sup>/H<sup>+</sup> Exchanger NHE2 Isoform Expressed in Na<sup>+</sup>/H<sup>+</sup> Exchanger-Deficient Chinese Hamster Ovary Cells**

Frank H. Yu, Gary E. Shull, and John Orlowski

This study was designed and all experiments were carried out by F.H.Yu. G.E. Shull provided the rat NHE2 cDNA. The study was coordinated and supervised by J. Orlowski.

The text and figures of this chapter were published in the *Journal of Biological Chemistry* (1993) **268**: 25536-25541.

## SUMMARY

The primary structure and functional expression of the rat  $\text{Na}^+/\text{H}^+$  exchanger NHE2 isoform has recently been reported (Wang, Z., Orlowski, J., and Shull, G.E., (1993) *J. Biol. Chem.* **268**; 11925-11928). To further characterize some of its functional properties, biochemical and pharmacological analyses were performed on exchanger-deficient Chinese hamster ovary cells (AP-1) that had been stably transfected with a full-length NHE2 cDNA. Transport activity for NHE2 was assayed by measuring amiloride-inhibitable  $^{22}\text{Na}^+$  influx following an acute intracellular acid load. Pharmacological analyses revealed that NHE2 had a relatively high affinity for amiloride and some of its analogues. The most potent analogue was 5-(*N*-ethyl-*N*-isopropyl)amiloride (EIPA) ( $K_{0.5} = 79$  nM), followed by 5-(*N,N*-dimethyl)amiloride (DMA) ( $K_{0.5} = 250$  nM), amiloride ( $K_{0.5} = 1.4$   $\mu\text{M}$ ), and benzamil ( $K_{0.5} = 320$   $\mu\text{M}$ ). Nonamiloride compounds known to inhibit the activity of other  $\text{Na}^+/\text{H}^+$  exchanger isoforms also inhibited NHE2 with the following order of potency: clonidine ( $K_{0.5} = 42$   $\mu\text{M}$ ) > harmaline ( $K_{0.5} = 330$   $\mu\text{M}$ )  $\approx$  cimetidine ( $K_{0.5} = 330$   $\mu\text{M}$ ). Biochemical analyses showed that the extracellular  $\text{Na}^+$  dependence of NHE2 followed simple, saturating Michaelis-Menten kinetics with an apparent affinity constant for  $\text{Na}^+$  ( $K_{\text{Na}}$ ) of 50 mM. In contrast, intracellular  $\text{H}^+$  appeared to activate NHE2 by a positive cooperative mechanism with an apparent half-maximal activation value of p*K* 6.90. Other cations, such as extracellular  $\text{Li}^+$  and  $\text{H}^+$ , acted as competitive inhibitors of  $^{22}\text{Na}^+$  influx by NHE2, with apparent  $K_i$  values of 3.0 mM and 10 nM, respectively. In contrast, extracellular  $\text{K}^+$  had no effect on the transport activity of NHE2. These results indicated that the rat NHE2 cDNA encodes a functional  $\text{Na}^+/\text{H}^+$  exchanger isoform with distinct properties compared to rat NHE1 and NHE3.

## INTRODUCTION

All mammalian cells contain an integral plasma membrane glycoprotein that mediates the electroneutral transport of extracellular  $\text{Na}^+$  in exchange for intracellular  $\text{H}^+$ . This  $\text{Na}^+/\text{H}^+$  exchanger (NHE) participates in a number of important cellular processes, including the regulation of intracellular pH and maintenance of cell volume as well as the facilitation of cell growth and proliferation in response to growth factor and mitogen stimulation. Furthermore, it is also involved in more specialized functions, such as the transepithelial absorption and secretion of electrolytes in kidney and intestine (reviewed in Refs. 4,5,81).

The diverse physiological roles fulfilled by the plasma membrane  $\text{Na}^+/\text{H}^+$  exchanger can be attributed to the existence of multiple isoforms. Prior studies have provided evidence for at least two forms of this cation transporter (8,9,16,93,174). More recently, molecular cloning studies have confirmed and extended these earlier observations by identifying four distinct members (NHE1, NHE2, NHE3, NHE4) of this gene family (27,33,34,47-49,54). The deduced amino acid sequences of these isoforms exhibit approximately 40–60% amino acid identity to each other. Northern blot analyses of rat tissues have revealed that the NHE1 mRNA is present in all tissues while the other isoforms are expressed in a more restricted range of tissues (33,47). The NHE3 transcripts are predominantly expressed in the small intestine and colon with significant levels also present in the kidney and stomach. The NHE2 and NHE4 transcripts are most abundant in the gastrointestinal tract, especially the stomach, but are also present in other tissues at lower abundance.

The functional features that distinguish these isoforms have yet to be fully elucidated. Current efforts to characterize some of their biochemical and pharmacological properties have involved the use of  $\text{Na}^+/\text{H}^+$  exchanger-deficient cells stably transfected



with the NHE1 (27,71,108,121,124) and NHE3 (108) isoforms. Based on this and other evidence (3,7,31), NHE1 is the amiloride-sensitive, growth factor-activatable exchanger that is expressed in most cells and regulates cytoplasmic pH and cell volume. In polarized epithelial cells, this isoform is generally localized to the basolateral membrane (34,45). In comparison, NHE3 has a substantially lower affinity for amiloride and exhibits many of the molecular features attributed to the  $\text{Na}^+/\text{H}^+$  exchanger present in apical membranes of renal proximal tubule epithelia (108). As such, this isoform most likely participates in the renal transepithelial reabsorption of  $\text{Na}^+$  and the luminal secretion of  $\text{H}^+$  which is necessary for  $\text{HCO}_3^-$  reabsorption.

In contrast to NHE1 and NHE3, the biochemical and pharmacological properties of the remaining two isoforms have not yet been examined in detail. We have recently shown that the rat NHE2 cDNA encodes a functional transporter capable of mediating the influx of  $^{22}\text{Na}^+$  following an acute intracellular acid load (47). The present study was initiated to further define the functional properties of this isoform with respect to its affinity for various pharmacological agents as well as extra- and intracellular cations that are known to influence  $\text{Na}^+/\text{H}^+$  exchanger activity. Here, we demonstrate that NHE2 exhibits distinct pharmacological and kinetic properties in comparison to rat NHE1 and NHE3.

## EXPERIMENTAL PROCEDURES

*Materials* – Carrier-free  $^{22}\text{NaCl}$  (5 mCi/ml) was obtained from NEN Research Products (Du Pont Canada Inc., Mississauga, Ontario). Amiloride and the amiloride analogues 5-(*N*-ethyl-*N*-isopropyl)amiloride (EIPA), 5-(*N,N*-dimethyl)amiloride (DMA), and benzamil were kindly provided by Dr. D. Pon (Merck Sharp & Dohme, Kirkland, Québec). Cimetidine, clonidine, harmaline, ouabain, bumetanide and nigericin were purchased from Sigma Chemical Co. (St. Louis, MO).  $\alpha$ -Minimal essential medium, fetal bovine serum, kanamycin sulfate, and trypsin-EDTA were from GIBCO BRL (Burlington, Ontario). Cell culture dishes and flasks were purchased from Becton-Dickenson and Co. (Fisher Scientific, Montréal, Québec). All other chemicals and reagents were from BDH Inc. (St. Laurent, Québec) or Fisher Scientific, and were of the highest grade available.

*Preparation of Pharmacological Reagents* – Stock solutions of the following compounds were prepared in dimethyl sulfoxide at the indicated concentrations: amiloride (0.5 M), EIPA (0.1 M), DMA (0.1 M), benzamil (0.1 M), bumetanide (0.1 M), cimetidine (1 M), clonidine (0.1 M), and harmaline (1 M). Ouabain was prepared as an aqueous stock at a concentration of 10 mM and nigericin was prepared as a 1 M stock in ethanol.

*Cell Culture* – A Chinese hamster ovary cell line (AP-1; a generous gift from Dr. S. Grinstein of Hospital for Sick Children, Toronto, Ontario) that is devoid of endogenous  $\text{Na}^+/\text{H}^+$  exchanger activity was stably transfected with a full-length rat NHE2 cDNA (AP-1<sup>NHE2/C12</sup>) (47). This cell line was used between passages 3 and 17. The cells were maintained in complete  $\alpha$ -minimal essential medium supplemented with 10% fetal bovine serum, 100  $\mu\text{g}/\text{ml}$  kanamycin sulfate and 25 mM  $\text{NaHCO}_3$  (pH 7.4), and incubated in an humidified atmosphere of 95% air/5%  $\text{CO}_2$  at 37 °C.

*<sup>22</sup>Na<sup>+</sup> Influx Measurements* – The cells were grown to confluence in 24-well plates. Prior to <sup>22</sup>Na<sup>+</sup> influx measurements, the cells were incubated with isotonic NH<sub>4</sub>Cl medium (50 mM NH<sub>4</sub>Cl, 70 mM choline chloride, 5 mM KCl, 1 mM MgCl<sub>2</sub>, 2 mM CaCl<sub>2</sub>, 5 mM glucose, 20 mM HEPES-Tris, pH 7.4) for 30 min at 37 °C in a nominally CO<sub>2</sub>-free atmosphere. Following preloading with H<sup>+</sup>, the cell monolayers were rapidly washed twice with isotonic choline chloride solution (125 mM choline chloride, 1 mM MgCl<sub>2</sub>, 2 mM CaCl<sub>2</sub>, 5 mM glucose, 20 mM HEPES-Tris, pH 7.4). <sup>22</sup>Na<sup>+</sup> influx assays were initiated by incubating the cells in 0.25 ml of isotonic choline chloride solution containing 1 mM ouabain and 1 μCi of <sup>22</sup>NaCl (carrier-free)/ml. The Na<sup>+</sup> concentration in the uptake solution ranged 20-30 nM, depending on the radioactive batch. The assay medium was K<sup>+</sup>-free and included ouabain to prevent the transport of <sup>22</sup>Na<sup>+</sup> catalyzed by the Na<sup>+</sup>/K<sup>+</sup>/Cl<sup>-</sup>-cotransporter and Na<sup>+</sup>/K<sup>+</sup>-ATPase. In experiments designed to examine the effect of extracellular K<sup>+</sup> on <sup>22</sup>Na<sup>+</sup> influx, the assay medium was further supplemented with 0.1 mM bumetanide to inhibit the Na<sup>+</sup>/K<sup>+</sup>/Cl<sup>-</sup>-cotransporter. Under the conditions of H<sup>+</sup> loading, the time course of <sup>22</sup>Na<sup>+</sup> influx was linear up to 10 min at low Na<sup>+</sup> concentrations at 22 °C (data not shown). Therefore, a time course of 5 min was chosen for most studies with the following exceptions.

In studies examining the kinetics of Na<sup>+</sup>/H<sup>+</sup> exchanger activity as a function of extracellular Na<sup>+</sup> concentration, the uptake of <sup>22</sup>Na<sup>+</sup> was linear for only 2 min when Na<sup>+</sup> concentration was increased to 100 mM. Hence, for these studies, an uptake time of 1 min was selected.

In studies examining Na<sup>+</sup>/H<sup>+</sup> exchanger activity as a function of intracellular pH (pH<sub>i</sub>), <sup>22</sup>Na<sup>+</sup> influx was linear for approximately 4 min. Therefore, a 2 min uptake time point was used. The pH<sub>i</sub> was set over the range of 6.0 to 8.0 using the K<sup>+</sup>-nigericin method as detailed by others (175). Briefly, the cells were washed twice with two

volumes of isotonic choline chloride solution. The cells were then incubated for 5 min at 22 °C with 0.5 ml of KCl solutions (130 mM KCl, 5 mM choline chloride, 1 mM  $\text{MgCl}_2$ , 1 mM  $\text{CaCl}_2$ , 5 mM glucose, 20 mM HEPES-Tris, and 10  $\mu\text{M}$  nigericin) that were adjusted from pH 6.0 to 8.0 at increments of 0.25 units. Under these conditions, the intracellular pH approaches that of the extracellular medium. The acid-loading was terminated by two washes of 1 ml isotonic choline chloride solution containing 5 mg/ml bovine serum albumin to scavenge the ionophore from the plasma membrane (83). The  $^{22}\text{Na}^+$  uptake assay was essentially as described above with the exception that 5 mg/ml bovine serum albumin was also present.

Measurements of  $^{22}\text{Na}^+$  influx specific to the  $\text{Na}^+/\text{H}^+$  exchanger were determined as the difference between the initial rates of  $\text{H}^+$ -activated  $^{22}\text{Na}^+$  influx in the absence and presence of 1 mM amiloride or 100  $\mu\text{M}$  EIPA and expressed as amiloride- or EIPA-inhibitable  $^{22}\text{Na}^+$  influx.

The influx of  $^{22}\text{Na}^+$  was terminated by washing the cells three times with four volumes of ice-cold isotonic saline solution (130 mM NaCl, 1 mM  $\text{MgCl}_2$ , 2 mM  $\text{CaCl}_2$ , 20 mM HEPES-NaOH, pH 7.4). The washed monolayers were solublized with 0.5 ml of 0.5 N NaOH and the wells were washed with 0.5 ml of 0.5 N HCl. Both the solublized cell extract and wash solutions were combined and radioactivity was determined by liquid scintillation spectroscopy. Protein content was determined using the Bio-Rad DC protein assay kit as per manufacturer's protocol. Each data point represents the average of at least 2 experiments, each performed in quadruplicate.

## RESULTS

*Pharmacological Properties of Rat NHE2* –  $\text{Na}^+/\text{H}^+$  exchanger isoforms are known to exhibit differential sensitivities to amiloride-based compounds. To define the amiloride analogue sensitivity of rat NHE2, the rate of  $\text{H}^+$ -activated  $^{22}\text{Na}^+$  influx was measured as a function of the concentration of amiloride, EIPA, DMA, and benzamil. The results are presented in Fig. 2.1, and the values for apparent half-maximal inhibition ( $K_{0.5}$ ) are summarized in Table I. The order of potency of these compounds was  $\text{EIPA} > \text{DMA} > \text{amiloride} \gg \text{benzamil}$  with apparent  $K_{0.5}$  values of 79 nM, 250 nM, 1.4  $\mu\text{M}$ , and 320  $\mu\text{M}$ , respectively. Comparison of rat NHE1, NHE2, and NHE3 revealed that NHE2 had intermediate sensitivity to EIPA and DMA relative to NHE1 and NHE3. Interestingly, NHE2 had the same affinity for amiloride as NHE1. Hence, amiloride cannot be used to distinguish these two isoforms.

A number of nonamiloride compounds, including cimetidine (10), clonidine (10), and harmaline (10,107), have also been reported to have significant inhibitory effects on  $\text{Na}^+/\text{H}^+$  exchanger activity. In order to assess their effects on NHE2, similar concentration-response experiments were performed. As shown in Fig. 2.2, the order of potency of these compounds was  $\text{clonidine} > \text{harmaline} \approx \text{cimetidine}$ , with values for apparent half-maximal inhibition of 42, 330, and 330  $\mu\text{M}$ , respectively. These values were generally intermediate to those found for NHE1 and NHE3 with the notable exception of clonidine which showed a 5-fold greater affinity for NHE2 than NHE1.

*Kinetic Properties of Rat NHE2* – To determine the extracellular  $\text{Na}^+$  ( $\text{Na}^+_o$ ) affinity of NHE2, the initial rates of  $\text{H}^+$ -activated  $^{22}\text{Na}^+$  influx as a function of the  $\text{Na}^+_o$  concentration were examined in AP-1<sup>NHE2/C12</sup> cells. As illustrated in Fig. 2.3, the rate of EIPA-inhibitable  $^{22}\text{Na}^+$  influx was a saturable process that conformed to simple Michaelis-Menten kinetics. Analysis of the data using the algorithm of Eadie-Hofstee (V

versus  $V/[S]$ ; Fig. 2.3, *inset*) showed a linear relationship, consistent with  $\text{Na}^+_o$  interacting at a single site. Calculation of the value of the negative slope yielded an apparent affinity constant for  $\text{Na}^+_o$  ( $K_{\text{Na}}$ ) of  $50.0 \pm 5.8$  mM. The transport activity of NHE2 was also measured as a function of intracellular pH ( $\text{pH}_i$ ). Nigericin, an ionophore that couples the transmembrane  $\text{K}^+$  and  $\text{H}^+$  gradients, was used to set the  $\text{pH}_i$  over the range of 6.0 to 8.0. The results are presented in Fig. 2.4 and expressed as a percentage of amiloride-inhibitable  $^{22}\text{Na}^+$  influx at  $\text{pH}_i$  6.0. The rates of  $\text{Na}^+/\text{H}^+$  exchange were minimally responsive to a decrease in  $\text{pH}_i$  from 8.0 to 7.5, but increased markedly thereafter as  $\text{pH}_i$  was further decreased to 6.0. An Eadie-Hofstee plot of the data is shown in Fig. 2.4 (*inset*). The analysis revealed a nonlinear distribution of the data, and suggested that NHE2 might also possess a  $\text{H}^+$ -modifier site in addition to the  $\text{H}^+_i$  transport site. However, this nonlinearity was not as well defined as that observed for NHE1 and NHE3 (108), and hence the presence of a  $\text{H}^+$ -modifier site is less apparent. The half-maximal  $\text{H}^+_i$ -activation value for the high capacity site of NHE2 was estimated to be  $\text{pK}_i$   $6.90 \pm 0.05$ . Thus, in comparison to NHE1 and NHE3, NHE2 has a substantially lower affinity for  $\text{Na}^+_o$  and slightly higher affinity for  $\text{H}^+_i$  (summarized in Table II).

*Influence of Other Extracellular Cations on Transport Activity of Rat NHE2* – The presence of certain extracellular monovalent cations, including  $\text{H}^+_o$ ,  $\text{Li}^+_o$ , and  $\text{NH}_4^+_o$ , has been shown to competitively inhibit the influx of  $^{22}\text{Na}^+$  by  $\text{Na}^+/\text{H}^+$  exchangers (83,92,100,101,108,176). However, disparate results have been reported for the influence of other monovalent cations such as  $\text{K}^+_o$  and  $\text{Cs}^+_o$ , with some studies reporting inhibition (86) while others showing no effect (83,92,100). Our recent study indicated that  $\text{K}^+_o$  can inhibit rat NHE1 activity, but not that of NHE3 (108). Thus, it was of interest to determine the influence of  $\text{H}^+_o$ ,  $\text{Li}^+_o$ , and  $\text{K}^+_o$  on the transport activity of NHE2. As shown in Fig. 2.5A, the rate of  $\text{H}^+_i$ -activated  $^{22}\text{Na}^+$  influx of AP-1<sup>NHE2/C12</sup> cells

was markedly inhibited by increasing concentrations of  $H^+_o$ , with an apparent half-maximal inhibition value of  $pK\ 7.9 \pm 0.1$ . To further define the molecular mechanism underlying  $H^+_o$  inhibition of NHE2 activity, the initial rates of 1 mM and 10 mM  $^{22}Na^+$  influx were measured as a function of the  $H^+_o$  concentration. Analysis of the data by Dixon plot ( $1/V$  versus  $[H^+]_o$ ; Fig. 2.5A, *inset*) resulted in linear lines, with the slope of the line decreasing in the presence of increased  $Na^+_o$  levels. This result indicated that  $H^+_o$  was acting as a competitive inhibitor of  $^{22}Na^+$  influx at a single site. Determination of the value for the intercept of the two lines yielded an inhibition constant ( $pK_i$ ) of  $8.00 \pm 0.12$ . To confirm this observation, the influence of different  $H^+_o$  concentrations (pH<sub>o</sub> 7.4, 7.9, and 8.4) on the rate of  $^{22}Na^+$  influx was also examined as a function of increasing  $Na^+_o$  concentration. Transformation of the data by the algorithm of Eadie-Hofstee showed that the negative slope of the line increased as the  $H^+_o$  concentration increased, indicating an increased apparent  $K_{Na}$  (*i.e.*, a decreased apparent affinity) for  $Na^+_o$  with no significant change in the maximal velocity (Fig. 2.5B). These results are again consistent with a competitive mechanism of inhibition where  $H^+_o$  and  $Na^+_o$  compete for the same extracellular binding site.

Similar conclusions were also drawn for  $Li^+_o$  inhibition of  $H^+_i$ -activated  $^{22}Na^+$  influx. As presented in Fig. 2.6B,  $Li^+_o$  inhibited  $^{22}Na^+$  influx with an apparent  $K_{0.5}$  of  $2.2 \pm 0.4$  mM. To characterize the nature of this inhibition in greater detail, the initial rates of 1 mM and 10 mM  $^{22}Na^+$  influx were measured as a function of the  $Li^+_o$  concentration. Analysis of the data by Dixon plot (Fig. 2.6A, *inset*) yielded straight lines, with the slope of the line decreasing in the presence of increased  $Na^+_o$  levels. This suggested that these cations also interacted in a competitive manner with an apparent  $K_i$  of  $3.0 \pm 0.7$  mM. To further examine this mechanism, the effect of different  $Li^+_o$  concentrations (0, 1, and 2.5 mM) on the rate of  $^{22}Na^+$  influx was measured as a function of the  $Na^+_o$  concentration. As shown in Fig. 2.6B, increasing concentrations of  $Li^+_o$  increased the apparent  $K_{Na}$  without

affecting the maximal velocity, consistent with a mechanism involving competitive inhibition. Thus the data indicated that extracellular  $H^+_o$  and  $Li^+_o$  inhibited  $^{22}Na^+$  influx by interacting at a single binding site. In contrast to  $H^+_o$  and  $Li^+_o$ , concentrations of  $K^+_o$  ranging from 1 to 100 mM had no significant effect on the initial transport rates of  $H^+$ -activated  $^{22}Na^+$  influx by AP-1<sup>NHE2/C12</sup> cells (Fig. 2.7).



## DISCUSSION

In this study, the pharmacological and kinetic properties of rat NHE2 were characterized in a heterologous expression system utilizing AP-1 cells, a mutant Chinese hamster ovary cell line devoid of endogenous  $\text{Na}^+/\text{H}^+$  exchange activity. The results revealed that the general functional properties of NHE2 are similar to those of other  $\text{Na}^+/\text{H}^+$  exchanger isoforms. However, significant differences in the affinity of NHE2 for amiloride analogues and nonamiloride compounds as well as  $\text{Na}^+_o$ ,  $\text{H}^+_o$  and  $\text{H}^+_i$  clearly distinguish this isoform from NHE1 and NHE3.

The present study demonstrated that  $\text{H}^+_i$ -activated  $^{22}\text{Na}^+$  influx of AP-1<sup>NHE2/C12</sup> cells was inhibited by amiloride and its analogues. The value for apparent half-maximal inhibition ( $K_{0.5}$ ) by amiloride was 1.4  $\mu\text{M}$  and is virtually identical to that of rat NHE1 (108). In accordance with other observations for NHE1 and NHE3 (10,97,102,108,177), the 5'-alkyl substituted analogues, EIPA and DMA, were more potent inhibitors of NHE2 than amiloride itself. Lastly benzamil, a potent inhibitor of epithelial  $\text{Na}^+$  channels (178,179) was a poor inhibitor of NHE2 activity, similar to that observed for NHE1 and NHE3. Comparison of the half-maximal inhibition constants for both EIPA ( $K_{0.5} = 79$  nM) and DMA ( $K_{0.5} = 250$  nM) indicated that rat NHE2 had intermediate affinities for these compounds relative to rat NHE1 and NHE3 (108). Thus, these two analogues provide a pharmacological means of distinguishing these three isoforms. Although the mechanism of amiloride inhibition of NHE2 was not investigated, available evidence for other  $\text{Na}^+/\text{H}^+$  exchangers strongly supports the view that amiloride competes with extracellular  $\text{Na}^+$  at the same, or a closely associated, binding site (82,86,92,100,101).

Other pharmacological agents are also known to inhibit the  $\text{Na}^+/\text{H}^+$  exchanger. Clonidine, an  $\alpha_2$ -adrenergic receptor agonist (10), was a more potent inhibitor of NHE2 than cimetidine, a histamine  $\text{H}_2$ -receptor antagonist (10), or harmaline, a hallucinogenic

drug known to inhibit amine oxidase and antagonize other  $\text{Na}^+$ -dependent transport proteins (86,107). This order of potency was similar to that found for NHE3 but the reverse of that for NHE1 (108). It was of interest to note that while most of the pharmacological agents tested tended to display a higher affinity for NHE1 relative to NHE2 and NHE3, only clonidine exhibited a significantly greater affinity for NHE2 compared to NHE1 and NHE3 (108). Overall, the pharmacological properties of rat NHE2 (Table I) clearly distinguish it from the other isoforms and provide a functional basis for its identification.

In addition to the inhibitory effects of these pharmacological agents, a number of monovalent cations are also known to antagonize the influx of  $^{22}\text{Na}^+$  via the  $\text{Na}^+/\text{H}^+$  exchanger. External  $\text{H}^+$ ,  $\text{Li}^+$  and  $\text{NH}_4^+$  have been shown to interact competitively at the  $\text{Na}^+$  binding site. Furthermore, the latter two cations can stimulate a net  $\text{H}^+$  efflux by serving as alternative substrates. Thus, the  $\text{Na}^+/\text{H}^+$  exchanger is capable of functioning in multiple exchange modes (reviewed in Ref. 81). As shown in the present study, the apparent half-maximal inhibitory constant of  $\text{Li}^+_o$  ( $K_i = 3.0 \pm 0.7 \text{ mM}$ ) for NHE2 was similar to that determined for rat NHE1 and NHE3 (108). Additional mechanistic studies demonstrated that this inhibition was competitive (Fig. 2.6A (*inset*), 2.6B). Extracellular  $\text{H}^+$  also competed with  $\text{Na}^+$  for binding at a single site on NHE2 (Fig. 2.5B). Interestingly, the affinity of  $\text{H}^+_o$  for NHE2 was an order of magnitude greater than that for NHE1 and NHE3, with an apparent  $K_i$  estimated to be  $10 \text{ nM}$  ( $\text{p}K_i = 8.00 \pm 0.12$ ). In contrast to  $\text{Li}^+_o$  and  $\text{H}^+_o$ ,  $\text{K}^+_o$  had no effect on  $\text{H}^+_i$ -activated  $^{22}\text{Na}^+$  influx mediated by NHE2. This result was similar to that found for NHE3 but opposite to that of NHE1 where  $\text{K}^+_o$  acted as a weak competitive inhibitor (108).

The  $\text{Na}^+_o$  and  $\text{H}^+_i$  dependence of  $^{22}\text{Na}^+$  influx were also characterized in AP-1<sup>NHE2/C12</sup> cells.  $\text{Na}^+/\text{H}^+$  exchanger activity has generally been found to be proportional to

the extracellular concentration of  $\text{Na}^+$ . The rate of activation of NHE2 by  $\text{Na}^+_{\text{o}}$  followed a rectangular hyperbola, consistent with simple, saturating Michaelis-Menten kinetics. Half-maximal stimulation by  $\text{Na}^+_{\text{o}}$  was attained at 50 mM, within the range of  $K_{\text{Na}}$  values (5 to 59 mM) characterized for the  $\text{Na}^+/\text{H}^+$  exchanger in various other systems (9,21,83,100,107,108,177). In comparison to rat NHE1 and NHE3 expressed in AP-1 cells (108), NHE2 exhibited a 5- and 10-fold lower affinity for  $\text{Na}^+_{\text{o}}$ , respectively. In contrast to  $\text{Na}^+_{\text{o}}$ , the  $\text{H}^+_{\text{i}}$  dependence of NHE2 did not appear to follow simple Michaelis-Menten kinetics. Eadie-Hofstee transformation of the data revealed a nonlinear plot composed of two components, although this nonlinearity was not as readily apparent as those detected for rat NHE1 and NHE3 (108). As suggested by Aronson *et al.* (93), this characteristic of the  $\text{Na}^+/\text{H}^+$  exchanger could be accounted for by the existence of a  $\text{H}^+_{\text{i}}$ -sensitive modifier site in addition to the transport site. This apparent allosteric activation by  $\text{H}^+_{\text{i}}$  can be interpreted most simply by assuming the presence of one or more ionizable groups that, upon protonation, alter the conformation of the protein and cause activation. Additional evidence supporting this paradigm was recently provided by Wakabayashi *et al.* (124) who, using deletion mutagenesis, reported that the *N*-terminal transmembrane region of human NHE1 most likely contains the  $\text{H}^+$ -modifier site while the *C*-terminal cytoplasmic domain modulates the  $\text{pH}_{\text{i}}$  set point value. Furthermore, in a related study, site-directed mutagenesis was used to identify a histidine residue ( $\text{His}^{226}$ ) as a component of the pH sensor of the Nha A isoform of the *Escherichia coli*  $\text{Na}^+/\text{H}^+$  antiporter (180). Presumably an analogous residue(s) in the mammalian  $\text{Na}^+/\text{H}^+$  exchanger fulfills a similar role. The apparent half-maximal  $\text{H}^+_{\text{i}}$ -activation value for the high capacity site of NHE2 was pK 6.90. Thus, this isoform appears to be slightly more sensitive to intracellular pH than NHE1 (pK 6.75) and NHE3 (pK 6.45) when expressed in AP-1 cells.

Comparison of the biochemical and pharmacological properties of rat NHE2 in AP-1 cells with other mammalian systems reveals a high degree of functional similarity with the endogenous  $\text{Na}^+/\text{H}^+$  exchanger present in rat thymic lymphocytes (83). This exchanger is highly sensitive to inhibition by amiloride (apparent  $K_i = 2.5 \mu\text{M}$ ) and  $\text{H}^+_{\text{o}}$  (apparent  $\text{p}K_i \approx 7.6$ ) and has a low affinity for  $\text{Na}^+$  (apparent  $K_m = 59 \text{ mM}$ ). Thus, it is conceivable that rat thymic lymphocytes express NHE2 or an NHE2-like isoform, although this remains to be verified. As well, the  $\text{Na}^+/\text{H}^+$  exchanger systems characterized in primary cultures of rat skeletal myotubes (21) and a rat smooth muscle cell line (177) exhibit affinities for amiloride analogues,  $\text{H}^+_{\text{o}}$  and  $\text{Na}^+_{\text{o}}$  that are intermediate to those determined for AP-1<sup>NHE1</sup> and AP-1<sup>NHE2</sup> cells, suggesting that these muscle cell types may express both NHE1 and NHE2. In keeping with this suggestion, RNA blot analyses of adult rat hind leg skeletal muscle and uterus have revealed moderate levels of expression of both NHE1 and NHE2 mRNAs, as well as very low amounts of NHE4 (33,47). The physiological significance of NHE2 in muscle tissue is unclear. However, the slightly higher affinity of NHE2 for intracellular  $\text{H}^+$  may possibly be important for a precise regulation of  $\text{H}^+$  in muscle tissues since several studies have demonstrated that increased intracellular  $\text{H}^+$  concentrations reduce force development in cardiac and skeletal muscles by decreasing the affinity of myofilaments for  $\text{Ca}^{2+}$  (181,182), and by reducing the actomyosin ATPase activity in smooth (183) and skeletal (184) muscles. However, while comparisons of rat NHE2 functional properties with  $\text{Na}^+/\text{H}^+$  exchanger activities in other tissues are interesting, they should be interpreted judiciously since it has been suggested that host cell regulatory influences may modulate the kinetic properties of the exchanger, particularly the set-point of the  $\text{H}^+$  modifier site (185).

In summary, the transport dynamics of NHE2 expressed in AP-1 cells are similar to that of other  $\text{Na}^+/\text{H}^+$  exchanger isoforms, although it is distinguished by its different

affinities for various pharmacological agents and extracellular and intracellular cations. The physiological function of this particular isoform remains to be established.

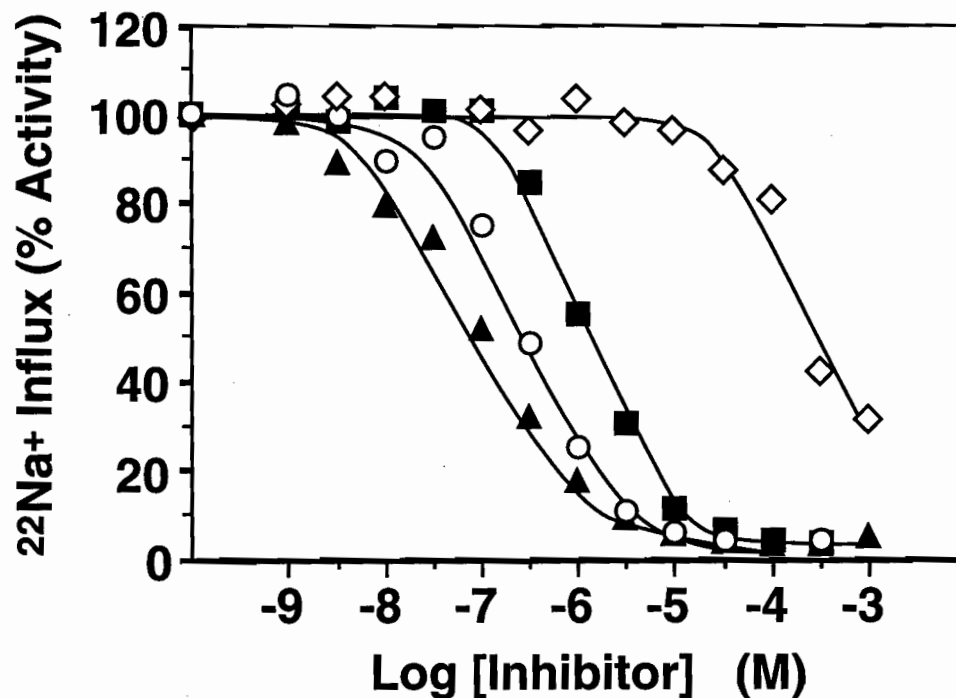


Fig. 2.1 Concentration-response profiles for inhibition of rat NHE2 transport activity in AP-1 cells by amiloride and its analogues. AP-1 cells expressing rat NHE2 (AP-1<sup>NHE2/C12</sup>) were grown to confluence in 24-well plates. Prior to  $^{22}\text{Na}^+$  influx measurements, the cells were loaded with  $\text{H}^+$  using the  $\text{NH}_4\text{Cl}$  prepulse technique. Initial rates of  $\text{H}^+$ -activated  $^{22}\text{Na}^+$  influx were measured in the presence of increasing concentrations ( $10^{-9}$  to  $10^{-3}$  M) of amiloride (*closed square*), EIPA (*closed triangle*), DMA (*open circle*), and benzamil (*open diamond*) as detailed in "Experimental Procedures." Data were normalized as a percentage of the maximal rate of  $\text{H}^+$ -activated  $^{22}\text{Na}^+$  influx in the absence of inhibitor. Values represent the average of two experiments, each performed in quadruplicate.

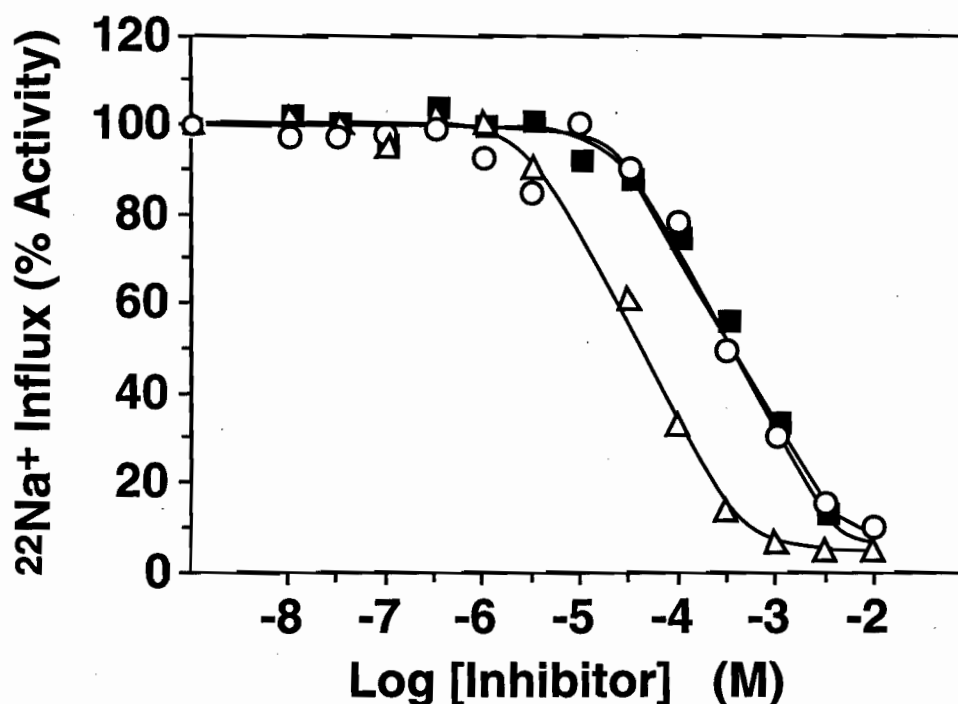


Fig. 2.2 Concentration-response profiles for inhibition of rat NHE2 transport activity in AP-1 cells by cimetidine, clonidine, and harmaline. AP-1 cells expressing rat NHE2 (AP-1<sup>NHE2/C12</sup>) were grown to confluence in 24-well plates. Prior to  $^{22}\text{Na}^+$  influx measurements, the cells were loaded with  $\text{H}^+$  using the  $\text{NH}_4\text{Cl}$  prepulse technique. Initial rates  $\text{H}^+$ -activated  $^{22}\text{Na}^+$  influx were measured in the presence of increasing concentrations ( $10^{-8}$  to  $10^{-2}$  M) of clonidine (*open triangle*), cimetidine (*open circle*), and harmaline (*closed square*). Data were normalized as a percentage of the maximal rate of rates  $\text{H}^+$ -activated  $^{22}\text{Na}^+$  influx in the absence of inhibitor. Values represent the average of two experiments, each performed in quadruplicate.

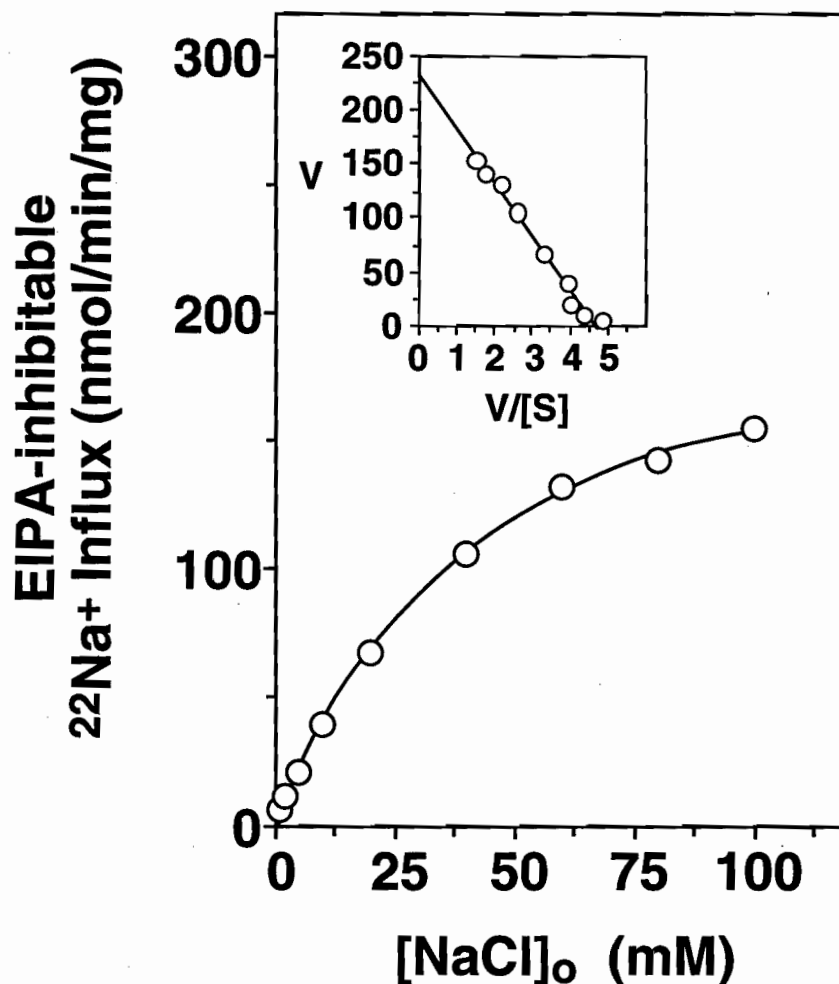


Fig. 2.3. Transport activity of rat NHE2 in AP-1 cells as a function of the extracellular  $\text{Na}^+$  concentration. AP-1<sup>NHE2/C12</sup> cells were preloaded with  $\text{H}^+$  using the  $\text{NH}_4\text{Cl}$  prepulse technique. Initial rates  $\text{H}^+$ -activated  $^{22}\text{Na}^+$  influx were measured at increasing concentrations of extracellular  $\text{Na}^+$ . Isoosmolarity was maintained by adjusting the choline chloride concentration. Low levels of background  $^{22}\text{Na}^+$  that were not inhibitable by 0.1 mM EIPA were subtracted from the total influx.  $\text{Na}^+/\text{H}^+$  exchanger activity is expressed as EIPA-inhibitable  $^{22}\text{Na}^+$  influx (nmol/min/mg protein). The apparent affinity constant ( $K_{\text{Na}}$ ) for  $\text{Na}^+_o$  was calculated from the linear transformation of the data (*inset*) according to the algorithm of Eadie-Hofstee. Values represent the average of two experiments, each performed in quadruplicate.



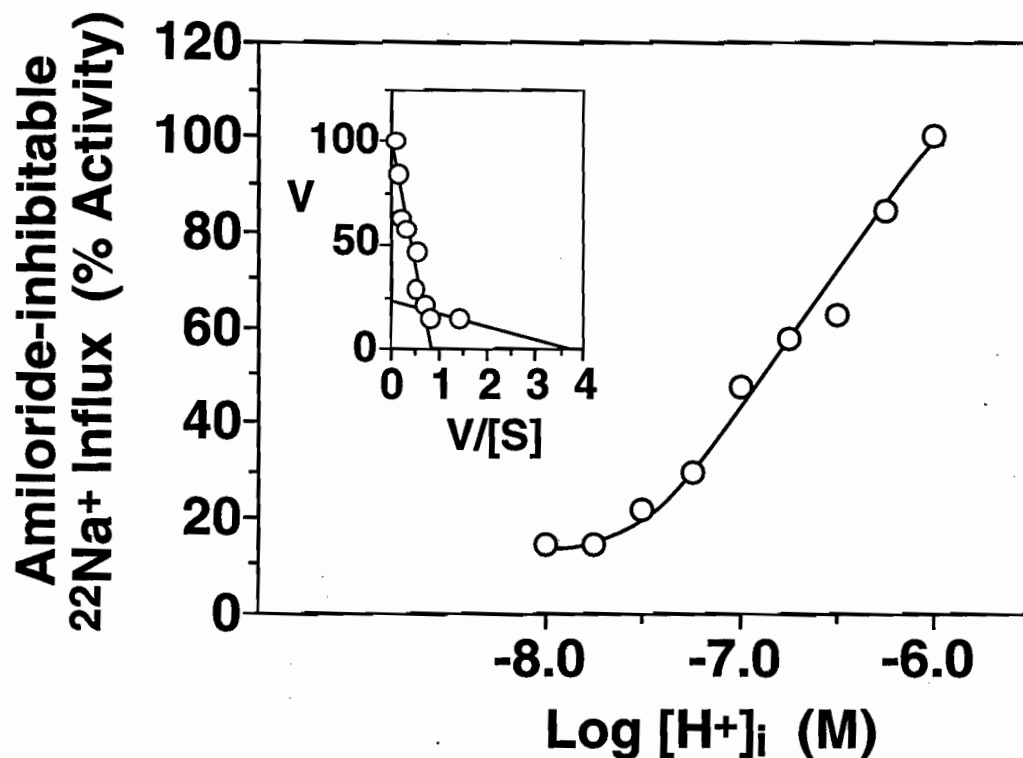
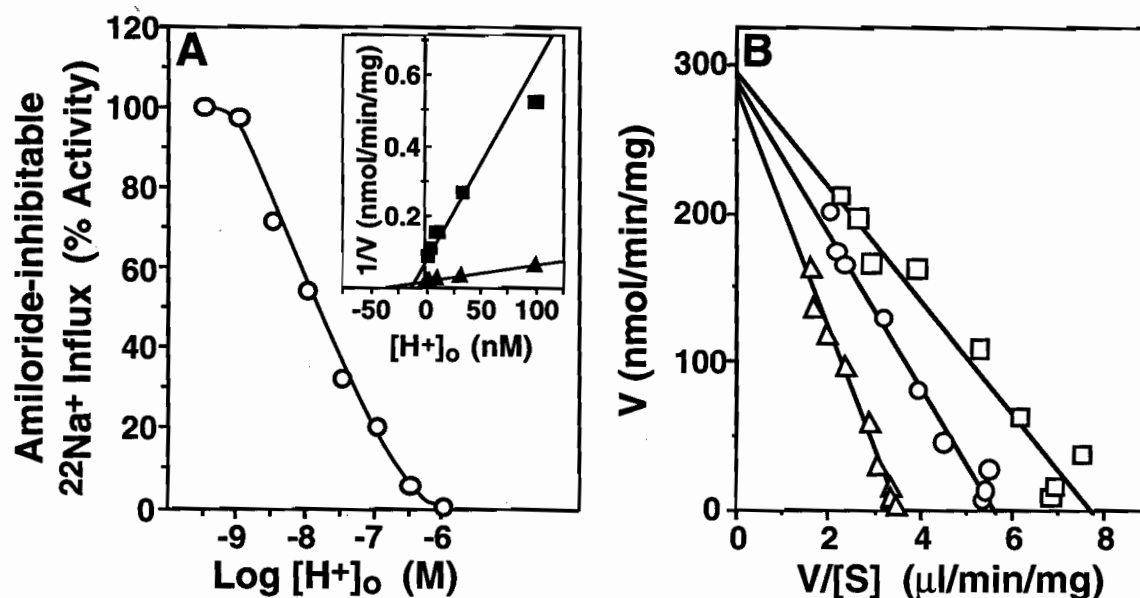


Fig. 2.4. Transport activity of rat NHE2 in AP-1 cells as a function of the intracellular  $\text{H}^+$  concentration. The initial rates of amiloride-inhibitable  $^{22}\text{Na}^+$  influx by AP-1<sup>NHE2/C12</sup> cells were measured at various intracellular  $\text{H}^+$  concentrations over the range of  $\text{pH}_i$  6.0 to 8.0. The intracellular  $\text{H}^+$  concentrations were adjusted by the  $\text{K}^+$ -nigericin method as described in "Experimental Procedures." Data were normalized as a percentage of the maximal rate of  $^{22}\text{Na}^+$  influx at  $\text{pH}_i$  6.0. The apparent affinity constant ( $K_H$ ) for  $\text{H}^+$ , was calculated from the linear transformation of the data (*inset*) according to the algorithm of Eadie-Hofstee. Values represent the average of two experiments, each performed in quadruplicate.



**Fig. 2.5. Influence of extracellular  $\text{H}^+$  on amiloride-inhibitable  $^{22}\text{Na}^+$  influx in AP-1 cells expressing rat NHE2.** *A*) AP-1<sup>NHE2/C12</sup> cells were preloaded  $\text{H}^+$  using the  $\text{NH}_4\text{Cl}$  prepulse technique. Initial rates  $\text{H}^+$ -activated  $^{22}\text{Na}^+$  influx were measured as a function of increasing extracellular  $\text{H}^+$  ( $\text{pH}_o$  6.0 to 9.5). The  $^{22}\text{Na}^+$  influx medium containing carrier-free  $^{22}\text{NaCl}$  (1  $\mu\text{Ci}/\text{ml}$ ) was buffered with 30 mM Mes-Tris (pH 6.0 to 6.5), 30 mM Mops-Tris (pH 7.0), 30 mM HEPES-Tris (pH 7.5-9.5). Data were normalized as a percentage of the maximal rate of  $^{22}\text{Na}^+$  influx at pH 9.5. The apparent  $K_i$  for  $\text{H}^+$  was determined from linearization of the rate of 1 mM (closed square) and 10 mM (closed triangle)  $^{22}\text{Na}^+$  influx (inset) according to algorithm of Dixon. *B*) Inhibition kinetics of  $\text{H}^+$  were determined for the initial rates of  $\text{H}^+$ -activated  $^{22}\text{Na}^+$  influx over a  $\text{Na}^+$  concentration range of 1.25 to 100 mM. The initial rates of  $^{22}\text{Na}^+$  influx at  $\text{pH}_o$  7.4 (open triangle), 7.9 (open circle), 8.4 (open square) were transformed by the algorithm of Eadie-Hofstee. Values represent the average of two experiments, each performed in quadruplicate.

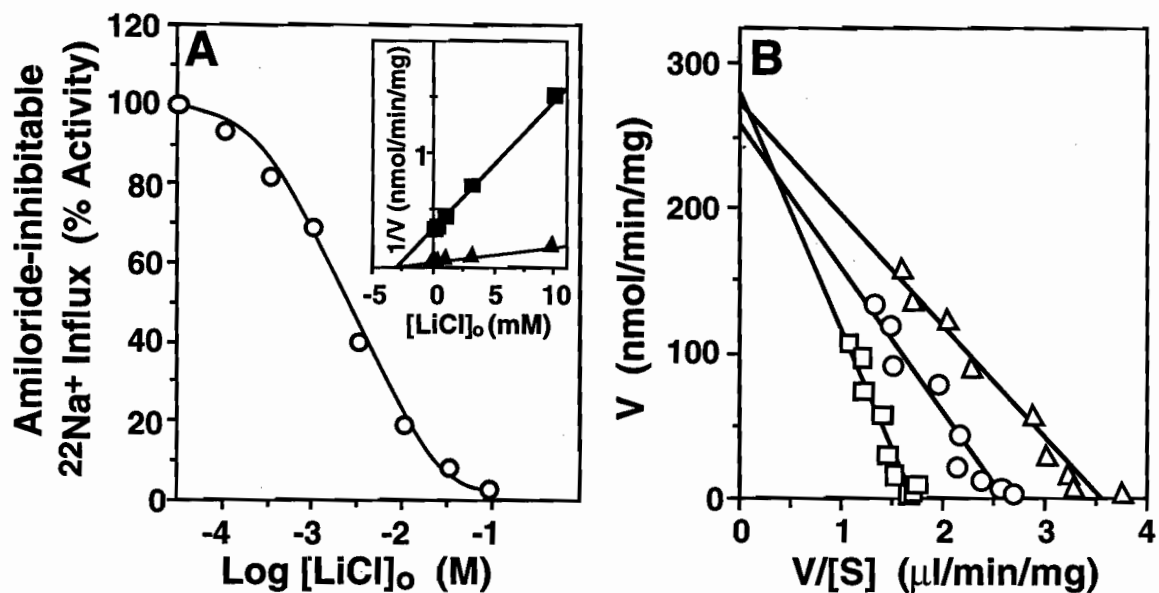


Fig. 2.6. Influence of extracellular  $\text{Li}^+$  on amiloride-inhibitable  $^{22}\text{Na}^+$  influx in AP-1 cells expressing rat NHE2. **A)** AP-1<sup>NHE2/C12</sup> cells were preloaded with  $\text{H}^+$  using the  $\text{NH}_4\text{Cl}$  prepulse technique. Initial rates of  $^{22}\text{Na}^+$  influx were measured in the presence of increasing concentrations of  $\text{Li}^+_o$  ( $10^{-4}$  to  $10^{-1}$  M). Isoosmolarity was maintained by adjusting the choline chloride concentration. Data were normalized as a percentage of the maximal rate of  $^{22}\text{Na}^+$  influx in the absence of  $\text{Li}^+_o$ . The apparent  $K_i$  for  $\text{Li}^+_o$  was determined from linearization of the rate of 1 mM (closed squares) and 10 mM (closed triangle)  $^{22}\text{Na}^+$  influx (inset) according to algorithm of Dixon. **B)** Inhibition kinetics of  $\text{Li}^+_o$  were determined for the initial rates of  $\text{H}^+$ -activated  $^{22}\text{Na}^+$  influx over a  $\text{Na}^+_o$  concentration range of 1.25 to 100 mM. The initial rates of  $^{22}\text{Na}^+$  influx in the absence of (open triangle) or presence of 1 mM (open circle) and 2.5 mM (open square)  $\text{Li}^+_o$  were transformed by the algorithm of Eadie-Hofstee. Values represent the average of two experiments, each performed in quadruplicate.

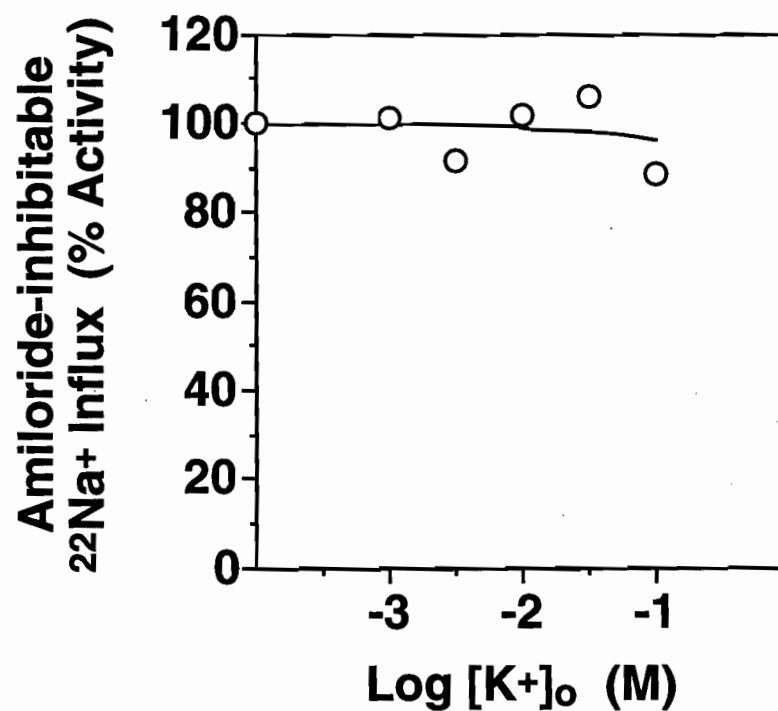


Fig. 2.7. Influence of extracellular  $K^+$  on amiloride-inhibitable  $^{22}Na^+$  influx in AP-1 cells expressing rat NHE2. AP-1<sup>NHE2/C12</sup> cells were preloaded with  $H^+$  using the  $NH_4Cl$  prepulse technique. Initial rates of  $^{22}Na^+$  influx were measured in the presence of increasing concentrations of extracellular  $K^+$  ( $10^{-3}$  to  $10^{-1}$  M). Isoosmolarity was maintained by adjusting the choline chloride concentration. Data were normalized as a percentage of the maximal rate of  $^{22}Na^+$  influx in the absence of  $K^+$ . Values represent the average of two experiments, each performed in quadruplicate.

**TABLE I**

**Comparison of the inhibition constants of the NHE1, 2, and 3 isoforms of the rat Na<sup>+</sup>/H<sup>+</sup> exchanger for amiloride and nonamiloride compounds**

Inhibitor	Inhibition Constants ( $K_{0.5}$ ) (M)		
	NHE1 <sup>a</sup>	NHE2	NHE3 <sup>b</sup>
Amiloride Compounds			
Amiloride	$1.6 \pm 0.1 \times 10^{-6}$	$1.4 \pm 0.2 \times 10^{-6}$	$1.0 \pm 0.1 \times 10^{-4}$
EIPA	$1.5 \pm 0.2 \times 10^{-8}$	$7.9 \pm 0.8 \times 10^{-8}$	$2.4 \pm 0.2 \times 10^{-6}$
DMA	$2.3 \pm 0.1 \times 10^{-8}$	$2.5 \pm 0.3 \times 10^{-7}$	$1.4 \pm 0.1 \times 10^{-5}$
Benzamil	$1.2 \pm 0.1 \times 10^{-4}$	$3.2 \pm 0.6 \times 10^{-4}$	$1.0 \pm 0.1 \times 10^{-4}$
Nonamiloride Compounds			
Cimetidine	$2.6 \pm 0.2 \times 10^{-5}$	$3.3 \pm 0.3 \times 10^{-4}$	$6.2 \pm 0.4 \times 10^{-3}$
Clonidine	$2.1 \pm 0.2 \times 10^{-4}$	$4.2 \pm 0.5 \times 10^{-5}$	$6.2 \pm 0.5 \times 10^{-4}$
Harmaline	$1.4 \pm 0.2 \times 10^{-4}$	$3.3 \pm 0.3 \times 10^{-4}$	$1.0 \pm 0.1 \times 10^{-3}$

a,b –  $K_{0.5}$  values for NHE1 and NHE3 were obtained from Ref. (108).

Values are expressed as the mean  $\pm$  S.D.

**TABLE II**

**Comparison of the affinity constants of the NHE1, 2, and 3 isoforms of the rat  $\text{Na}^+/\text{H}^+$  exchanger for various intra- and extracellular cations**

Cation	Apparent Affinity Constants ( $K_{0.5}$ )		
	NHE1 <sup>a</sup>	NHE2	NHE3 <sup>b</sup>
$\text{Na}^+_o$ (mM)	$10.0 \pm 1.4$	$50.0 \pm 5.8$	$4.7 \pm 0.6$
$\text{H}^+_i$ (pK)	$6.75 \pm 0.05$	$6.90 \pm 0.05$	$6.45 \pm 0.08$
$\text{H}^+_o$ (pK)	$7.0 \pm 0.1$	$7.9 \pm 0.1$ ( $\text{pK}_i = 8.00 \pm 0.12$ )	$7.0 \pm 0.1$
$\text{Li}^+_o$ (mM)	$3.4 \pm 0.3$	$2.2 \pm 0.4$ ( $K_i = 3.0 \pm 0.7$ )	$2.6 \pm 0.6$
$\text{K}^+_o$ (mM)	$19.5 \pm 1.3$ ( $K_i = 180 \pm 23$ )	none	none

a,b –  $K_{0.5}$  values for NHE1 and NHE3 were obtained from Ref. (108).

Values are expressed as the mean  $\pm$  S.D.

## **Chapter III.**

### **Distinct Structural Domains Confer cAMP Sensitivity and ATP Dependence to the Na<sup>+</sup>/H<sup>+</sup> Exchanger NHE3 Isoform**

Ana G. Cabado, Frank H. Yu, Andras Kapus, Gergely Lukacs, Sergio Grinstein, and John Orlowski

This study was a collaborative effort with Sergio Grinstein's research group. The design and initial experiments were carried out by F.H.Yu – more specifically the design, construction, and stable transfection of all mutant Na<sup>+</sup>/H<sup>+</sup> exchangers, as well as the radioisotopic determinations. S. Grinstein supervised the fluorimetric measurements that were carried out by A.G. Cabado and A. Kapus, as well as the immunoblot analysis done by G. Lukas. The study was coordinated and supervised by J. Orlowski.

The text and figures of this chapter were published in the *Journal of Biological Chemistry* (1996) **271**, 3590-3599.

## SUMMARY

Agents known to increase cAMP levels in renal and intestinal epithelia decrease sodium absorption by inhibiting NHE3, an isoform of the  $\text{Na}^+/\text{H}^+$  exchanger expressed at high levels in apical membranes of these cells. In contrast, the ubiquitous, housekeeping isoform of the exchanger (NHE1) is stimulated by cAMP in some cell types. To gain insight into the molecular mechanisms of ATP dependence and cAMP regulation of NHE3, a series of mutations were constructed by progressively truncating segments of the C-terminal cytoplasmic domain of the transporter at amino acid positions 684, 638, and 579 (named NHE3 $\Delta$ 684, NHE3 $\Delta$ 638, and NHE3 $\Delta$ 579). In addition, chimeric antiporters were constructed with the N-terminal transmembrane domain of NHE3 linked to the entire cytoplasmic region of NHE1 (chimera NHE3/1) or *vice-versa* (chimera NHE1/3). These constructs were heterologously expressed in antiport-deficient Chinese hamster ovary cells and their activities were assessed by fluorimetric measurements of intracellular pH and by radioisotope determinations of  $\text{Na}^+$  influx. Forskolin, which directly stimulates adenylate cyclase inhibited NHE3 as well as NHE1/3, but not NHE3/1, suggesting that the cytoplasmic domain of NHE3 was sufficient to confer sensitivity to inhibition by cAMP. Forskolin also inhibited the truncated mutant NHE3 $\Delta$ 684 to a similar extent as wild type NHE3. However, the inhibitory effect was greatly reduced in NHE3 $\Delta$ 638 and more profound truncations (NHE3 $\Delta$ 579) obliterated the effect of forskolin. These findings suggest that a region found between amino acids 579 and 684 is essential for cAMP response of NHE3. In contrast, comparable ATP dependence was observed in all exchanger constructs examined. These observations indicate that ATP dependence is conferred by a region of the molecule in or adjacent to the transmembrane domain, which is most conserved between isoforms. It is concluded that different sites, and therefore different mechanisms, underlie inhibition of NHE3 by cAMP and by depletion of ATP.



## INTRODUCTION

$\text{Na}^+/\text{H}^+$  exchange (NHE1) activity is present in virtually all mammalian cells and catalyzes the electroneutral exchange of one sodium for one proton. The exchange of  $\text{Na}^+$  for  $\text{H}^+$ , which is characteristically sensitive to inhibition by amiloride and its analogues (2,81), is driven by the concentration gradients of these ions and does not require direct expenditure of metabolic energy. Nevertheless, the presence of ATP is required for optimal exchanger activity by a mechanism that is poorly understood (18).

$\text{Na}^+/\text{H}^+$  exchanger activity is thought to be essential for pH homeostasis (5,186), transepithelial ion and water transport (13) and cell volume regulation (152), and may also play a role in cell proliferation (5) and adhesion (187,188). This functional versatility prompted the search for variant forms of the transporter. To date, five mammalian isoforms of the  $\text{Na}^+/\text{H}^+$  exchanger (NHE1 to NHE5) have been identified (27,33,47,48,61,108). The isoforms share a similar hydropathy profile that indicates the existence of two major structural domains; a predominantly hydrophobic transmembranous *N*-terminus and a more hydrophilic cytoplasmic *C*-terminus. The *N*-terminal domain, which is highly conserved among isoforms, is predicted to span the membrane 10-12 times and is believed responsible for catalyzing  $\text{Na}^+$  and  $\text{H}^+$  exchange and conferring amiloride sensitivity (17,189). The more variable *C*-terminus is thought to extend into the cytosol and to play a role in regulating the activity and subcellular distribution of the exchangers (17). It contains potential sites for phosphorylation by protein kinases and in some isoforms includes a segment with affinity for calmodulin (27,33,71,126,127).

NHE1, the "housekeeping" isoform, is present in nearly all mammalian cells examined to date. In epithelial cells, it localizes predominantly to the basolateral membrane. The other isoforms have a more restricted tissue distribution: NHE2 to NHE4

are abundant in epithelial cells of kidney, intestine and stomach whereas NHE5 resides primarily in brain, spleen and testis. Of these, NHE3 has been studied in most detail. It is restricted to the apical (brush border) membranes of some epithelial cells of the renal and gastrointestinal tracts, where it mediates  $\text{Na}^+$  reabsorption (43,57,150). In these tissues, the rate of  $\text{Na}^+$  reabsorption is variable and stringently controlled, primarily by agents that modulate the levels of adenosine 3',5'-cyclic monophosphate (cAMP). Because NHE3 is the predominant exchanger in epithelial brush border membranes, this isoform is postulated to be the direct target of the cAMP dependent protein kinase A (PKA) (137). However, direct demonstration of the regulation of NHE3 by PKA in native tissues is complicated by the coexistence of multiple isoforms in different cell types and even in different membranes of the same cell. These confounding factors can be overcome by heterologous transfection of NHE3 into cells devoid of endogenous exchanger activity. Using this approach, it has recently been demonstrated that the activity of NHE3 is markedly depressed by elevating intracellular cAMP using agents such as forskolin (141).

The molecular basis of the regulatory effects of cAMP on NHE3 is not clear. The cytosolic domain of this isoform contains several consensus sites for phosphorylation by PKA (33), some of which may mediate the observed inhibition. On the other hand, phosphorylation-independent regulation of other isoforms has been described (123,152). In an attempt to better understand the regulation of NHE3, a mutational analysis was conducted by generating a series of progressive truncations of the regulatory C-terminal domain which contains the putative phosphorylation sites. For comparative purposes, the behaviour of NHE1 was also examined since, in osteoblasts, it has been reported to be *activated* by cAMP (132). Definition of the site(s) that confer NHE3-specific sensitivity to cAMP was accomplished by creating chimeras of NHE1 and NHE3. The functional behaviour of these mutants was studied in isolation by transfection into AP-1 cells, a

Chinese hamster ovary cell line that lacks endogenous  $\text{Na}^+/\text{H}^+$  exchange (190). These transfectants were also used to analyze the structural basis of the paradoxical ATP dependence of the exchanger.

## EXPERIMENTAL PROCEDURES

*Materials, Solutions and Antibodies* – Nigericin and 2',7'-bis(2-carboxyethyl)-5(6)-carboxyfluorecein (BCECF) acetoxymethylester were from Molecular Probes, Inc. Antimycin A, deoxyglucose, pepstatin A, phenylmethanesulphonylfluoride, iodoacetamide, forskolin and amiloride were obtained from Sigma. The BCA protein assay reagent was purchased from Pierce Chemical Co. HOE694 [(3-methylsulphonyl-4-piperidinobenzoyl) guanidine methanesulphonate] was a generous gift from Hoechst, AG. Enhanced chemiluminescence reagents were from Amersham.

Polyclonal antibodies to the NHE1 isoform of the  $\text{Na}^+/\text{H}^+$  exchanger were raised by injecting rabbits with a fusion protein constructed with  $\beta$ -galactosidase of *Escherichia coli*, containing the last 157 residues (658-815) of the human NHE1. Polyclonal antibodies to the NHE3 isoform were generated against a glutathione-S-transferase fusion protein with residues 565-690 of the rat NHE3. Antibodies were affinity-purified as described (152,191).

Bicarbonate-free medium RPMI 1640 were buffered with 25 mM HEPES to pH 7.3 and adjusted to  $290 \pm 5$  mosM. Phosphate-buffered saline consisted of (in mM): 140 NaCl, 10 KCl, 8 sodium phosphate, 2 potassium phosphate, pH 7.4. The isotonic  $\text{Na}^+$ -rich medium used in the fluorimetric pH measurements contained (in mM): 140 NaCl, 3 KCl, 1  $\text{MgCl}_2$ , 10 glucose, 20 HEPES, pH 7.3. The isotonic  $\text{Na}^+$ -free medium contained the same salts, but NaCl was substituted by *N*-methyl-D-glucamine. The isotonic  $\text{K}^+$ -rich medium had the same composition as  $\text{Na}^+$ -rich medium, except that NaCl was replaced by KCl. In all cases the osmolarity was set to  $290 \pm 5$  mosM with the major salt.

*Construction of  $\text{Na}^+/\text{H}^+$  Exchanger Chimeras and Deletion Mutations* – Complementary DNA fragments of rat NHE1 (*NotI*-*NsiI* fragment, nucleotides -761 to

+3820) and NHE3 (*KpnI-SmaI* fragment, nucleotides -44 to +4288) were initially subcloned into the mammalian expression plasmid pCMV and called pCMV/NHE1 and pCMV/NHE3, respectively, as previously described (108). To facilitate the construction of Na<sup>+</sup>/H<sup>+</sup> exchanger chimeras and deletion mutants, it was necessary to remove parts of the 5' and/or 3' untranslated regions of NHE1 and NHE3 in order to create a number of useful restriction endonuclease sites. For NHE1, nucleotides -761 to -42 in the 5' untranslated region were removed by PCR mutagenesis. As well, nucleotides +3454 to +3820 in the 3' untranslated region and part of the pCMV polylinker region were eliminated by removing *XbaI-XbaI* fragment. For NHE3, nucleotides +2950 to +4288 in the 3' untranslated region and part of the polylinker were eliminated by removing an *NsiI-NsiI* fragment. A unique *EagI* restriction endonuclease site was then engineered into each cDNA by site directed mutagenesis (192) at the predicted junction between the *N*-terminal transmembranous and the *C*-terminal cytoplasmic regions. For NHE1, the introduction of an *EagI* site (CGG CCG) at amino acid positions 504-505 did not alter its coding sequence (*i.e.*, Arg-Pro). For NHE3, insertion of an *EagI* site at amino acid positions 454-455 resulted in a conservative substitution, altering its coding sequence from Lys-Pro to Arg-Pro. The cDNAs were sequenced to confirm the presence of the *EagI* site. These modified plasmids were called pNHE1 and pNHE3 (Fig. 3.1A). Chimeric Na<sup>+</sup>/H<sup>+</sup> exchangers were constructed by the reciprocal exchange of the *EagI-XbaI* fragments which comprise the entire *COOH*-terminal cytoplasmic regions of NHE1 and NHE3 to generate NHE1/3 and NHE3/1 (Fig. 3.1B). Mutations of NHE3 were also constructed by deleting segments of *COOH*-terminal cytoplasmic region according to following procedures (Fig. 3.1B): NHE3Δ684 was generated by cleaving pNHE3 with *BssHII* and removing the *BssHII-BssHII* fragment of NHE3. The resulting linear plasmid containing the *BssHII* 5' overhang ends was then blunt-ended by a fill-in reaction using Klenow, followed by cleavage of a single downstream *ApaI* site in the polylinker to remove the intervening fragment. The *ApaI* 3' overhang end was subsequently blunt-

ended by the 3' exonuclease activity of T4 DNA polymerase and the remaining linear plasmid was then re-ligated with T4 DNA ligase. This procedure resulted in NHE3 being truncated at amino acid position 684 followed by the addition of two non-native amino acids (Ile-Leu) and a TAG stop codon in the proper reading frame. NHE3 $\Delta$ 638 was generated by cleaving pNHE3 with *SacI* and removing the *SacI-SacI* fragment containing the entire coding region up to amino acid position 638. This *SacI-SacI* fragment was subcloned into a modified pCMV vector where the bulk of the multiple cloning site was removed (*Bam*HI to *Xba*I) in order to leave a unique *SacI* site. Plasmids containing the *SacI-SacI* fragment in the proper orientation relative to the CMV promoter were selected for further analysis. This procedure yielded a NHE3 truncation mutant at amino acid position 638 with the addition of two non-native amino acids (Gly-Ser) and a TAG stop codon. NHE3 $\Delta$ 579 was generated by engineering a *KasI* site in pNHE3 at amino acid positions 578-579. The modified pNHE3 was then cleaved with *KasI* and *XbaI* to remove the 3' terminal *KasI-XbaI* fragment which contained amino acids 580 to 831. The remaining linear plasmid containing 5' overhang ends were blunt-ended by a fill-in reaction using Klenow and then re-ligated with T4 DNA ligase. This procedure resulted in an in-frame TAG stop codon being placed immediately adjacent to amino acid position 579 and the penultimate amino acid being changed from Glu to Gly. The *KasI* site was not present in the other cDNA constructs. All deletion mutations were sequenced at the C-terminal ends to verify the constructions.

*Stable Transfection and Expression of the Na<sup>+</sup>/H<sup>+</sup> Exchanger Chimeric and Deletion Mutation cDNAs* – Chemically-mutagenized Chinese hamster ovary (AP-1) cells devoid of endogenous Na<sup>+</sup>/H<sup>+</sup> exchange activity (190) were transfected with plasmids containing the various Na<sup>+</sup>/H<sup>+</sup> exchanger constructs by the calcium phosphate-DNA coprecipitation technique of Chen and Okayama (193). Starting 48 h after transfection, the AP-1 cells were selected for survival in response to repeated (5-6 times over a two

week period) acute  $\text{NH}_4\text{Cl}$ -induced acid loads (30,108) in order to discriminate between  $\text{Na}^+/\text{H}^+$  exchanger positive and negative transfectants.

*Cell Culture* – Transfected cells were grown in a humidified 95% air/5%  $\text{CO}_2$  atmosphere and maintained in  $\alpha$ -MEM supplemented with 10% fetal calf serum and antibiotic (penicillin/streptomycin). Cells expressing  $\text{Na}^+/\text{H}^+$  exchanger activity were regularly selected by an acute acid challenge, as described above. This process was repeated to eliminate possible revertants and maintain stable functional expression of the exchanger.

*ATP Depletion* – For depletion of ATP, cells were incubated for 10 min in a glucose-free medium containing 100 mM potassium glutamate, 30 mM KCl, 10 mM NaCl, 1 mM  $\text{MgCl}_2$ , 10 mM HEPES (pH 7.2), 5 mM deoxyglucose plus 10  $\mu\text{g}/\text{ml}$  antimycin A as described (194). This high  $\text{K}^+$ , low  $\text{Na}^+$ , and  $\text{Ca}^{2+}$ -free medium was used to prevent  $\text{Na}^+$  and/or  $\text{Ca}^{2+}$  loading of the cells upon inhibition of the  $\text{Na}^+/\text{K}^+$  or  $\text{Ca}^{2+}$  pumps. Substitution of most  $\text{Cl}^-$  by the poorly permeant glutamate $^-$  minimizes cell swelling. This procedure reduces ATP content by > 90% (194). Control cells were incubated for the same time in potassium glutamate medium devoid of deoxyglucose and antimycin A, but containing instead 10 mM glucose.

*Measurement of  $\text{Na}^+/\text{H}^+$  Exchanger Activity* – Cytosolic pH measurements: Stably transfected cells were grown to 60-70% confluence on glass coverslips and serum starved for at least 16 h. Next, cells were incubated for 20 min in HPMI or in potassium glutamate medium (to study the effect of forskolin or ATP depletion, respectively), with 2  $\mu\text{g}/\text{ml}$  BCECF acetoxymethylester at 37 °C. Cells were pulsed with 50 mM  $\text{NH}_4\text{Cl}$  during the last 15 min of the incubation with the dye. Cells were next washed three times with  $\text{NH}_4\text{Cl}$ - and  $\text{Na}^+$ -free solution and resuspended in this medium. In order to study the sodium-dependent  $\text{pH}_i$  recovery, cells were next incubated in isotonic  $\text{Na}^+$ -rich

medium. To measure the fluorescence of BCECF, the coverslip was placed in a thermostatted Leiden holder on the stage of a Nikon TMD-Diaphot microscope equipped with a Nikon Fluor 40X oil-immersion objective. An Empix Imaging filter wheel was used to alternately position the two excitation filters ( $500 \pm 10$  nm and  $440 \pm 10$  nm) in front of a xenon lamp. In order to minimize dye bleaching and photodynamic damage, neutral density filters were used to reduce the intensity of the excitation light reaching the cells. The excitation light was directed to the cells via a 510 nm dichroic mirror and fluorescence emission was collected by a  $535 \pm 25$  nm band-pass filter. Data were recorded every 10 sec by irradiating the cells for 500 ms at each of the excitation wavelengths. The fluorescence image was captured on a Star 1 liquid-cooled CCD camera (Photometrics Ltd.), then downloaded to a Dell 486 computer where the Metafluor Imaging System software from Universal Imaging Corp. was used to acquire and ratio the two images created by dual excitation.

Calibration of the fluorescence ratio *versus* pH was performed for each experiment by equilibrating the cells in isotonic  $K^+$ -rich medium buffered to varying pH values (between 7.45 and 5.85) in the presence of the  $K^+/H^+$  ionophore nigericin ( $5 \mu M$ ). Calibration curves were constructed by plotting the extracellular pH, which is assumed to be identical to the internal pH, against the corresponding fluorescence ratio (175).

Cellular buffering power was determined in the  $pH_i$  range studied by pulsing cells with weak electrolytes, as described (1).  $H^+$  efflux rates (mM/s) were calculated by multiplying the rate of  $pH_i$  recovery ( $dpH_i/dt$ ) times the buffering capacity, at the corresponding pH values.  $Na^+/H^+$  exchange rates were analyzed using the general allosteric model described by the Hill equation shown in Equation 1.



$$V/(V_{\max} - V) = K[S]^n$$

or

(Eq.1)

$$V = (V_{\max} \cdot [S]^n) / (K^{-1} + [S]^n)$$

V is the H<sup>+</sup> (equivalent) efflux at a particular cytosolic H<sup>+</sup> concentration [S]; V<sub>max</sub> is the maximal H<sup>+</sup> efflux rate, and n, is the Hill coefficient, a minimal estimate of the number of binding sites for H<sup>+</sup>. Though n was greater than 1, data were adequately fit using a single intrinsic binding constant, K, suggesting that the affinities of the individual sites were of the same order. Experimental results were fit to the above model using a nonlinear regression data analysis program, Enzfitter from Bios Corp.

*Measurement of <sup>22</sup>Na<sup>+</sup> Influx* – Na<sup>+</sup>/H<sup>+</sup> exchanger activity was also measured as the rate of amiloride-inhibitable <sup>22</sup>Na<sup>+</sup> influx at a constant intracellular H<sup>+</sup> concentration. For these studies, pH<sub>i</sub> was set at 6.3 by incubating confluent cell monolayers on 24-well plates in medium containing the appropriate K<sup>+</sup> concentration and the K<sup>+</sup>/H<sup>+</sup> exchange ionophore nigericin (175). Since at equilibrium [K<sup>+</sup>]<sub>i</sub>/[K<sup>+</sup>]<sub>o</sub> = [H<sup>+</sup>]<sub>i</sub>/[H<sup>+</sup>]<sub>o</sub>, the desired pH<sub>i</sub> was calculated from the imposed [K<sup>+</sup>] gradient and the extracellular pH (pH<sub>o</sub> = 7.4), assuming an intracellular [K<sup>+</sup>] of 140 mM. To clamp pH<sub>i</sub> at 6.3, the cell monolayers were first washed with a N-methyl-D-glucamine<sup>+</sup>-balanced salt solution and then preincubated in a K<sup>+</sup>-nigericin solution containing 153 mM N-methyl-D-glucamine chloride, 11.2 mM KCl, 2 mM NaCl, 1 mM MgCl<sub>2</sub>, 10 μM nigericin, 10 mM HEPES, pH<sub>o</sub> 7.4 for 3 min at room temperature. This solution was then removed and <sup>22</sup>Na<sup>+</sup> influx measurements were initiated in the same K<sup>+</sup>-nigericin solution supplemented with 1 μCi <sup>22</sup>NaCl/ml (~20-30 nM Na<sup>+</sup>) and 1 mM ouabain (to inhibit Na<sup>+</sup>/K<sup>+</sup>-ATPase and minimize <sup>22</sup>Na<sup>+</sup> efflux) in the absence or presence of 2 mM amiloride. <sup>22</sup>Na<sup>+</sup> influx was terminated after 10 min by aspirating the radiolabeled medium and rapidly washing the cells 3 times with ice-cold NaCl stop solution (130 mM NaCl, 1 mM MgCl<sub>2</sub>, 2 mM CaCl<sub>2</sub>, 20 mM HEPES-NaOH, pH 7.4). To extract the radiolabel, 0.25 ml of 0.5N NaOH was added to each well and the

wells were washed with 0.25 ml of 0.5N HCl. Both the solublized cell extract and wash solutions were suspended in 5 ml scintillation fluid and the radioactivity assayed by liquid scintillation spectroscopy.  $^{22}\text{Na}^+$  influx was linear for at least 10 min under these experimental conditions.

*Membrane Isolation* – Cells grown to 80-90% confluence on 10 cm dishes and washed three times with ice-cold phosphate buffered saline. Next, cells were scraped into a hypotonic solution containing 10 mM HEPES, 18 mM potassium acetate, 1 mM EDTA, 1  $\mu\text{M}$  phenylmethylsulphonylfluoride and 1 mM iodoacetamide (pH 7.2) and homogenized by 50 strokes of a Dounce homogenizer. The lysate was centrifuged at 1000 Xg for 5 min to remove nuclei and incompletely broken cells and the resulting supernatant was sedimented at 100,000 xg for 60 min at 4 °C. The resulting microsomal pellet was resuspended in Laemmli sample buffer for electrophoresis.

*SDS-Polyacrylamide Gel Electrophoresis and Immunoblotting* – To assess the expression of the gene products, immunoblotting was carried out using polyclonal antibodies against NHE1 and NHE3. Samples containing 25  $\mu\text{g}$  of membrane protein were subjected to electrophoresis in 7.5% acrylamide gels and transferred to nitrocellulose. Blots were blocked with 0.2% gelatin and exposed to one of the primary polyclonal anti-NHE antibodies described above. Affinity-purified antibodies against human NHE1 (residues 658-815) and NHE3 (residues 565-690) were used at 1:5000 dilution. The secondary antibody, goat anti-rabbit coupled to horseradish peroxidase, was applied at 1:5000 dilution. Immunoreactive bands were visualized using enhanced chemiluminescence (Amersham Corp.).

## RESULTS

*Structural Analysis of the Regulation of NHE3 by cAMP* – A series of truncated mutants and chimeras was used to define the structural basis of the inhibitory effect of cAMP on the activity of NHE3. These are diagrammatically illustrated in Fig. 3.1. The mammalian expression plasmids containing the parental rat  $\text{Na}^+/\text{H}^+$  exchanger isoforms NHE1 and NHE3 are shown in *panel A*. The diagram includes the relevant restriction endonuclease sites used in the construction of the deletion mutants of NHE3 and NHE1/NHE3 chimeras. *Panel B* of Fig. 3.1 illustrates the linear profiles and nomenclature used to designate the resulting truncation and chimeras.

$\text{Na}^+/\text{H}^+$  exchange was initially assessed fluorimetrically in cells treated with or without forskolin, an agent that stimulates adenylate cyclase and increases intracellular cAMP. No attempt was made to compare the absolute rates of transport between stable transfectants, which can reflect parameters other than the length of construct, such as the site(s) of genomic integration, the number of incorporated cDNA copies per cell and differences in intracellular processing of mutated proteins. Acid-loaded cells were exposed to  $\text{Na}^+$  and the rate of recovery of  $\text{pH}_i$  was used as a measure of exchanger activity. It is noteworthy that in all cases the rate of alkalization was negligible in the absence of  $\text{Na}^+$ . As shown in Fig. 3.2A, untreated cells transfected with the full-length NHE3 recovered readily from the acid load upon reintroduction of  $\text{Na}^+$  (*solid circles*). Consistent with observations in renal proximal tubule cells (25,41), pretreatment with forskolin markedly depressed the activity of NHE3 (*open circles*). To more precisely evaluate the mechanism of inhibition, the rate of  $\text{Na}^+/\text{H}^+$  exchange was estimated at varying  $\text{pH}_i$ .  $\text{H}^+$  (equivalent) fluxes were calculated from the rate of change of  $\text{pH}_i$  ( $\Delta\text{pH}/\Delta t$ ) and the buffering power, determined independently throughout the pH range studied. As summarized in Fig. 3.2B, the  $\text{H}^+$  efflux rate in control cells was highest at

acidic  $\text{pH}_i$  and decreased thereafter approaching quiescence near pH 6.8. As described in isolated renal brush borders (93), the exchange process showed cooperativity with respect to  $\text{H}^+$ . The data were fit adequately by the Hill equation (Fig. 3.2B, *inset*), yielding a coefficient of  $\sim 3$ . Treatment with 10  $\mu\text{M}$  forskolin (141) reduced  $\text{Na}^+/\text{H}^+$  exchange activity at all  $\text{pH}_i$  values tested. Importantly, the  $\text{pH}_i$  dependence of the exchanger was shifted to more acidic  $\text{pH}_i$  by nearly 0.4 units. The Hill coefficient was not markedly different when cAMP was elevated ( $\sim 2.7$ ), suggesting that cooperativity with respect to  $\text{H}^+$  persisted under these conditions. Therefore, the effect of cAMP appears to be largely due to a reduced affinity for intracellular H. The effect of cAMP on  $V_{\text{max}}$  could not be properly assessed due to insufficient data points below pH 6.0. Such data were not collected because of concerns regarding potential cellular damage caused by extreme acidic conditions. Prolonged exposure to acidic intracellular pH can fix or cause CHO cells to lift off the tissue culture dishes (unpublished observations, F.H. Yu, and J. Orłowski). In this figure the data are means  $\pm$  SE of 27/54 (control/treated) individual determinations.

The inhibitory effect of forskolin on NHE3 was confirmed by measuring amiloride-sensitive  $\text{Na}^+$  uptake. As illustrated in Fig. 3.3A, activation of the adenylate cyclases reduced influx by nearly 50% at  $\text{pH}_i$  6.3, in good agreement with the fluorescence determinations of  $\text{pH}_i$ .

The behaviour of the  $\Delta 684$  truncation was almost indistinguishable from that of the full length NHE3. As shown in Fig. 3.2 (C and D), this mutant displayed similar recovery rates, a sharp  $\text{pH}_i$  dependence and cooperativity with a Hill coefficient of  $\sim 2.6$ . Importantly, NHE3 $\Delta 684$  was also susceptible to inhibition by cAMP which, as in wild type NHE3, was manifested as an acidic shift in the activation threshold. The data are means  $\pm$  SE of 34/27 (control/treated) individual determinations.  $^{22}\text{Na}^+$  uptake

determinations also reflected the inhibitory effect. The isotope influx rates were over 60% lower in the forskolin treated samples (Fig. 3.3A). Together, these findings imply that the C-terminal 147 amino acids are not required for the cAMP response.

Truncation at amino acid 638 had little effect on the basal functional behaviour of untreated cells, but greatly reduced its responsiveness to cAMP. The activation threshold and cooperativity of unstimulated NHE3 $\Delta$ 638 were similar to those of the full length NHE3 (Fig. 3.2E and F; Hill coefficient  $\sim 2$ ). However, the inhibitory effect of forskolin was only marginal in this mutant, with a small divergence noted primarily at higher pH. In this figure the data are means  $\pm$  SE of 35/27 (control/treated) individual determinations. The reduced effectiveness of forskolin was also apparent when activity was assessed radioisotopically (Fig. 3.3A).

A further loss of responsiveness was noted in the NHE3 $\Delta$ 579 truncated mutant. The absolute recovery rates of these cells were low (note time scale in Fig. 3.2G), precluding detailed analysis at near neutral pH<sub>i</sub>. Nevertheless, in the range where the measurements were reliable elevation of cAMP did not inhibit exchange. In fact, a slight stimulatory effect was recorded. The data are means  $\pm$  SE of 37/31 (control/treated) individual determinations. The loss of susceptibility to forskolin was also noted when  $^{22}\text{Na}^+$  uptake was measured (Fig. 3.3A). The influx rates with and without forskolin were indistinguishable. In summary, the region encompassed by residues 579 and 684 appears to play a central role in mediating the inhibitory action of cAMP.

*Structural Analysis of the Regulation of NHE3 by ATP* – As described initially for NHE1, depletion of cellular ATP induces a pronounced inhibition of NHE3 activity (Fig. 3.4A and Ref. 53). In the pH<sub>i</sub> range investigated, the rate of H<sup>+</sup> efflux of the full length exchanger is almost eliminated upon metabolic depletion. The data are means  $\pm$  SE of 51/72 (control/treated) individual determinations. The extent of the inhibition was also

apparent when measuring  $^{22}\text{Na}^+$  influx (Fig. 3.3B), which showed only marginal uptake in depleted cells. As shown in Fig. 3.4B, the  $\text{pH}_i$  dependence of the exchanger undergoes a large acid shift under these conditions, with quiescence attained near  $\text{pH}_i$  6.2. The cooperative behaviour towards  $\text{H}^+$  (Hill coefficient  $\sim 2.8$ ), was preserved following ATP depletion. It must be pointed out, however, that the need to calculate the maximal velocity by iteration in profoundly inhibited samples makes these estimates less accurate.

The inhibitory effect of ATP depletion was preserved in NHE3 $\Delta$ 684 truncated mutants. The data are means  $\pm$  SE of 20/20 (control/treated) individual determinations. Internally consistent results are obtained when  $\text{pH}_i$  recoveries were measured fluorimetrically (Fig. 3.4C and D) and when  $\text{Na}^+$  uptake was determined radioisotopically (Fig. 3.3B). Similarly, a profound inhibition of  $\text{H}^+$  extrusion (Fig. 3.4F and H)<sup>1</sup> and  $\text{Na}^+$  influx (Fig. 3.3B) was noted when NHE3 $\Delta$ 638 and NHE3 $\Delta$ 579 transfectants were subjected to the ATP depletion protocol. In this figure the data are means  $\pm$  SE of 61/59 and 47/29 (control/treated) individual determinations, respectively. Thus, unlike the effect of cAMP, the inhibition induced by metabolic depletion remains essentially unaffected when most of the cytosolic tail of the exchanger has been deleted.

#### *cAMP Sensitivity and ATP Dependence of NHE3 and NHE1 chimeric exchangers –*

The behaviour of the full-length NHE3 and NHE1 towards challenge with cAMP is diametrically opposed: the former is inhibited, while the latter is stimulated. This divergence provides a convenient system to test the structural conclusions derived from analysis of the truncated mutants. To this end, we constructed two chimeras: one was composed of the transmembrane domain (residues 1-504) of NHE1 and the cytosolic tail (residues 456-831) of NHE3 (designated NHE1/3) (see Fig. 3.1). The reciprocal chimera

---

<sup>1</sup> The absolute rate of the  $\text{pH}_i$  recovery for NHE3 $\Delta$ 638 was found to be much higher in cells preincubated in  $\text{K}^+$ -glutamate medium compared to HPMI (*cf.*, Figs. 3.2E and 3.4E). While we do not have a definitive explanation for this observation, it is possible that this mutant is more sensitive to the presence of chloride than the other truncation mutants.

was also constructed with the transmembrane domain (residues 1-455) of NHE3 and the cytosolic tail (residues 505-820) of NHE1 (designated NHE3/1).

The expression of the chimeras was probed using antibodies directed to the cytosolic domains of either NHE1 or NHE3 (see "Experimental Procedures"). As shown earlier, anti-NHE1 antibodies recognized a wide band of approximately 110 kDa in NHE1 transfected AP-1 cells (Fig. 3.5A). The width of this band has been attributed to carbohydrate heterogeneity (77). The specificity of the antibody is indicated by its failure to react with NHE3 or with the NHE1/3 chimera. However, positive reactivity was detected in the NHE3/1 chimera, supporting the presence of the cytosolic domain of NHE1. Interestingly, the immunoreactive band was sharper and had a molecular mass of ~ 80 kDa, similar to that of NHE3, which unlike NHE1 is apparently not glycosylated (74). This observation is consistent with the notion that the transmembrane domain of the chimera is that of NHE3.

The immunoreactivity of the NHE3 antibody was weaker and therefore required longer exposure times. This intensified two nonspecific bands of ~75 and 110 kDa, which were present in all samples. Nevertheless, a band of 80 kDa was also discernible in NHE3 transfectants, as expected. In the NHE1/3 cells, an additional reactive band of 105-110 kDa was seen, but not in the NHE3/1 transfectants. The higher molecular weight of the latter band suggests glycosylation of the NHE1 transmembrane domain. These findings are compatible with the predicted primary structure of the chimeras.

Additional confirmation of the composition of the chimeric constructs was obtained using amiloride and a substituted benzoyl guanidine, compound HOE694. These inhibitors are thought to act externally on the *N*-terminal transmembrane region of the protein (77). More importantly, the isoforms are differentially sensitive to these drugs. As illustrated in Fig. 3.6, NHE1 activity was almost entirely inhibited by 1  $\mu$ M HOE694,

in agreement with the inhibitory constant ( $K_i = 0.16 \mu\text{M}$ ) reported in an earlier study (104). Similar inhibition was observed when NHE1 transfectants were exposed to 1 mM amiloride (Fig. 3.6). In contrast, a much higher concentration of HOE694 (500  $\mu\text{M}$ ) produced only a modest inhibition of NHE3. The nearly complete inhibition obtained with 1 mM amiloride indicates that the HOE694-resistant component of  $\text{H}^+$  transport is mediated by the exchanger (Fig. 3.6).

The inhibitor sensitivity of the NHE1/3 chimera was virtually identical to that of NHE1, implying that the two exchanger constructs share a common transmembrane domain. Conversely, the NHE3/1 chimera was resistant to 1  $\mu\text{M}$  HOE694, resembling the behaviour of NHE3. Together with the immunoblotting data of Fig. 3.5, these pharmacological findings confirm the composition of the chimeric constructs.

The sensitivity of the chimeras to forskolin and to ATP depletion was tested next. NHE1/3 transfectants displayed cooperativity towards  $\text{H}^+$  (Hill coefficient  $\sim 2.3$ ) and had a set point near  $\text{pH}_i$  7.0. Treatment of this chimera with forskolin resulted in a moderate inhibition of transport and was only noticeable at more acidic  $\text{pH}_i$  (Fig. 3.7A and B). In this figure the data are means  $\pm$  SE of 24/20 (control/treated) individual determinations. The occurrence of a small yet significant inhibition was confirmed by measuring  $^{22}\text{Na}^+$  uptake (Fig. 3.9A). In contrast, the NHE3/1 chimera was not inhibited by cAMP. Only a small, insignificant stimulation was noted at more alkaline  $\text{pH}_i$  (Fig. 3.7C and D). The data are means  $\pm$  SE of 20/24 (control/treated) individual determinations. Again, determinations of  $^{22}\text{Na}^+$  influx yielded consistent results (Fig. 3.9A). These findings confirm that the transmembrane region of NHE3 is not sufficient to confer sensitivity to inhibition by forskolin. Moreover, the results of Fig. 3.7A and B imply that while the cytosolic tail of NHE3 is necessary for the response, the participation of other regions of



the protein is likely required to fully mimic the inhibitory effect observed in wild type NHE3.

The ATP dependence of transport by the chimeras was also tested. Both the NHE3/1 and the NHE1/3 constructs were severely inhibited when the cells were depleted metabolically. The data are means  $\pm$  SE of 34/42 and 22/20 (control/treated) individual determinations, respectively. The inhibition was apparent when both  $H^+$  extrusion (Fig. 3.8) and  $Na^+$  influx was measured (Fig. 3.9*B*). For both chimeras, inhibition appeared to be mediated by a leftward displacement of the  $pH_i$  dependence of the rate of transport, as found for the full-length parental exchangers.

## DISCUSSION

Sodium and bicarbonate reabsorption in renal and intestinal epithelial cells is mediated mainly by  $\text{Na}^+/\text{H}^+$  exchange across their apical membranes. The isoform of the exchanger responsible for this exchange is believed to be NHE3. This isoform has a higher affinity for Na, and is substantially less sensitive to amiloride derivatives and HOE694 than the housekeeping NHE1 (108). The differential sensitivity to HOE694 was confirmed in the heterologous expression model illustrated in Fig. 3.6. Moreover, complementary chimeras constructed with NHE3 and NHE1 indicated that the transmembrane domain suffices to dictate the degree of sensitivity to these inhibitors. This conclusion is in good agreement with earlier findings that identified unique residues within the transmembrane domain as important determinants of the affinity for amiloride and its analogs (189,195).

*Regulation by cAMP* – Epithelial sodium and bicarbonate reabsorption is stringently controlled by a number of variables, including hormones that elevate the cytosolic concentration of cAMP (196). These effects are thought to be mediated by modulation of the activity of NHE3 in renal cells. Accordingly, forskolin was recently reported to inhibit amiloride-sensitive  $\text{Na}^+$  uptake in cells transfected with NHE3 (141), an observation reproduced in present studies (Figs. 3.2 and 3.3). It was therefore of interest to understand the structural basis of the regulation of NHE3 by cAMP. To this end, the responsiveness of a series of NHE3 chimeras and deletion mutants stably expressed in exchanger-deficient AP-1 cells to forskolin treatment was analyzed.

Inhibition of exchanger activity persisted in the NHE1/3 chimera, which contains the C-terminal cytoplasmic domain of NHE3, but was not observed in the reciprocal chimera, NHE3/1. These findings imply that the cytoplasmic domain of NHE3 is required for cAMP to exert its inhibitory action. This conclusion was confirmed by

deletion studies. Truncation of NHE3 at position 579 similarly prevented modulation by forskolin (Figs. 3.2 and 3.3). However, only a fraction of the cytoplasmic tail is essential for the cAMP effect, since the inhibition was intact following truncation of NHE3 at position 684. Loss of responsiveness occurred in two stages: partial effects were seen in NHE3 $\Delta$ 638, while complete unresponsiveness was apparent in NHE3 $\Delta$ 579. This behaviour is suggestive of multiple target sites for cAMP, resembling the reported behaviour of  $\beta$ NHE, the trout red cell isoform of the exchanger that is also responsive to cAMP. However, unlike NHE3,  $\beta$ NHE is stimulated by cAMP and has two distinct sites that are substrates for phosphorylation by PKA (38). Elimination of these sites greatly reduces but does not abolish the stimulatory effect of cAMP (135). It is noteworthy that  $\beta$ NHE has the highest homology to the mammalian NHE1 isoform which is also stimulated by cAMP in certain cell types (132).

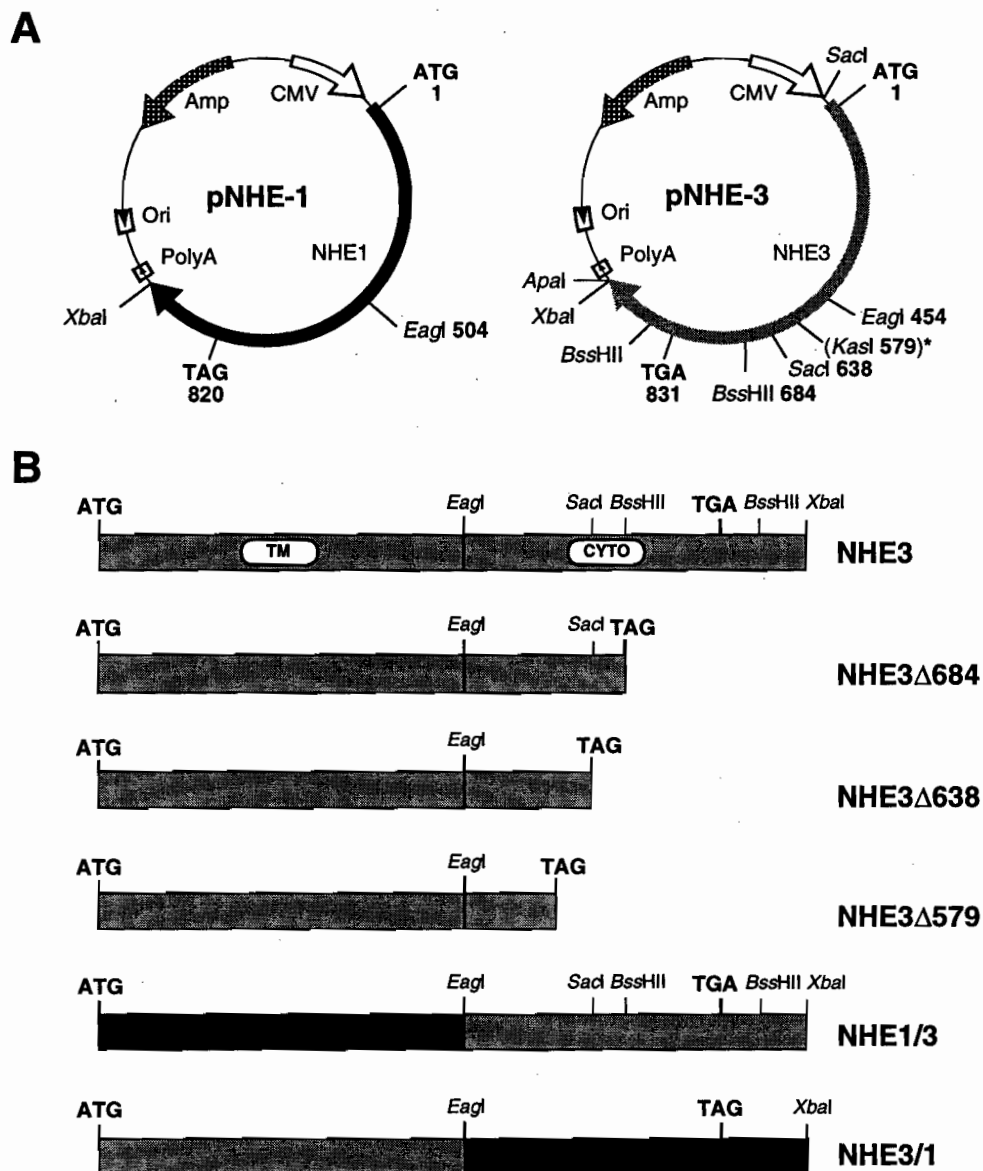
NHE3 differs from  $\beta$ NHE in that loss of responsiveness to forskolin occurs upon deletion of residues 579-684, a region that does not contain the optimal consensus sequence (R-R/K-X-S\*/T\*) for PKA phosphorylation (197). However, phosphorylation of this region by PKA may occur at variant sites (R-X<sub>2</sub>-S\*/T\* or R-X-S\*/T\*) such as RELS<sup>661</sup> or RRRS<sup>605</sup>IR, which more closely resemble a classical PKC consensus sequence ((R/K<sub>1-3</sub>, X<sub>2-0</sub>)-S\*/T\*-(X<sub>2-0</sub>, R/K<sub>1-3</sub>)) (197). In this regard, it is noteworthy that Levine *et al.* (142) recently demonstrated that the same region of NHE3 mediates inhibition of the rabbit homologue by PKC, which kinetically resembles the effect of PKA. Alternatively, it is conceivable that the structure or disposition of the 579-684 domain changes upon phosphorylation of potential upstream targets (*e.g.*, RRS<sup>520</sup>, RRGs<sup>552</sup>, RPS<sup>575</sup>), thereby contributing to the transduction of the inhibitory signal. It is also possible that NHE3 may not be directly phosphorylated by PKA, in which case ancillary cAMP-sensitive regulatory protein(s) may be the target of the kinase. This notion is supported by the recent discovery of a soluble cytoplasmic protein required for inhibition of Na<sup>+</sup>/H<sup>+</sup>

exchange by cAMP in renal brush border vesicles (144,145) More detailed studies to test these hypotheses are currently ongoing in order to precisely delineate the molecular mechanism responsible for cAMP-dependent regulation of NHE3.

*Regulation by ATP* – NHE1 was initially found to be inhibited by depletion of cellular ATP, despite the passive (thermodynamic downhill) nature of the exchange process (191). Subsequent studies demonstrated that the two other isoforms analyzed this far, NHE2 and NHE3, are similarly dependent on ATP (53). While the extent of inhibition differs somewhat between isoforms, the general pattern is comparable, suggesting similar underlying mechanisms. In accordance with this notion, the NHE1/3 and NHE3/1 chimeras were both susceptible to inhibition by metabolic ATP depletion.

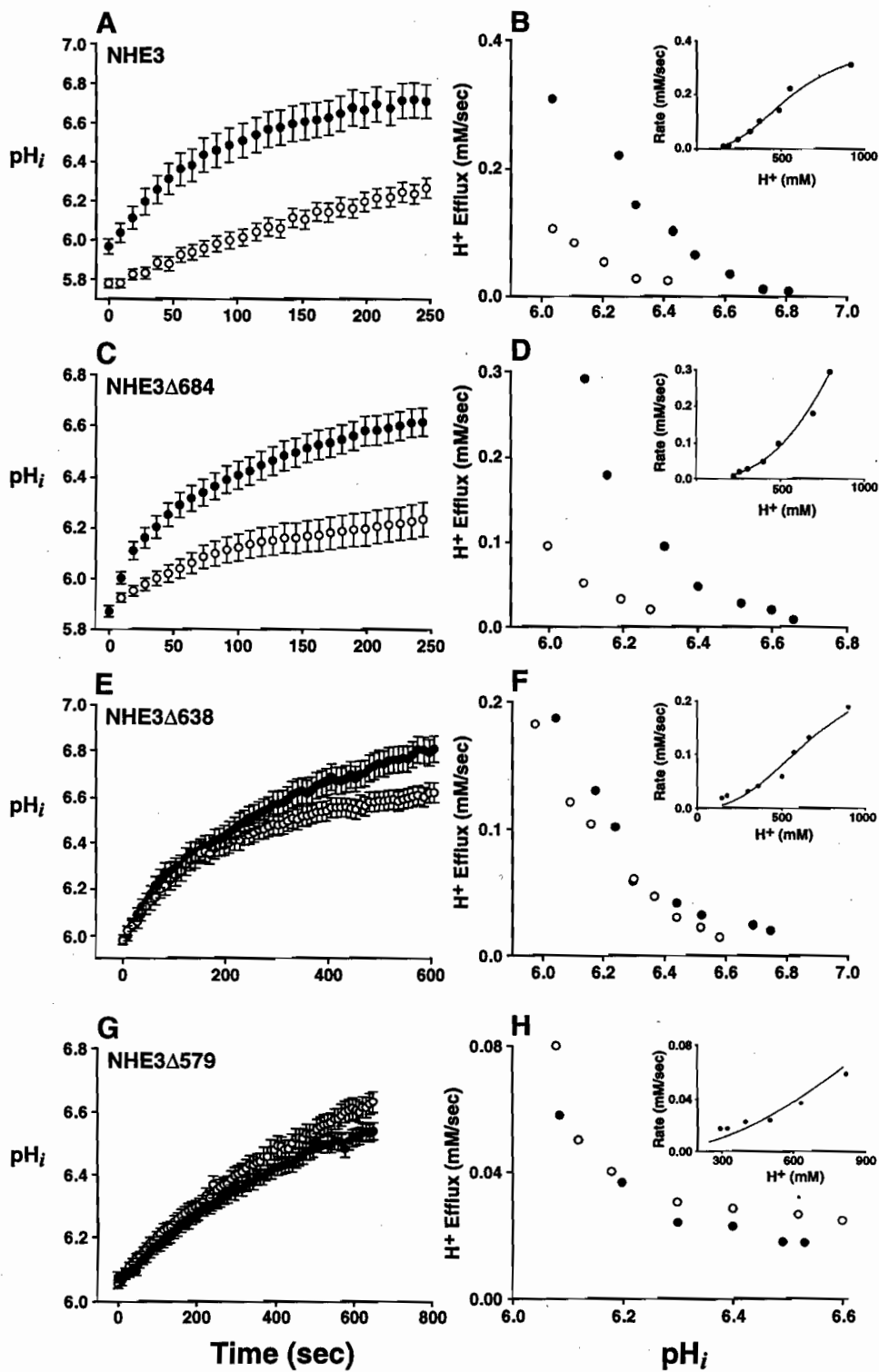
Structure-function analysis of the ATP dependence was also performed by examining progressive deletions of the C-terminal tail of NHE3. In contrast to the forskolin response, the inhibitory effect of ATP depletion was preserved even in the most profound truncation studied, NHE3 $\Delta$ 579. It is concluded from these findings that the site(s) responsible for the ATP requirement are situated in the transmembrane domain or in a portion of the tail near its emergence from the membrane. It is noteworthy that ATP dependence persisted in NHE3 $\Delta$ 579 despite deletion of most consensus phosphorylation sites. For NHE1, it has been suggested that regulation by ATP is independent of changes in the phosphorylation of the exchanger itself (194). Hence, a similar mechanism may mediate the metabolic dependence of NHE3. No conventional nucleotide-binding sites are identifiable from the sequence of either NHE1 or NHE3, suggesting that perhaps associated proteins are required to confer ATP sensitivity to the exchangers. The cytoskeleton, which is drastically rearranged upon depletion of ATP, may contribute to this effect.

In summary, a similar kinetic profile is observed upon inhibition of NHE3 by cAMP and by depletion of cellular ATP. Both procedures induce a shift in the  $pH_i$  sensitivity of the exchanger to more acidic values. Nevertheless, the mutational analysis reported here implies that the mode of regulation by ATP and cAMP is unlikely to be identical. The latter required the presence of most of the cytosolic tail, while the ATP dependence persisted after more severe deletions. This points to the existence of distinct domains of NHE3 that are responsible for unique regulatory functions. More precise definition of the specific inhibitory mechanisms may require detailed information of the putative accessory proteins and their sites of interaction with NHE3.

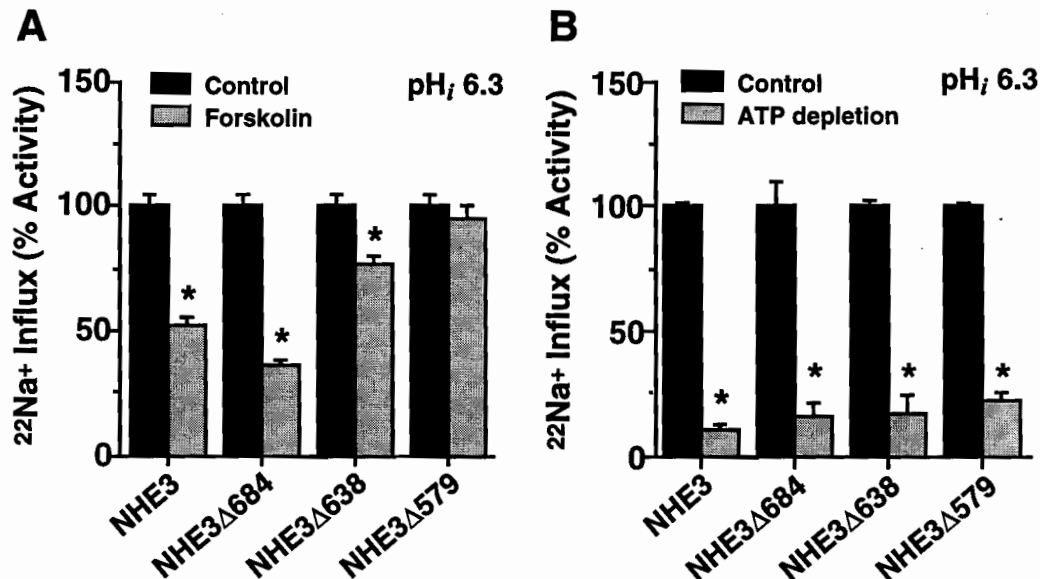


**Fig. 3.1. Diagram of Na<sup>+</sup>/H<sup>+</sup> exchanger chimeras and deletion mutants.** *A*) Diagram of the mammalian expression vector plasmids containing the rat parental Na<sup>+</sup>/H<sup>+</sup> exchanger isoforms NHE1 and NHE3. Indicated in the figure are relevant restriction endonuclease sites used in the construction of chimeras of NHE1 and NHE3 and deletion mutants of NHE3. *B*) Linear profile and nomenclature of chimeras of NHE1 and NHE3 and deletion mutants of NHE3. Details of their construction are provided in "Experimental Procedures."



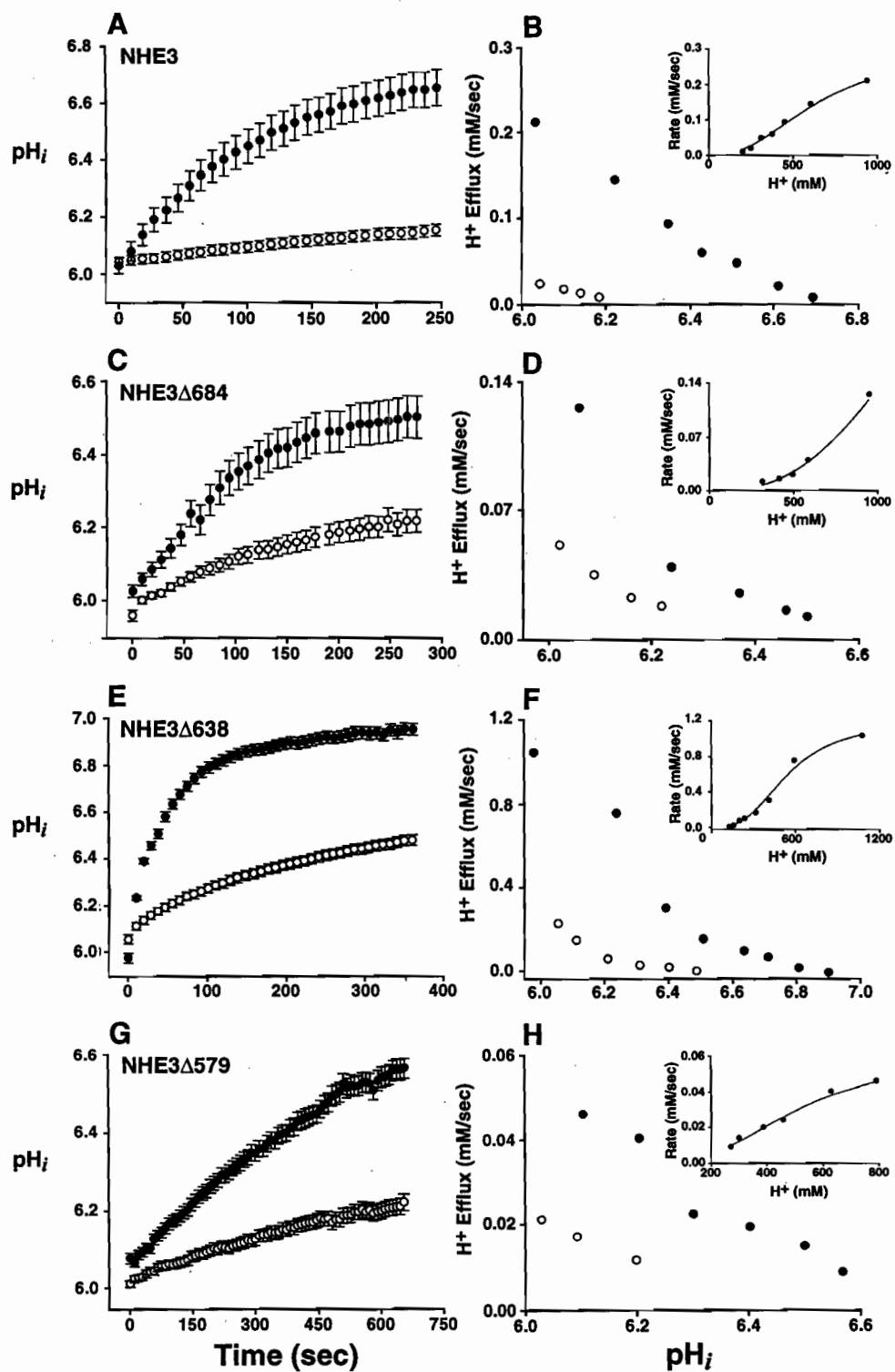






**Fig. 3.3. Effects of forskolin and ATP depletion on the activity of full-length and C-terminally truncated NHE3: Na<sup>+</sup> uptake determinations.** AP-1 cells transfected with either full length NHE3, NHE3Δ684, NHE3Δ638 or NHE3Δ579 were grown to confluence on 24-well plates. *A*) The monolayers were washed twice with Na<sup>+</sup>-medium (see Experimental Procedures for composition of media). The cells were then preincubated in the same solution in the absence or presence of 10 μM forskolin for 15 min at 37 °C. Next, the medium was removed and the cells were preincubated for 3 min in K<sup>+</sup>-nigericin solution to clamp the intracellular pH at 6.3 in the continued absence or presence of 10 μM forskolin. At the end of this equilibration period, the solutions were aspirated and replaced with the same media supplemented with <sup>22</sup>NaCl (1 μCi/ml), 1 mM ouabain, with or without 2 mM amiloride. Radioisotope uptake was terminated after 10 min by aspiration and extensive washing with ice-cold Na<sup>+</sup>-solution and the samples were processed as described under "Experimental Procedures." Background <sup>22</sup>Na<sup>+</sup> influx that was not inhibitable by 2 mM amiloride was subtracted from the total influx. Data are expressed as the mean percentage of amiloride-inhibitable <sup>22</sup>Na<sup>+</sup> influx ± SE (*n* = 16) from four independent experiments. *B*) The cell monolayers were incubated for 10 min in control or ATP-depleting solutions at 37 °C. Na<sup>+</sup>/H<sup>+</sup> exchanger activity was then measured as described above. Data are expressed as the mean percentage of amiloride-inhibitable <sup>22</sup>Na<sup>+</sup> influx ± SE from 2-3 independent experiments each done in quadruplicate. Significance of differences between control and experimental measurements was calculated using two-tailed Student's *t*-test and is indicated by an asterisk (*p* < 0.001).





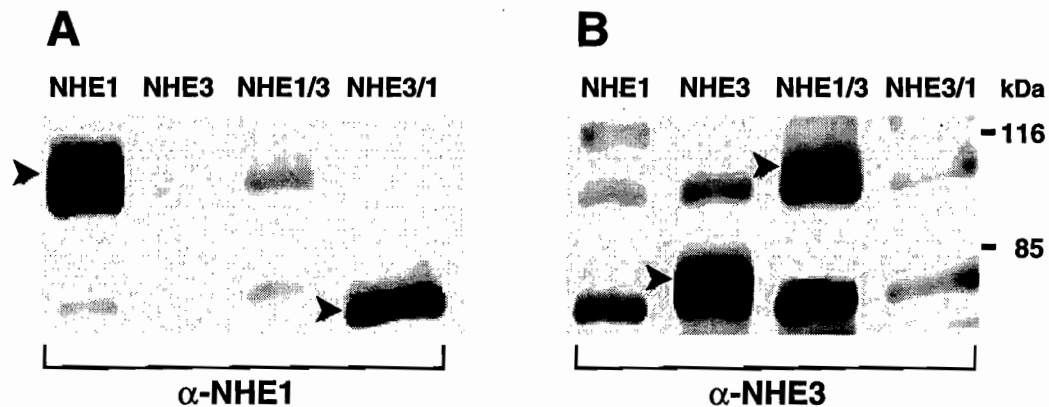


**Fig. 3.5. Immunoblotting of the full-length NHE1 and NHE3 and chimeric NHE1/3 and NHE3/1 exchangers in AP-1 cells.** Membranes (microsomal fraction) isolated from cells stably transfected with the indicated NHE were subjected to immunoblot analysis and probed with antibodies raised against NHE1 ( $\alpha$ NHE1, panel *A*) or NHE3 ( $\alpha$ NHE3, panel *B*). Specific immunoreactive bands are indicated by *arrowheads*. Lighter, nonspecific bands ~75 and 110 kDa were routinely observed in all lanes. Blots are representative of three independent experiments.

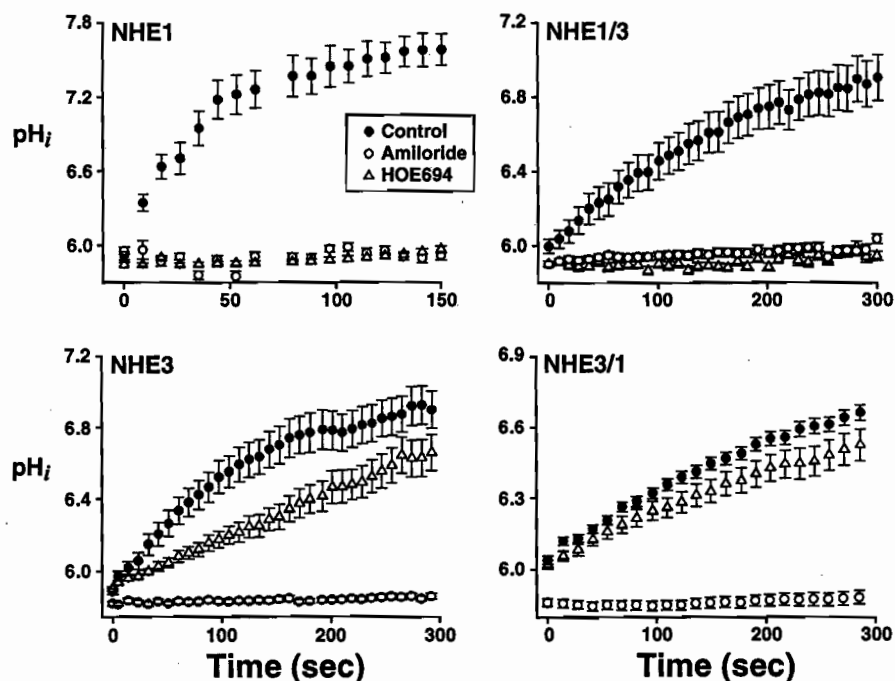


Fig. 3.6. Effects of amiloride and HOE694 on the activity of full-length and chimeric exchangers. AP-1 cells transfected with full-length NHE1 or NHE3 (*left column*), or with the chimeric NHE1/3 or NHE3/1 (*right column*) were loaded with BCECF in bicarbonate-free medium. The cells were acid-loaded with ammonium and the  $pH_i$  recovery induced by addition of  $Na^+$  was measured fluorimetrically in the presence (*open symbols*) or absence (*solid circles*) of inhibitors. The inhibitors used were amiloride (1 mM throughout; *open circles*) or HOE694 (*triangles*). The concentration of HOE694 used was 1  $\mu M$  for full-length NHE1 and the NHE1/3 chimera and 500  $\mu M$  for NHE3 and NHE3/1. Results are the mean  $\pm$  SE of at least 20 cells from three separate experiments.

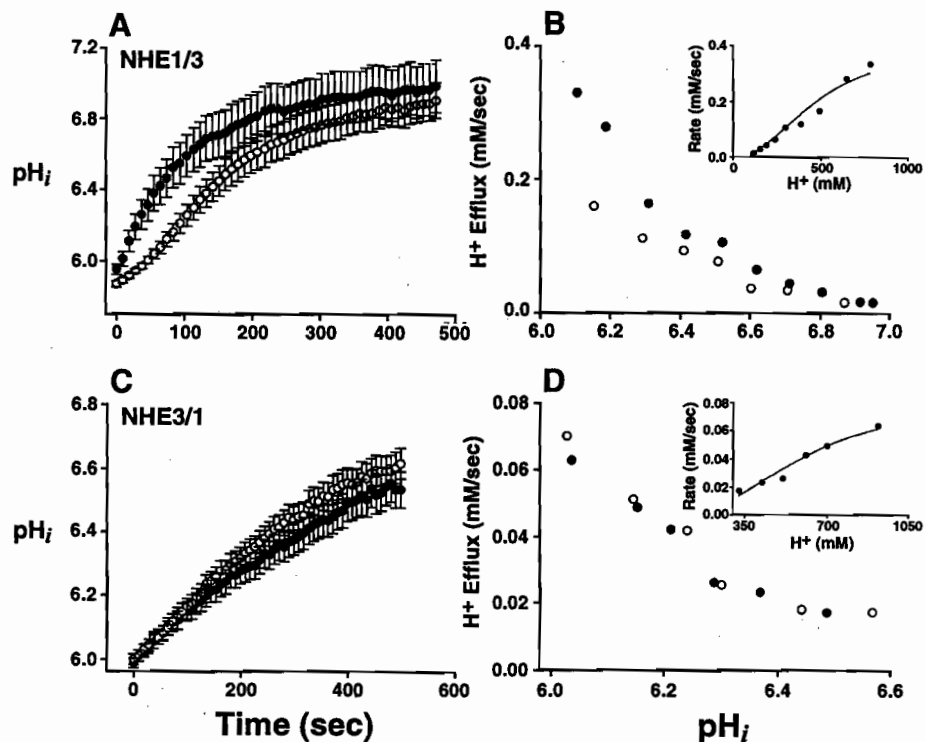
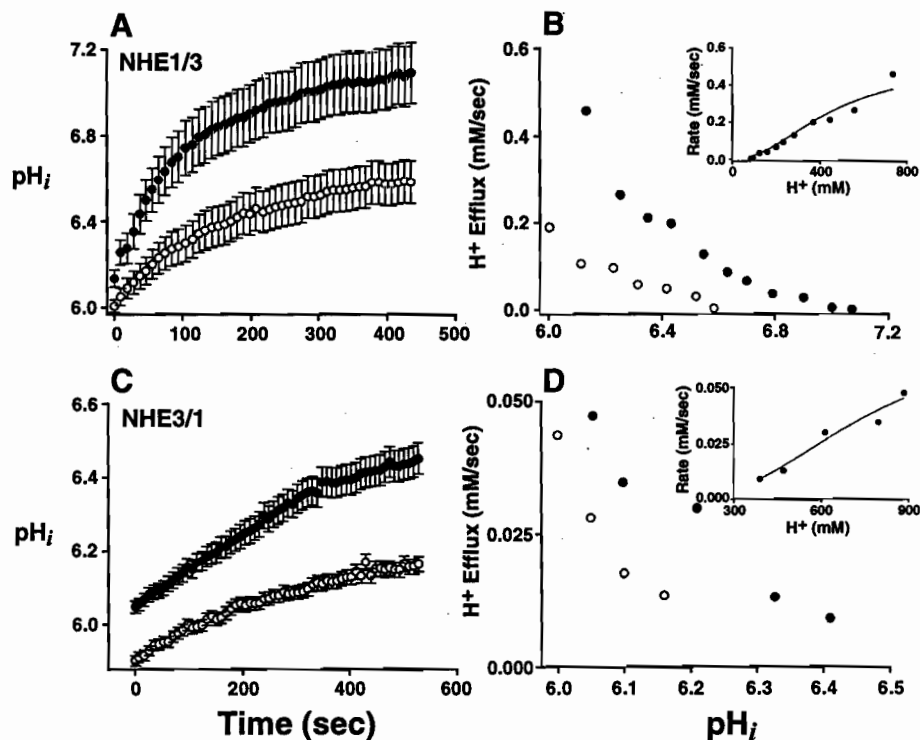
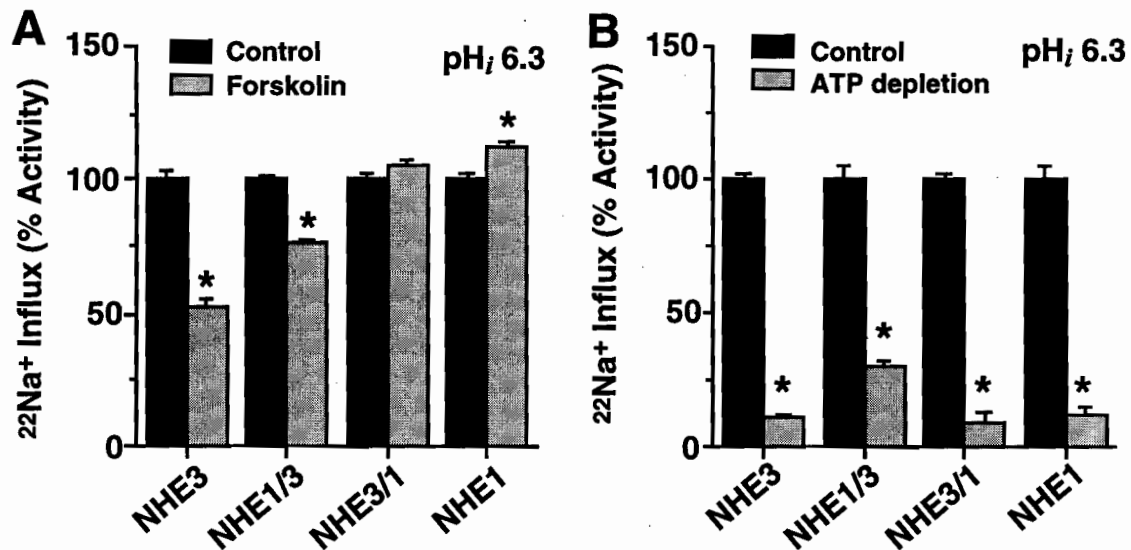


Fig. 3.7. Effect of forskolin on the activity of chimeric exchangers: pH determinations. AP-1 cells transfected with full length NHE1/3 (A and B), NHE3/1 (C and D) were loaded with BCECF in bicarbonate-free medium. The cells were acid-loaded with ammonium and treated with (*open symbols*) or without (*solid symbols*) 10  $\mu$ M forskolin during the final 10 min of incubation with the dye. Next, the pH<sub>i</sub> recovery induced by addition of Na<sup>+</sup> was measured fluorimetrically. Results in each panel are the mean  $\pm$  SE of at least 20 cells from three separate experiments. Other details were as in Fig. 3.2.



**Fig. 3.8. Effect of ATP depletion on the activity of chimeric exchangers: pH determinations.** AP-1 cells transfected with full length NHE1/3 (A and B), NHE3/1 (C and D) were loaded with BCECF in bicarbonate-free medium. The cells were acid-loaded with ammonium and treated with (*open symbols*) or without (*solid symbols*) a glucose-free medium containing 5 mM deoxyglucose plus 1 μg/ml antimycin in order to deplete ATP during the final 10 min of incubation with the dye. Next, the pH<sub>i</sub> recovery induced by addition of Na<sup>+</sup> was measured fluorimetrically. Results in each panel are the mean ± SE of at least 20 cells from three separate experiments. Other details were as in Fig. 3.4.



**Fig. 3.9. Influence of forskolin and ATP-depletion on the activities of wild type and chimeric Na<sup>+</sup>/H<sup>+</sup> exchangers: Na<sup>+</sup> uptake determinations.** AP-1 cell transfectants stably expressing wild type rat Na<sup>+</sup>/H<sup>+</sup> exchanger isoforms NHE1 and NHE3 and chimeric exchangers NHE1/3 and NHE3/1 were grown to confluence on 24-well plates. *A*) The effect of 10  $\mu\text{M}$  forskolin on the transport activities of the exchanger was studied exactly as described in the legend to Fig. 3.3. Data are expressed as the mean percentage of amiloride-inhibitable <sup>22</sup>Na<sup>+</sup> influx  $\pm$  SE ( $n = 16$ ) from four independent experiments. *B*) The influence of cellular ATP depletion on the transport activities of the exchanger was performed as described in the legend to Fig. 3.3. Data are expressed as the mean percentage of amiloride-inhibitable <sup>22</sup>Na<sup>+</sup> influx  $\pm$  SE from 2-3 independent experiments each done in quadruplicate. Significance of differences between control and experimental measurements was calculated using two-tailed Student's *t*-test and is indicated by an asterisk ( $p < 0.001$ ).



## **Chapter IV.**

### **Localization of an Osmoresponsive Inhibitory Domain of the Na<sup>+</sup>/H<sup>+</sup> Exchanger NHE3 Isoform**

Frank H. Yu, Jonathan D. Wasserman, and John Orlowski

This study was designed and all experiments were carried out by F.H.Yu. Under supervision by F.H. Yu, J.D. Wasserman (an undergraduate honours physiology student) helped to generate and analyze some of the chimeric exchangers; his contribution is included in Fig. 4.4. The research project was supervised by J. Orlowski.

This manuscript is in preparation for submission to the *Journal of Biological Chemistry*.

## SUMMARY

The  $\text{Na}^+/\text{H}^+$  exchanger NHE1 and NHE3 isoforms are stimulated and inhibited, respectively, by hyperosmotic medium. In order to test the hypothesis that hyperosmotic inhibition of NHE3 is mediated by a distinct structural domain of the transporter, a mutational analysis of NHE3 was conducted by examining chimeras of NHE1 and NHE3, and a series of C-terminally truncated mutants of NHE3. These mutant proteins were heterologously expressed in  $\text{Na}^+/\text{H}^+$  exchanger-deficient Chinese hamster ovary cells (AP-1), and their responsiveness to hyperosmotic stress was determined by measuring amiloride-inhibitable  $\text{H}^+$ -activated  $^{22}\text{Na}^+$  influx. The NHE3/1 chimera (*N*-terminal transmembranous region of NHE3 linked to the *C*-terminal cytoplasmic region of NHE1) was activated by hyperosmotic medium, suggesting that the major determinants of this response are confined to the cytoplasmic *C*-terminal region of NHE1. In contrast, the NHE1/3 chimera was unresponsive to hyperosmotic challenge, suggesting that an interaction of both the *N*- and the *C*-termini of NHE3 may be requisite for hyperosmolarity-mediated inhibition of NHE3. Hyperosmotic responsiveness of the truncation mutant NHE3 $\Delta$ 684, which lacks the most *C*-terminal 147 amino acids, was indistinguishable from the full-length NHE3. However, the inhibitory effect was totally ablated in NHE3 $\Delta$ 649. Deletion of the next 11 amino acid residues (mutant NHE3 $\Delta$ 638) unexpectedly resulted in a stimulatory response to hyperosmotic medium, whereas a more profound truncation (NHE3 $\Delta$ 579) completely abrogated this effect. These findings suggest that two distinct and opposite osmoresponsive domains exist in NHE3: a hyperosmotically activatable region between amino acids 579 and 638, and an inhibitory region between amino acids 649 and 684, the latter acting in a dominant manner. This latter domain is distinct from the adjacent region (amino acids 579 to 638) which has also previously been found to confer inhibition by cAMP.

## INTRODUCTION

The mammalian  $\text{Na}^+/\text{H}^+$  exchanger (NHE) participates in several vital homeostatic processes such as the maintenance of intracellular pH, control of cell volume, transepithelial reabsorption of  $\text{Na}^+$  and  $\text{HCO}_3^-$ , and facilitation of cell proliferation in response to various mitogenic signals (reviewed in 2-5). The diverse physiological functions of  $\text{Na}^+/\text{H}^+$  exchanger are partly attributed to the existence of multiple  $\text{Na}^+/\text{H}^+$  exchanger isoforms.

To date, five members (NHE1 to NHE5) of this multigene family have been identified in mammals (27,33,47,48,61,108). These isoforms share moderate amino acid identity (~40-70%), and exhibit similar predicted membrane topology with 10-12 *N*-terminal transmembrane-spanning regions and a large *C*-terminal cytoplasmic region. The isoforms display distinct patterns of tissue distribution: NHE1, the "housekeeping" isoform, is the predominant species in nonepithelial cells and is also localized to the basolateral membrane of polarized epithelial cells; NHE2, NHE3 and NHE4 are most abundant in kidney, intestine, and stomach; and NHE5 is predominantly restricted to brain, spleen, and testis. Amongst the isoforms, the greatest divergence in sequence homology occurs in the cytoplasmic tail region where the regulation of exchanger activity is believed to occur (17,124). Indeed, this region contains several consensus sequences for potential phosphorylation by serine/threonine protein kinases (27,33,71), and in the case of NHE1, also contains a regulatory binding site for calmodulin (126,127).

In most cells, restoration of cell volume following hyperosmotic-induced cell shrinkage is mediated by activation of  $\text{Na}^+/\text{H}^+$  exchanger NHE1 activity (53,152) which is functionally coupled to stimulation of cation-independent  $\text{Cl}^-/\text{HCO}_3^-$  exchange (87,149). The net effect is a cellular uptake of NaCl and osmotically obliged water. Although the mechanism remains unclear, osmotic regulation of NHE1 is dependent on the presence of

cellular ATP (53) and the first 566 amino acids of NHE1 (198), but does not require increased phosphorylation of the molecule (152). Considerably less is known about the involvement of other  $\text{Na}^+/\text{H}^+$  exchanger isoforms in cell volume regulation. Recently, rat NHE2 was also found to be stimulated by hyperosmotic stress, whereas rat NHE3 was inhibited by the same treatment in transfected Chinese hamster ovary cells (53). This latter effect precisely mimicked that observed for native NHE3 in renal and intestinal epithelia (150,151). Osmotic inhibition of NHE3 may be physiologically relevant during pathological conditions causing serum hyperosmolarity, such as extreme dehydration, in order to limit the uptake of  $\text{Na}^+$  from the lumen (53).

To better understand the molecular mechanisms involved in the osmotic regulation of NHE3, we examined the effect of hyperosmotic stress on the activities of various NHE3 mutants expressed in exchanger-deficient Chinese hamster ovary cells (AP-1). Here, we report that hyperosmotic inhibitory response of NHE3 is conferred by a distinct region of its *C*-terminal cytoplasmic tail.

## EXPERIMENTAL PROCEDURES

*Materials* – Carrier-free  $^{22}\text{NaCl}$  (5 mCi/ml) was obtained from NEN Research Products (Du Pont Canada Inc., Mississauga, Ontario). Amiloride, ouabain, forskolin, phorbol 12-myristate 13 acetate (PMA) and nigericin were purchased from Sigma Chemical Co. (St. Louis, MO). The amiloride derivative 5-(*N*-ethyl-*N*-isopropyl) amiloride (EIPA) was purchased from Molecular Probes (Eugene, OR).  $\alpha$ -Minimal essential medium, fetal bovine serum, kanamycin sulfate, and trypsin-EDTA were from Life Technologies (Burlington, Ontario). Cell culture dishes and flasks were purchased from Becton-Dickenson and Co. (VWR Scientific, Montréal, Québec). All other chemicals and reagents were from British Drug House Inc. (St. Laurent, Québec) or Fisher Scientific (Montréal, Québec), and were of the highest grade available.

*Construction of  $\text{Na}^+/\text{H}^+$  exchanger mutants* – The mammalian expression plasmids, pNHE1 and pNHE3 contain the cDNA fragments of rat NHE1 (nucleotides -42 to +3454) and NHE3 (nucleotides -44 to +2950), respectively. The construction of the chimeric mutants NHE1/3 and NHE3/1 and the C-terminal truncation mutants NHE3 $\Delta$ 684, NHE3 $\Delta$ 638, and NHE3 $\Delta$ 579 (Fig. 4.1) were described previously (199). The NHE3 $\Delta$ 649 mutant was generated by engineering a unique *EcoRI* restriction endonuclease site into pNHE3 at amino acid positions 649-650. This modified pNHE3 was then cleaved with *EcoRI* and *XbaI* (site in polylinker) to remove the terminal *EcoRI*-*XbaI* fragment that contained amino acids 650 to 831. The 5' DNA overhang ends of this linearized plasmid were blunt-ended by a fill-in reaction using Klenow and then religated with T4 DNA ligase. This procedure resulted in NHE3 being truncated at amino acid residue 649 followed by the addition of a non-native amino acid (Phe) and a TAG stop codon in the proper reading frame. The NHE3 $\Delta$ 455 mutant was generated by cleaving pNHE3 with *EagI*, which cuts at the predicted junction between *N*- and *C*-termini, and

*Xba*I to remove the entire C-terminal tail region encoded by amino acids 456-831. The 5' DNA overhangs resulting from this double restriction endonuclease digest were blunt-ended by a fill-in reaction with Klenow and religated as described above. This NHE3 mutant contained an in-frame TAG stop codon immediately adjacent to amino acid position 455. NHE1/3 $\Delta$ 638 chimera was generated by excising the truncated cytoplasmic tail of NHE3 $\Delta$ 638 by *Eag*I and *Sph*I (site in vector) and subcloning the cDNA fragment into pNHE1 whose C-terminus was eliminated by the identical restriction digests.

To facilitate the construction of additional Na<sup>+</sup>/H<sup>+</sup> exchanger chimeras containing various homologous segments of the C-terminal regulatory regions of NHE1 and NHE3, three unique restriction endonuclease sites were engineered by site-directed mutagenesis into each cDNA in this region (192). For NHE1, the introduction of a *Kas*I site (GGC GCC) at amino acid residues 625-626 altered its coding sequence from Pro-Ala to Gly-Ala, an *Eco*RI site (GAA TTC) at residues 665-666 changed the coding sequence from Glu-Ala to Glu-Phe, and an *Afl*III site (CTT AAG) at residues 748-749 did not transform its coding sequence (*i.e.*, Leu-Lys). For NHE3, the insertion of a *Kas*I site at amino acid residues 578-579 changed the coding sequence from Glu-Ala to Gly-Ala, an *Eco*RI site at residues 649-650 altered its amino acid sequence from Glu-Ile to Glu-Phe, and an *Afl*III site (CTT AAG) at amino acid positions 715-716 transformed its coding sequence from Leu-Ser to Leu-Lys. These cDNAs were sequenced to confirm the presence of the restriction endonuclease sites and to ensure that other spurious mutations were not introduced during the mutational manipulations of the plasmids. These modified plasmids were called pNHE1'' and pNHE3'', respectively. The chimeric Na<sup>+</sup>/H<sup>+</sup> exchangers were constructed by the reciprocal exchange of the restriction endonuclease fragments that comprise the various segments of the C-terminal cytoplasmic regions of NHE1 and NHE3 (Fig. 4.1B).

*Stable transfection and expression of the  $\text{Na}^+/\text{H}^+$  exchanger mutant expression plasmids* – Chinese hamster ovary (AP-1) cells devoid of endogenous  $\text{Na}^+/\text{H}^+$  exchanger activity (190) were transfected with plasmids containing the various  $\text{Na}^+/\text{H}^+$  exchanger mutants by the calcium phosphate-DNA coprecipitation technique of Chen and Okayama (193). Starting 48 h after transfection, the AP-1 cells were selected for survival in response to repeated (5-6 times over a two week period), acute  $\text{NH}_4\text{Cl}$ -induced acid loads (30,108) in order to discriminate between  $\text{Na}^+/\text{H}^+$  exchanger positive and negative transfectants. Thereafter, clonal cell lines of stable transfectants were isolated and expanded for further analysis.

*Cell culture* – Transfected cells were grown in a humidified 95% air/5%  $\text{CO}_2$  atmosphere and maintained in complete  $\alpha$ -minimal essential medium supplemented with 10% fetal bovine serum, 100  $\mu\text{g}/\text{ml}$  kanamycin sulfate and 25 mM  $\text{NaHCO}_3$  (pH 7.4). Cells expressing  $\text{Na}^+/\text{H}^+$  exchanger activity were periodically selected by an acute acid challenge, as described above. This process was repeated to eliminate possible revertants and maintain stable, functional expression of the exchanger.

*Measurement of  $^{22}\text{Na}^+$  influx* –  $\text{Na}^+/\text{H}^+$  exchanger activity was measured as the rate of amiloride-inhibitable  $^{22}\text{Na}^+$  influx at a constant intracellular  $\text{H}^+$  concentration as described previously (199). Briefly, confluent cell monolayers in 24-well plates were washed with isotonic choline chloride solution (125 mM choline chloride, 5 mM  $\text{KCl}$ , 2 mM  $\text{MgCl}_2$ , 5 mM glucose, 20 mM HEPES-Tris, pH 7.4) at room temperature prior to commencement of the influx assay. To clamp  $\text{pH}_i$  at 6.3, the cell monolayers were preincubated in an isotonic  $\text{K}^+$ -nigericin solution containing 153 mM *N*-methyl-D-glucamine methanesulphonate, 11.2 mM potassium glutamate, 2 mM  $\text{NaCl}$ , 1 mM  $\text{MgCl}_2$ , 10  $\mu\text{M}$  nigericin, 10 mM HEPES, pH 7.4 at room temperature or a hyperosmotic solution which consisted of the same  $\text{K}^+$ -nigericin solution to which 200 mM mannitol was added.

In experiments that assessed the influence of agonists of PKA and PKC signaling pathways on  $\text{Na}^+/\text{H}^+$  exchanger activity, the composition of the  $\text{K}^+$ -nigericin solution consisted of 153 mM *N*-methyl-D-glucamine chloride, 11.2 mM KCl, 2 mM NaCl, 1 mM  $\text{MgCl}_2$ , 10  $\mu\text{M}$  nigericin, 10 mM HEPES, pH 7.4 with and without 10  $\mu\text{M}$  forskolin or 1  $\mu\text{M}$  PMA. After preincubation for 3 min, the solutions were then removed and  $^{22}\text{Na}^+$  influx measurements were initiated in the same  $\text{K}^+$ -nigericin solutions supplemented with 1  $\mu\text{Ci}$   $^{22}\text{NaCl}/\text{ml}$  and 1 mM ouabain (to inhibit  $\text{Na}^+/\text{K}^+$ -ATPase and minimize  $^{22}\text{Na}^+$  efflux) in the absence or presence of 2 mM amiloride.  $^{22}\text{Na}^+$  influx was terminated after 10 min by three rapid washes of 1 ml ice-cold NaCl stop solution (130 mM NaCl, 1 mM  $\text{MgCl}_2$ , 2 mM  $\text{CaCl}_2$ , 20 mM HEPES-NaOH, pH 7.4). To extract the radiolabel, 0.25 ml of 0.5 N NaOH was added to each well and subsequently washed with 0.25 ml of 0.5 N HCl. Both the solubilized cell extract and wash solutions were suspended in 3 ml of scintillation fluid and the radioactivity assayed by liquid scintillation spectroscopy.  $^{22}\text{Na}^+$  influx was linear for at least 10 min under these experimental conditions.



## RESULTS

*Involvement of the C-terminal region of NHE3 in hyperosmotic sensitivity* – To define the structural motifs of NHE3 that confer an inhibitory response to hyperosmotic medium, a series of chimeras of rat NHE1 and NHE3 and truncation mutants of NHE3 were engineered. A diagram of these constructs is illustrated in Fig. 4.1.

The effect of hyperosmotic stress on AP-1 cells stably expressing parental and mutant NHEs was compared by measuring amiloride-inhibitable  $^{22}\text{Na}^+$  influx. The intracellular pH ( $\text{pH}_i$ ) was clamped at 6.3 to attain near maximal velocity and to maintain a constant  $\text{H}^+$  concentration, thereby eliminating the potential effect of osmolarity-induced changes in  $\text{pH}_i$ . This pH was chosen from an initial experiment that profiled the initial rates of  $^{22}\text{Na}^+$  influx at varying  $\text{pH}_i$  (data not shown). Consistent with previous observations (53), hyperosmotic challenge inhibited the activity of NHE3 whereas it stimulated that of NHE1 (Fig. 4.2). As a first step towards delineating the structural segments of NHE3 that confer responsiveness to hyperosmolarity, we examined the NHE1/3 and NHE3/1 chimeras which contained reciprocally-exchanged C-terminal cytoplasmic domains (199). Exposure of the NHE3/1 chimera to hyperosmotic media resulted in a robust stimulation of transport activity. In contrast, the hyperosmotic media had no effect on the NHE1/3 chimera. This finding suggests that the cytosolic tail of NHE1 is sufficient to confer hyperosmotic stimulation, while that of NHE3 requires the participation of other regions of the protein to elicit the full hyperosmotic inhibitory effect.

*Structural analysis of NHE3 truncation mutants in osmotic response* – In order to more precisely delineate specific regions of NHE3 involved in the hyperosmotic inhibition of transport activity, a series of mutants that progressively truncate the cytosolic tail domain were analyzed. As shown in Fig. 4.3, the inhibitory effect of

hyperosmolarity on NHE3 $\Delta$ 684 was indistinguishable from that of the full-length rat NHE3. This result indicates that the C-terminal 147 amino acids are not required for this osmotic response. A further truncation at amino acid residue 649 totally ablated the hyperosmotic inhibition of NHE3 and suggests that the region between amino acids 649 to 684 is essential for manifesting the hyperosmotic inhibitory response. Unexpectedly, a truncation at amino acid residue 638 (NHE3 $\Delta$ 638) resulted in approximately 30% increase in  $^{22}\text{Na}^+$  influx rates upon hyperosmotic challenge. In fact, the osmotic activation of NHE3 $\Delta$ 638 was completely retained in two additional stable transfectant clones that were analyzed, substantiating that the initial observation was not an artifact of clonal selection (data not shown). Furthermore, this novel hyperosmotic stimulatory response was lost with a more profound truncation at position 579 (mutant NHE3 $\Delta$ 579), which exhibited rates of  $^{22}\text{Na}^+$  influx in hyperosmotic medium that were virtually indistinguishable from those determined under isotonic conditions. Finally, the removal of the entire proposed cytosolic tail resulted in a nonfunctional mutant (NHE3 $\Delta$ 455) by virtue of the fact that it failed to rescue transfected cells from imposed acid loads. In summary, these results indicate that a dominant autoinhibitory domain exists between amino acid positions 649 and 684 of the cytoplasmic tail of NHE3 that is essential for the inhibitory response to hyperosmolarity. Further removal of amino acids 639 to 649 exposes cryptic elements that now allow NHE3 to be stimulated in response to hyperosmolarity.

As described above, the NHE1/3 chimera was unresponsive to hyperosmolarity. However, in view of our observation that the C-terminal segment between amino acids 649 and 684 of NHE3 conferred a dominant inhibitory response to hyperosmolarity, we wished to ascertain whether this smaller segment, when inserted into NHE1, would be sufficient to cause inhibition of transport activity in response to hyperosmolarity.

To this end, three unique restriction endonuclease sites (*KasI*, *EcoRI* and *AflIII*) were engineered simultaneously into the C-terminal region of the NHE1 and NHE3 cDNAs to facilitate the exchange of homologous segments. The new parental exchangers were called NHE1" and NHE3". The results are shown in Fig.4.4. Unexpectedly, the full-length NHE3" resulted in a complete loss of regulation by hyperosmolarity. Chimeric exchangers derived from the NHE3" parental construct (Fig. 4.1B) showed similar unresponsiveness to hyperosmolarity (*cf.*, Fig. 4.4, NHE3KE1 and NHE3EA1).

In contrast, the hyperosmotic activation of NHE1" was identical to native NHE1 despite the substitution of two amino acid residues at positions 625 and 666 (see "Experimental Procedures"). The NHE1KE3 chimera (*i.e.*, containing the *KasI-EcoRI* fragment (amino acids 579 - 649)) of NHE3" was also stimulated by hyperosmolarity, although the degree of stimulation was reduced by about 30% compared to NHE1". However, the NHE1EA3 chimera (containing amino acids 649 to 715 of NHE3) was almost totally unresponsive to hyperosmolarity. The suppressive effect of the *EcoRI-AflIII* fragment of NHE3 on hyperosmotic stimulation of NHE1 activity is consistent with its involvement in the hyperosmotic inhibition of NHE3. However, it is also possible that the lack of hyperosmotic stimulation of NHE1EA3 may be due to a secondary alteration in the protein structure of this particular chimera. Nevertheless, the serendipitous creation of NHE3" which lacks responsiveness to hyperosmolarity, implicates one or more of the three substituted amino acids as important regulatory determinants. Determination of the critical residue(s) involved awaits further analyses.

*Sensitivity of the NHE3Δ638 mutant to phorbol ester and forskolin* – Because of the surprising hyperosmotic activation of NHE3Δ638, it was of interest to determine whether other regulatory properties of NHE3 were affected. We have recently demonstrated that activation of the PKA or PKC signaling pathways in AP-1 cells also

leads to the inhibition of NHE3, whereas they cause stimulation of NHE1 (141). Therefore, the effects of phorbol ester and forskolin on the transport activity of NHE3 $\Delta$ 638 were compared to three other chimeric constructs of NHE3 and NHE1, as illustrated in Fig. 4.5. Activation of PKC by phorbol esters caused stimulation of the NHE3 $\Delta$ 638 mutant. This response is similar to that observed following hyperosmotic shock, but contrary to what occurs in the full-length NHE3 (141). However, the cAMP-mediated inhibition of NHE3 was preserved in this truncation mutant as forskolin treatment caused approximately 30% reduction of activity compared to untreated cells, as previously described by us (199). This confirms that not all regulation of NHE3 activity is affected by the truncation of the terminal 196 amino acid residues. A virtually indistinguishable pattern of activation by phorbol ester and inhibition by forskolin was observed in the NHE1/3 $\Delta$ 638 chimera, which comprised the truncated C-terminus of NHE3 linked to the entire transmembrane region of NHE1. This result suggests that the NHE3 cytosolic tail segment spanned by amino acids 456 to 638 contains an intrinsic, but cryptic, capability to be activated by PKC. However, this stimulation of Na<sup>+</sup>/H<sup>+</sup> exchange activity is not observed when the entire cytosolic tail of NHE3 is present, as demonstrated by the total lack of PKC sensitivity of the NHE1/3 chimera. In contrast, a strong stimulation of NHE3/1 activity was noted in transfectants treated with PMA which was similar to the hyperosmotic response (Fig. 4.2). Thus the C-terminal cytosolic tail of NHE1 is sufficient to confer responsiveness to both the PKC and hyperosmotic signaling pathways when attached to N-terminal region of NHE3. The striking similarities between PKC- and hyperosmotic-mediated activation of NHE1 has been observed before (18,114,152) but the mechanism remains unknown.

To verify that the modifications of the C-terminal region did not affect other functional properties of the NHE3 mutants, the pharmacological sensitivity of some deletion mutants was compared to the full-length NHE3. The amiloride analogue, EIPA,

was used as it readily discriminates NHE3 from NHE1, the former being 30- to 160-fold more resistant to inhibition by EIPA (108,200). As shown in Fig. 4.6, all mutant constructs and wild type NHE3 displayed similar low sensitivities to EIPA. This finding confirms that the mutations created in the cytoplasmic tail region of NHE3 influenced only certain regulatory properties and that drug sensitivity is confined to the *N*-terminal domain of the exchanger, as previously reported (77,199).

## DISCUSSION

The apically targeted NHE3 isoform of renal proximal tubule cells is inhibited by agonists of the PKA and PKC signaling pathways (41,139), and by hyperosmotic stress (150). An identical pattern of inhibition is observed when rat NHE3 is expressed in AP-1 cells (53,141,199). Thus, AP-1 cells constitute a useful model system to examine the regulation of NHE3. To this end, hyperosmotic responsiveness of a series of NHE3 truncation mutants and chimeric exchangers was assessed in order to identify the relevant structural domain(s).

The most salient conclusion of the present study is the identification of a hyperosmotic inhibitory site in NHE3. While NHE3 $\Delta$ 684 was inhibited by hyperosmotic stress, this regulatory effect disappeared with a more profound truncation at amino acid 649. This finding implies that a deletion or disruption of a crucial domain between amino acids 649 and 684 is important for the hyperosmotic inhibitory response. This conclusion is further supported by the observation that two of three point mutations (*i.e.*, Glu579Gly, Ile650Phe) inserted into NHE3", that lie within or closely upstream of this crucial segment, render the exchanger completely refractory to hyperosmotic regulation. However, this domain by itself appears insufficient to manifest the full inhibitory effect of the full-length NHE3 since: a) replacement of the NHE1 cytoplasmic region with that of NHE3 (chimera NHE1/3) failed to transfer the inhibitory response (Fig. 4.2) and b) homologous substitution of this inhibitory segment (amino acids 649-715) into NHE1 markedly attenuated the stimulation by hyperosmotic medium, but did not bring about inhibition (Fig. 4.4). Thus, the ability of this segment to confer hyperosmotic inhibition appears to be sensitive to its spatial orientation within the molecule.

Although the precise molecular mechanisms has yet to be defined, the osmotic inhibition of NHE3 may involve a phosphorylation-dependent event. Recent evidence has implicated protein tyrosine kinases in hyperosmotic-mediated inhibition of the apical  $\text{Na}^+/\text{H}^+$  exchanger (*i.e.*, NHE3) in rat medullary thick ascending limb (156). A single consensus tyrosine kinase phosphorylation site (*i.e.*, Tyr<sup>553</sup>) is present in NHE3, although it lies outside the putative inhibitory domain. Whether NHE3 is directly phosphorylated at this or other sites in response to hyperosmotic stress remains unknown. It is conceivable that the tyrosine kinase- and hyperosmotic-induced effects converge upstream of NHE3. In support of this hypothesis, it has been recently demonstrated that hyperosmolarity activates several members of the mitogen-activated protein (MAP) kinase and MAP kinase kinase families (157,158) which are known to involve tyrosine phosphorylation. Alternatively, the putative inhibitory region may be targeted by hyperosmotically-sensitive ancillary protein(s) – possibly activated by protein tyrosine kinases – whose interaction with NHE3 mediates the repression of transport activity. Regardless of the precise mechanism, it appears to be distinct from the cAMP-mediated inhibition of NHE3 which appears to involve an upstream adjacent fragment (amino acids 579 to 638) of the exchanger (199).

A unexpected result of the present study is the reversed regulation of NHE3 $\Delta$ 638. Deletion of the terminal 196 amino acid residues of NHE3 created a mutant that was now *activatable* by both hyperosmotic stress and an agonist (PMA) of the PKC signaling pathway. However, it is notable that the NHE1/3 $\Delta$ 638 chimera was equally sensitive to cAMP-mediated inhibition as NHE3 $\Delta$ 638, demonstrating that not all inhibitory regulation of NHE3 was affected by this truncation. It seems that the capacity to confer hyperosmotic stimulation is intrinsic to this portion of the cytoplasmic tail (amino acids 455-638) only in the absence of terminal amino acids since NHE1/3 $\Delta$ 638, but not NHE1/3, was stimulated by hyperosmotic stress. The biological relevance of this

observation is unclear, but it may represent a residual function of an evolutionary ancestral protein (presumably NHE1-like) unmasked by mutagenic manipulations. In this regard, the hyperosmolarity- or volume-activatable site(s) of NHE1 likely resides in the foremost segment of the cytoplasmic tail that is more closely similar in sequence to NHE3. This notion is based on the recent findings that osmotic responsiveness persisted in a human NHE1 $\Delta$ 566 truncation mutant (198), and the results presented in Fig. 4.2 which demonstrate that the entire cytoplasmic tail of NHE1 confers hyperosmotic activation to the NHE3 *N* terminus (chimera NHE3/1). In addition, recent data presented by Levine *et al.* (142) indicate the existence of a stimulatory region in the proximal portions of the rabbit NHE3 cytoplasmic tail that is sensitive to serum, fibroblast growth factor and a phosphatase inhibitor, okadaic acid.

In summary, the mutational analysis reported here dissociates the hyperosmotic- and cAMP-sensitive inhibitory regions of NHE3 from each other. Furthermore, we have identified two distinct hyperosmolarity-responsive regions of NHE3: a cryptic stimulatory site between amino acids 579 to 638 whose effects are only revealed upon deletion of a dominant inhibitory site between amino acids 649-684.



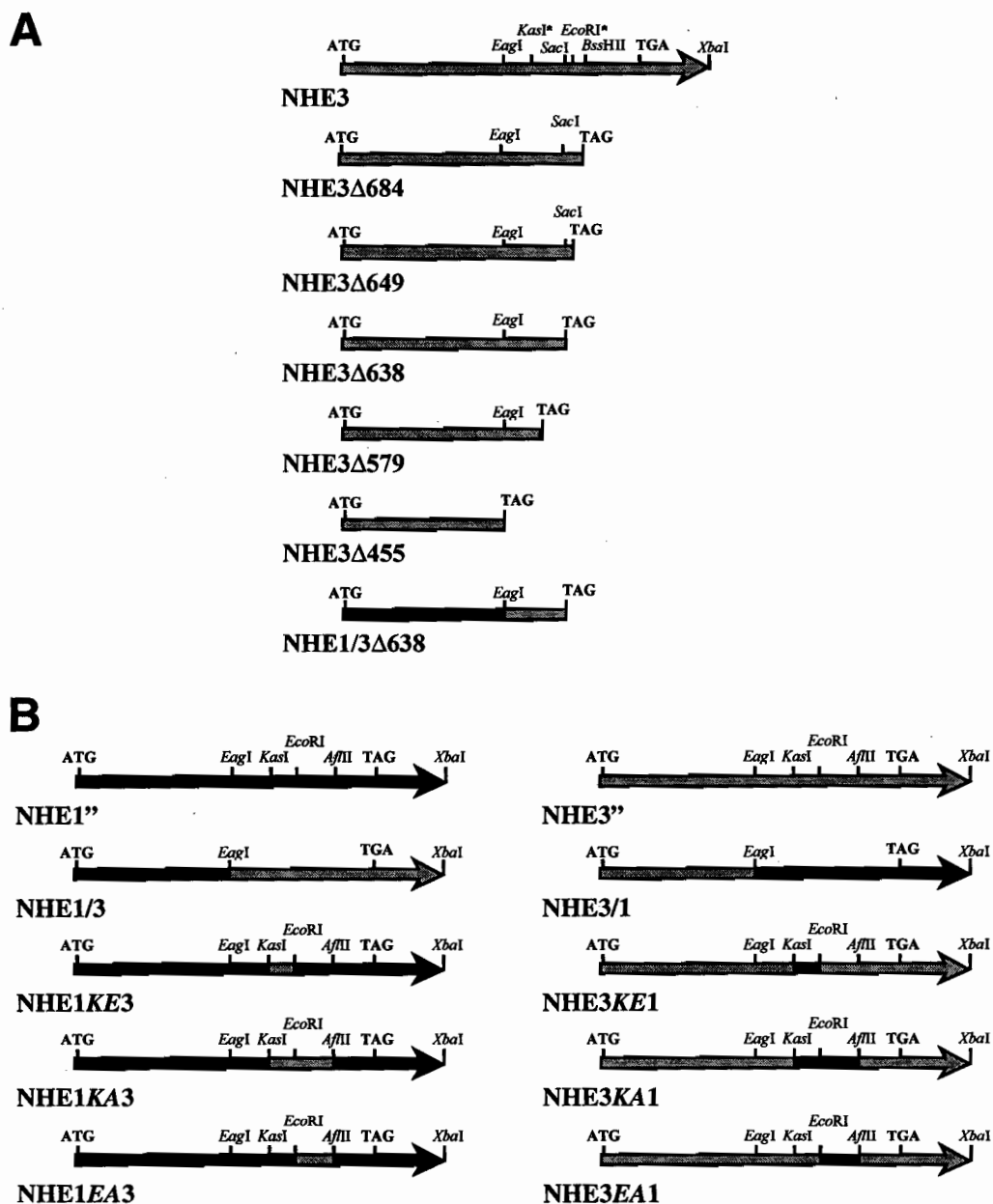


Fig. 4.1. Diagram of  $\text{Na}^+/\text{H}^+$  exchanger truncation and chimeric mutants. A) Linear profile and nomenclature of the full-length NHE1 and NHE3 and the various deletion mutants derived thereafter. Indicated in the diagram are the relevant restriction endonuclease sites used in the construction of the mutants. B) Linear diagram and nomenclature of chimeras of NHE1 and NHE3 that interchange reciprocal segments. Details of all mutant construction are outlined in "Experimental Procedures."

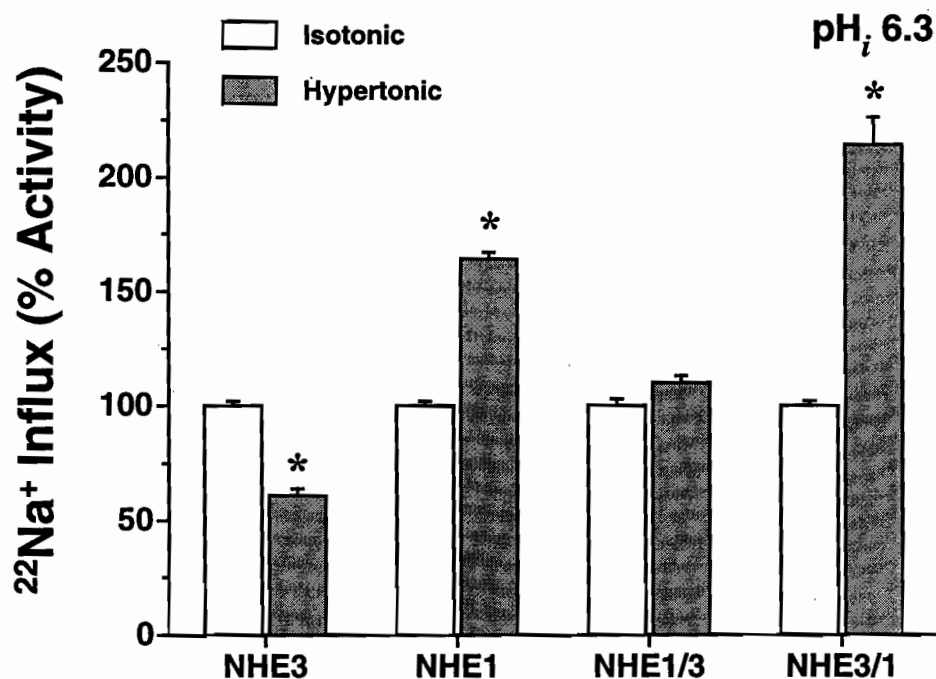


Fig. 4.2. Influence of hyperosmolarity on the activity of full-length NHE1 and NHE3 and chimeric NHE1/3 and NHE3/1 exchangers in AP-1 cells.  $\text{Na}^+/\text{H}^+$  exchanger activity was measured in cells stably transfected with indicated NHE constructs. Cell monolayers grown to confluence in 24-well plates were preincubated for 3 min in isotonic or hyperosmotic  $\text{K}^+$ -nigericin solution to clamp the intracellular pH at 6.3.  $^{22}\text{Na}^+$  influx was initiated by replacement of the same media supplemented with  $^{22}\text{NaCl}$  (1  $\mu\text{Ci}/\text{ml}$ ), 1 mM ouabain, with or without 2 mM amiloride. Radioisotope uptake was terminated after 10 min by rapid and expensive washing with ice-cold NaCl solution and the samples were processed as described under "Experimental Procedures." Background  $^{22}\text{Na}^+$  influx that was not inhibitable by 2 mM amiloride was subtracted from the total influx. Data are expressed as the mean percentage of amiloride-inhibitable  $^{22}\text{Na}^+$  influx  $\pm$  SE from 2-3 independent experiments each done in quadruplicate. Significant difference between isotonic and hyperosmotic measurements was determined by a two-tailed Student's *t*-test and is indicated by an asterisk ( $p < 0.001$ ).

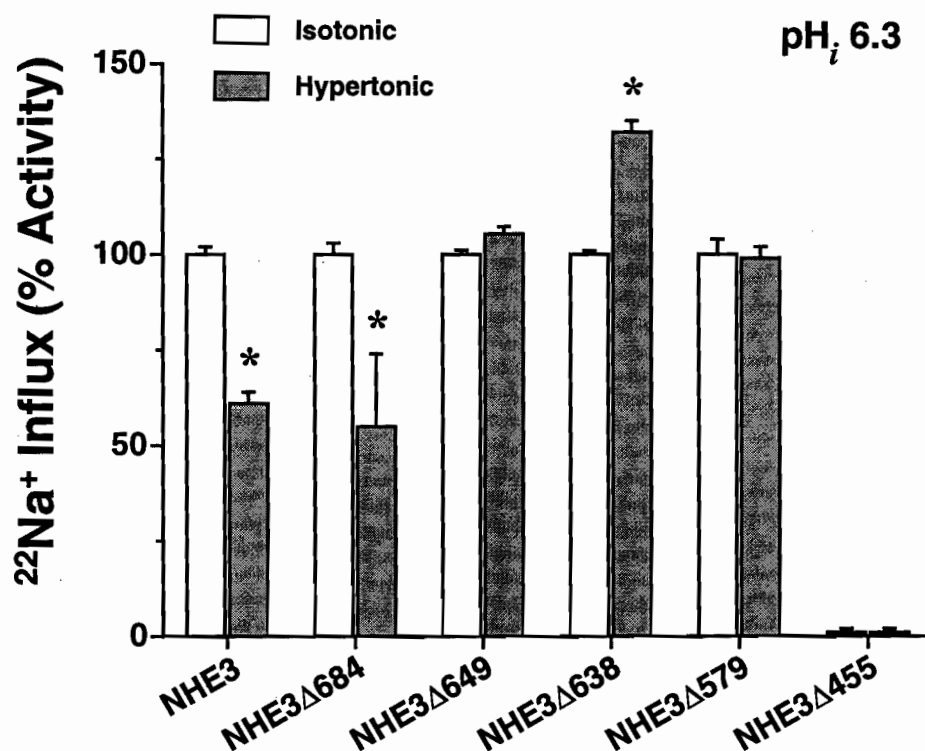


Fig. 4.3. **Influence of hyperosmolarity on the activity of full-length and C-terminally truncated NHE3.** AP-1 cells transfected with NHE3, NHE3Δ684, NHE3Δ649, NHE3Δ638, NHE3Δ579 were grown to confluence in 24-well plates and the effect of hyperosmolarity on the transport activities of the exchanger was studied exactly as described in the legend to Figure 4.2. Data are expressed as the mean percentage of amiloride-inhibitable  $^{22}\text{Na}^+$  influx  $\pm$  SE from 2-3 independent experiments each done in quadruplicate. Significant difference between isotonic and hyperosmotic measurements was determined by a two-tailed Student's *t*-test and is indicated by an *asterisk* ( $p < 0.001$ ).

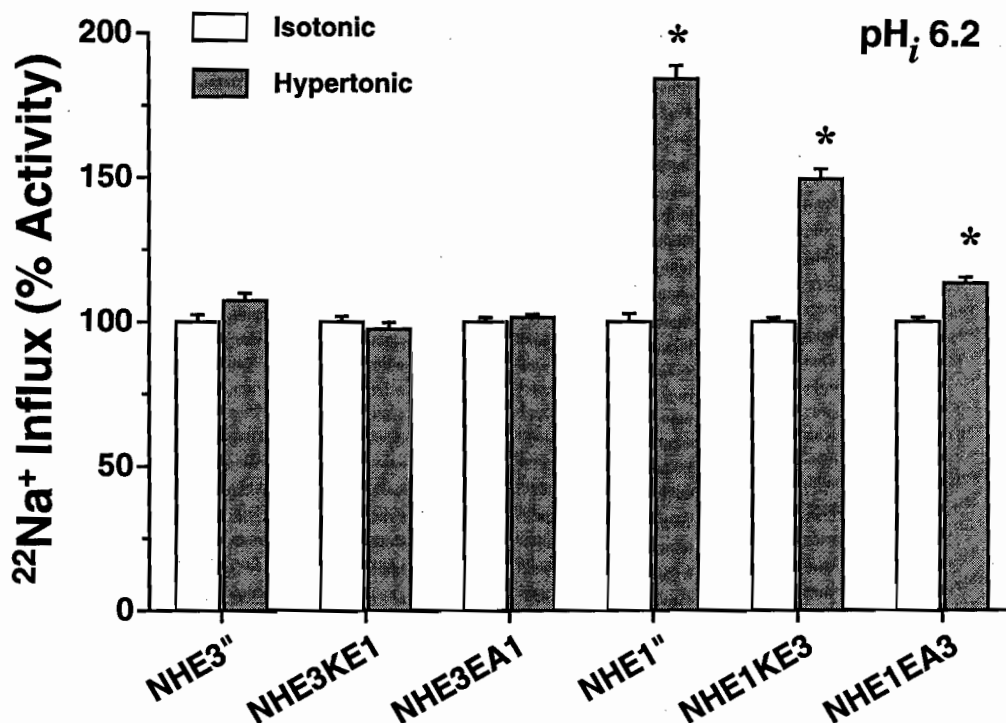


Fig. 4.4. Influence of hyperosmolarity on the activity of full-length  $\text{Na}^+/\text{H}^+$  exchanger NHE1 and NHE3 and their chimeric mutants of C-terminal segments. AP-1 cells were stably transfected with modified full-length  $\text{Na}^+/\text{H}^+$  exchanger isoforms NHE1 and NHE3 and chimeric exchangers that interchanged reciprocal C-terminal segments (detailed in "Experimental Procedures") and were grown to confluence in 24-well plates. The influence of hyperosmolarity on the transport activities of the exchangers was studied as described in the legend to Figure 4.2 with a minor modification. The intracellular pH was clamped at 6.2 by adjusting the concentration of *N*-methyl-D-glucamine methanesulphonate to 155 mM and potassium glutamate to 9 mM. Data are expressed as the mean percentage of amiloride-inhibitable  $^{22}\text{Na}^+$  influx  $\pm$  SE ( $n = 8$ ) from 2 independent experiments. Significant difference between control and experimental measurements was determined by Student's *t*-test and is indicated by an asterisk ( $p < 0.001$ ).

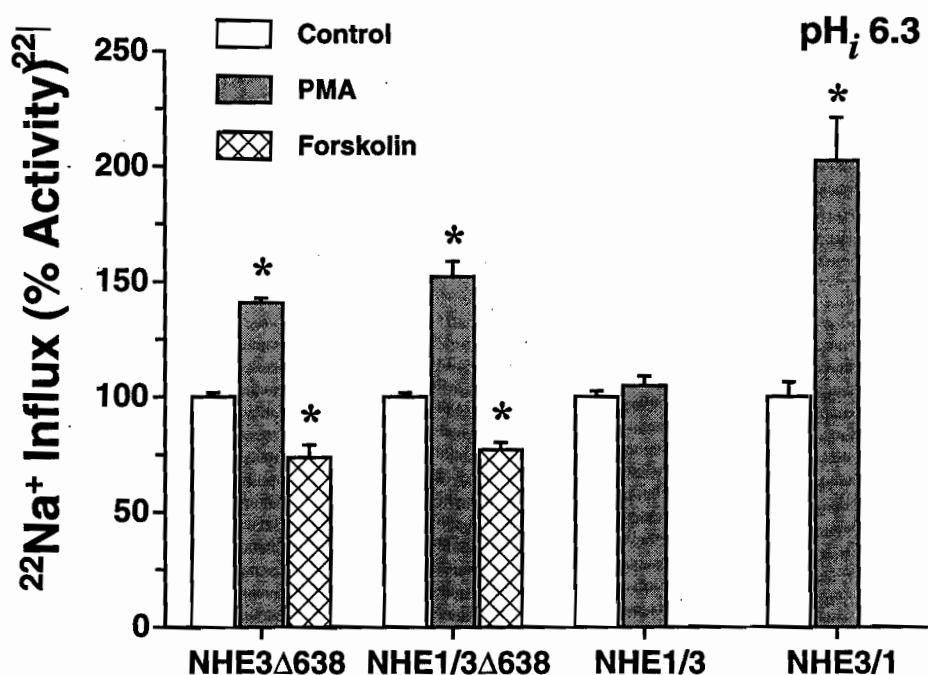


Fig. 4.5. Influence of phorbol ester (PMA) and forskolin on the transport activity of NHE3Δ638 and chimeric exchangers NHE1/3Δ638, NHE1/3 and NHE3/1. AP-1 cells stably transfected with indicated NHE constructs were grown to confluence in 24-well plates. The cell monolayers were washed twice with isotonic Na<sup>+</sup>-saline solution (130 mM NaCl, 5 mM KCl, 2 mM CaCl<sub>2</sub>, 1 mM MgCl<sub>2</sub>, 5 mM glucose, 20 mM HEPES-NaOH, pH 7.4). The cells were then preincubated in the same solution in the absence or presence of 10 μM forskolin for 15 min at 37 °C. Next, the medium was removed and the cells were preincubated for 3 min in K<sup>+</sup>-nigericin solution to clamp the intracellular pH at 6.3 in the presence and absence of 10 μM forskolin or 1 μM PMA. At the end of this equilibration period, the solutions were aspirated and replaced with the same media supplemented with <sup>22</sup>NaCl (1 μCi/ml), 1 mM ouabain, with or without 2 mM amiloride. Radioisotope uptake was terminated after 10 min by rapid and extensive washing with ice-cold NaCl stop solution and the samples were processed as described under "Experimental Procedures." Data are expressed as the mean percentage of amiloride-inhibitable <sup>22</sup>Na<sup>+</sup> influx ± SE from 2-3 independent experiments each done in quadruplicate. Significant difference between control and experimental measurements was determined by a two-tailed ANOVA and is indicated by an asterisk (*p* < 0.001).

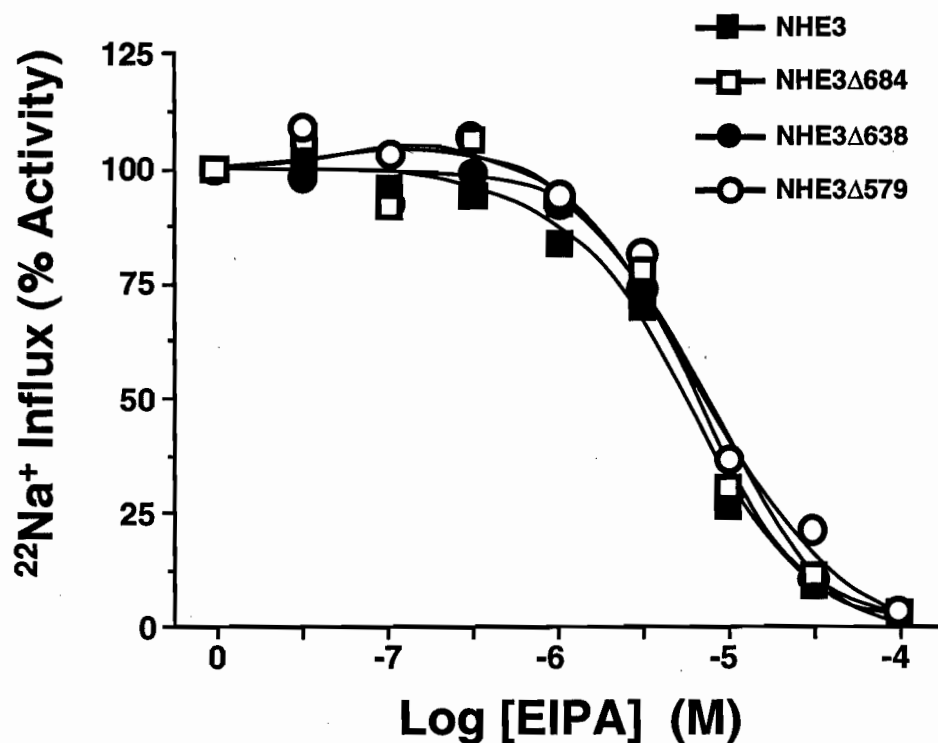


Fig. 4.6. **Concentration response profiles of inhibition of rat full-length NHE3 and truncation mutants by EIPA.** Stable transfectants of AP-1 cells expressing full-length rat NHE3 isoform (*closed square*) and various truncation mutants of NHE3 C-terminus, NHE3Δ684 (*open square*), NHE3Δ638 (*filled circle*) and NHE3Δ579 (*open circle*), were grown to confluence in 24-well plates. The Na<sup>+</sup>/H<sup>+</sup> exchanger transport activity was measured exactly as detailed previously (Refs. 108,200). The cells were loaded with H<sup>+</sup> using NH<sub>4</sub>Cl prepulse technique. Initial rates of H<sup>+</sup>-activated <sup>22</sup>Na<sup>+</sup> influx were measured in the presence of increasing EIPA concentrations up to 10<sup>-4</sup> M. Radioisotope uptake was terminated after 5 min by rapid and extensive washing with ice-cold Na<sup>+</sup>-solution and the samples were processed as described under "Experimental Procedures." Data were normalized as a percentage of the maximal rate of H<sup>+</sup>-activated <sup>22</sup>Na<sup>+</sup> influx in the absence of inhibitor. Values represent the average of duplicate wells.

## **Chapter V**

### **General Discussion and Conclusion**

The results of this thesis extend our understanding of the functional properties of members of the  $\text{Na}^+/\text{H}^+$  exchanger gene family. The data presented in Chapter II provided the first description of the general transport dynamics of NHE2 which are similar to those of the previously characterized NHE1 and NHE3 isoforms: that is a) reciprocal translocation of  $\text{Na}^+_o$  and  $\text{H}^+_i$ , and affinity for extracellular  $\text{H}^+$  and  $\text{Li}^+$ ; b) allosteric activation of the transport rate by  $\text{H}^+_i$ ; and c) inhibition by amiloride compounds and other antagonists. However, its affinities for the various drugs,  $\text{Na}^+$  and  $\text{H}^+$  clearly distinguished it from the other isoforms.

The functional properties of NHE2 in transfected cells most closely resemble those of NHE1, and hence it probably shares similar roles in  $\text{pH}_i$  and volume regulation. However its distinctive physiological role(s) in native tissues are less obvious. Future studies directed at understanding its transcriptional and post-translational regulation, as well as cellular or subcellular distribution may provide some greater insight into the physiological significance of this isoform. In this regard, the utilization of transgenic technology to knock out and/or overexpress the NHE2 gene may prove to be more informative and revealing.

The heterologous expression of rat NHE3 in AP-1 cells has also permitted more detailed investigation of its transport properties. The pharmacological and kinetic properties of this isoform in AP-1 cells are entirely consistent with the amiloride-insensitive  $\text{Na}^+/\text{H}^+$  exchanger localized to the apical membranes of polarized epithelia (108,134). In addition, agonists of the protein kinase A and C signaling pathways and hyperosmotic medium effectively depress NHE3 activity in AP-1 cells which are consistent with the responses observed for the endogenous NHE3 found in renal proximal tubule OK cells (41,139,150), rat medullary thick ascending limb (151), and rabbit renal



brush border membranes (137). However, the mechanism(s) by which these various molecular signals inhibit NHE3 activity has yet to be fully resolved.

The simplest interpretation of the observed loss of cAMP-dependent inhibition of the truncation mutant NHE3 $\Delta$ 579 is the removal of potential phosphorylation sites for PKA, although one must consider that an altered secondary structure in mutational analysis of protein may influence function or regulation without it being the actual site of function or regulation. Consistent with this notion, Moe *et al.* (140) have recently demonstrated that treatment of stable transfectants (AP-1 cells) of rat NHE3 with a cAMP analogue resulted in three-fold increase in phospho-content of the exchanger. Furthermore, the catalytic subunit of PKA phosphorylated the cytoplasmic domain of NHE3 on undefined serine residues *in vitro*. These findings support the suggestion that PKA-mediated inhibition of NHE3 may act through phosphorylation at RELS<sup>661</sup> or RRRS<sup>605</sup>IR, sites which resemble the optimal PKA consensus sequence (R-R-X-S\*/T\*) (197). Extensions of the present studies would be to compare the phosphorylation states of the truncation mutants NHE3 $\Delta$ 579 and NHE3 $\Delta$ 638 in response to PKA and to target the putative serine phosphorylation consensus sequences in this region for site-directed mutagenesis. With regard to the latter, a significant disruption of the consensus sequence would be expected to abrogate the cAMP-dependent inhibition whereas a conversion of the phosphorylation target, serine, to threonine would be predicted to have no influence on the inhibitory effect. These future studies assume that the mechanism of cAMP-dependent inhibition of NHE3 involves a direct phosphorylation of the exchanger by PKA and that this change causes the inhibitory effect; however, this has yet to be clearly demonstrated. An alternative mechanism has been proposed where PKA-mediated inhibition of the rabbit renal apical Na<sup>+</sup>/H<sup>+</sup> exchanger may occur via an intermediary phosphorylation-dependent ancillary protein (144,145).

A closer examination of NHE3's amino acid sequence between residues 579-684 reveals an intriguing possibility that the molecular basis of cAMP-dependent inhibition may involve additional components. Alignment of this region with those of rat NHE1, NHE2 and NHE4 reveals that 27 amino acids between residues S<sup>605</sup> and Y<sup>634</sup> appear to have been inserted (or not lost) during the course of evolution. Of these residues, the sequence <sup>606</sup>IRDTEDMVTHHTL<sup>618</sup> bear a reasonable homology to the EF-hand calcium binding domain (201). Whether this segment binds Ca<sup>2+</sup> is unknown. Nevertheless, the presence of calcium appears to be important for NHE3 activity. In preliminary experiments, the chelation of intracellular Ca<sup>2+</sup> using BAPTA-AM inhibited the transport activity of NHE3 by ~75%, whereas the transport rates of NHE1 and NHE2 were less depressed (25% and 40%, respectively) (unpublished observations, F.H. Yu and J. Orłowski). Thus, one speculative mechanism to account for cAMP-PKA regulation of NHE3 is that kinase phosphorylation of residues S<sup>605</sup> and/or S<sup>635</sup> alters the structural conformation of this potential Ca<sup>2+</sup> binding region, leading to decreased Ca<sup>2+</sup> affinity and reduction of NHE3 activity. This hypothesis predicts that direct binding of Ca<sup>2+</sup> is essential for the transport activity of NHE3. This could be tested by measuring the binding of radioactive <sup>45</sup>Ca<sup>2+</sup> to *in vitro* translated wild type and mutant NHE3 transporters that fail to respond to cAMP using the gel-overlay technique.

Similar to the cAMP-dependent response, the mechanism of hyperosmotic-mediated inhibition of NHE3 is also poorly defined. However, our results suggest that the underlying mechanisms are likely to be different due to the identification of distinct, but partly overlapping inhibitory regions. The strongest evidence that supports this notion is from the chimeric analysis of NHE1 and NHE3 that examined the capability of the C-terminal tail regions to transfer the regulatory characteristics to the ion translocating N-terminal regions. While the cAMP-mediated inhibition of wild type NHE3 appeared to be qualitatively preserved in the NHE1/3 chimera, the hyperosmotic-mediated inhibition

was lost. The latter results are suggestive of a mechanism that requires an interaction between the osmo-responsive inhibitory region of the cytoplasmic tail with the *N*-terminal transmembrane domain. To address this possibility, segments of the osmo-responsive inhibitory region could be used as probes in the yeast two-hybrid system or a phage-display system to screen peptide fragments constructed from the *N*-terminal transmembrane region.

A serendipitous finding from the structural analyses of NHE3 hyperosmotic response was the identification of a *C*-terminal tail segment spanning residues 455-638 that harbours an inherent potential to stimulate ion transport. It should be noted that this region of NHE3 was also similarly sensitive to activation by the PKC pathway. However, these stimulatory effects likely have little functional significance as it was apparent only upon removal of the *C*-terminal amino acids. The more plausible explanation is the conservation of amino acid residues through evolution in this segment of NHE3 tail that displays homology to that of NHE1 (which is stimulated by PMA- and hyperosmolarity).

Nonetheless, it is interesting to note that the hyperosmotic-mediated responses of the wild type and the various chimeras of NHE1 and NHE3 generally paralleled the PKC-mediated responses (*cf.*, Figs. 4.2, 4.5, and Ref. 141). These observations are suggestive of a converging common underlying mechanism. Indeed, independent processes may not be involved in the hyperosmolarity- or PMA-sensitive activations of  $\text{Na}^+/\text{H}^+$  exchangers as these effects have been shown to be not additive in lymphocytes (18). Furthermore, since no common phosphorylation consensus sequences are shared between the wild type NHE1 and the truncation mutant NHE3 $\Delta$ 638 and yet, both are similarly activated by hypertonicity and PMA, the mechanism may not require a direct phosphorylation of the transporter. Indeed, the hyperosmotic activation of NHE1 appears to occur without

additional phosphorylation (152). Thus, it is conceivable that the cellular signaling cascades which are recruited in response to hypertonicity and PMA converge upstream of the exchangers, perhaps at a level of a putative ancillary protein. If the hypothesis is correct, the previous findings (198) and the results presented in Chapters III and IV would predict a binding site that includes a portion of the tail near its emergence from the membrane, although an interaction site in *N*-terminal transmembrane domain cannot be ruled out.

Last, numerous attempts were also made to investigate the functional properties of the rat NHE4 isoform, although the data was not presented in this thesis. For reasons which are not well understood, we have been unable to obtain functional expression of rat NHE4 in our AP-1 cells (data not presented) despite the high degree of homology (~60% identity overall) that exists between NHE2 and NHE4 (33,47). Complete sequencing of rat genomic clones and reverse transcription-polymerase chain reaction (RT-PCR) products of NHE4 confirmed the coding sequence obtained from the initially isolated cDNA, thereby eliminating the possibility of a cDNA cloning artifact (data not shown). Conceivably, there may be cell-specific component(s) necessary for the functional expression of NHE4 that are lacking in the AP-1 cells. In contrast, Chang and colleagues have obtained very low levels of expression of rat NHE4 in PS120 cells (60). They were able to demonstrate amiloride-sensitive  $^{22}\text{Na}^+$  influx into NHE4 transfectants only under conditions of both low intracellular pH ( $\text{pH}_i$  ~6.0) and high extracellular osmolarity (~500 mosM). Based on the specific expression of NHE4 mRNA in the inner medullary collecting tubules, a region of the kidney where high osmolarity exists, it has been suggested that this isoform may have a specialized role in volume homeostasis in these cells (60).

However, it seems unlikely that such low transport activity of NHE4 would be physiologically relevant. In fact, our analysis of these transfectants expressing NHE4 that were obtained from Dr. Chang showed < 0.5% of the activity of NHE2 transfectants (data not shown). Furthermore, these cells failed to survive the standard  $\text{NH}_4^+$ -induced acid-recovery selection protocol that discriminates functional  $\text{Na}^+/\text{H}^+$  exchanger positive and negative stable transfectants (unpublished observation, F.H. Yu and J. Orlowski), most likely due to very low or negligible transport activity.

We have employed additional expression strategies to study this lack of function or very low transport activity of NHE4. These include: 1) treatment of NHE4 transfectants with a myriad of agents that activate the various intracellular signaling pathways during the acid survival selection procedure; 2) transfection of several different C-terminally truncated NHE4 mutants; 3) conversion of several non-conservative amino acid changes in the transmembrane domain of NHE4 to those of NHE2; 4) generation of chimeric exchanger that substitute the *N*-terminal leading sequence (80 amino acids) with the corresponding segment of NHE2; 5) generation of chimeric exchanger which replaced the *C*-terminal tail region of NHE4 with that of NHE2. All of these strategies were unsuccessful. Interestingly, the analysis of the converse chimeric exchangers revealed that when the *N*-terminal 80 amino acids or *C*-terminal tail of NHE4 were substituted into NHE2, functional chimeric  $\text{Na}^+/\text{H}^+$  exchangers were obtained (unpublished observations, F.H. Yu and J. Orlowski), indicating that the molecular basis of the defect in functional expression resides between amino acids 80 and 472 of the *N*-terminal transmembranous region of NHE4. One possible strategy to identify the amino acid residues that may be hindering the transport activity of NHE4 would be to use random mutagenesis of this region and then select for functional revertants using the acid selection protocol. An important question that also has not been addressed is whether the transfectants express mature NHE4 protein on the plasma membrane. Recent availability of NHE4-specific

antibody and epitope tagging of the NHE4 isoform should facilitate the determination of the subcellular localization of the NHE4 protein in transfected and native cells.

### **Concluding Remarks**

The results of this thesis make new contributions to our understanding of the structure-function relationships of the  $\text{Na}^+/\text{H}^+$  exchanger gene family. The deletion and chimeric analyses have provided significant insights into the structural regions of these transporters – in particular NHE3 – that are critical by acute regulation for various stimuli. Needless to say, further studies will be required to fully understand the molecular basis of  $\text{Na}^+/\text{H}^+$  exchanger regulation.

## BIBLIOGRAPHY

1. Roos, A. and Boron, W.F. (1981) Intracellular pH. *Physiol. Rev.* **61**: 296-434
2. Grinstein, S. and Rothstein, A. (1986) Mechanisms of regulation of the  $\text{Na}^+/\text{H}^+$  exchanger. *J. Membr. Biol.* **90**: 1-12
3. Mahnensmith, R.L. and Aronson, P.S. (1985) The plasma membrane sodium hydrogen exchanger and its role in physiological and pathophysiological processes. *Circ. Res.* **56**: 773-788
4. Moolenaar, W.H. (1986) Effects of growth factors on intracellular pH regulation. *Annu. Rev. Physiol.* **48**: 363-376
5. Grinstein, S., Rotin, D. and Mason, M.J. (1989)  $\text{Na}^+/\text{H}^+$  exchange and growth factor-induced cytosolic pH changes. Role in cellular proliferation. *Biochim. Biophys. Acta* **988**: 73-97
6. Murer, H., Hopfer, U. and Kinne, R. (1976) Sodium/proton antiport in brush-border membrane vesicles isolated from rat small intestine and kidney. *Biochem. J.* **154**: 597-604
7. Clark, J.D. and Limbird, L.E. (1991)  $\text{Na}^+/\text{H}^+$  exchanger subtypes: A predictive review. *Am. J. Physiol.* **261**: C945-C953
8. Haggerty, J.G., Agarwal, N., Reilly, R.F., Adelberg, E.A. and Slayman, C. (1988) Pharmacologically different Na/H antiporters on the apical and basolateral surfaces of cultured porcine kidney cells (LLC-PK1). *Proc. Natl. Acad. Sci. USA* **85**: 6797-6801
9. Knickelbein, R.G., Aronson, P.S. and Dobbins, J.W. (1990) Characterization of  $\text{Na}^+/\text{H}^+$  exchangers on villus cells in rabbit ileum. *Am. J. Physiol.* **259**: G802-G806
10. Kulanthaivel, P., Liebach, F.H., Mahesh, V.B., Cragoe, E.J. and Ganapathy, V. (1990) The  $\text{Na}^+/\text{H}^+$  exchanger of the placental brush border membrane is pharmacologically distinct from that of the renal brush-border membrane. *J. Biol. Chem.* **265**: 1249-1252
11. Casavola, V., Helmle-Kolb, C. and Murer, H. (1989) Separate regulatory control of apical and basolateral  $\text{Na}^+/\text{H}^+$  exchange in renal epithelial cells. *Biochem. Biophys. Res. Commun.* **165**: 833-837
12. Montrose, M.H., Friedrich, T. and Murer, H. (1987) Measurements of intracellular pH in single LLC-PK<sub>1</sub> cells: recovery from an acid load via basolateral  $\text{Na}^+/\text{H}^+$  exchange. *J. Membr. Biol.* **97**: 63-78

13. Knickelbein, R.G., Aronson, P.S. and Dobbins, J. (1988) Membrane distribution of sodium-hydrogen and chloride-bicarbonate exchangers in crypt and villus cell membranes from rabbit ileum. *J. Clin. Invest.* **82**: 2158-2163
14. Ganapathy, M.E., Liebach, F.H., Mahesh, V.B., Devoe, L.D. and Ganapathy, V. (1986) Interaction of clonidine with human placental  $\text{Na}^+\text{-H}^+$  exchanger. *Biochem. Pharmacol.* **35**: 3989-3994
15. Kulanthaivel, P., Furesz, T.C., Moe, A.J., Smith, C.H., Mahesh, V.B., Liebach, F.H. and Ganapathy, V. (1992) Human placental syncytiotrophoblast expresses two pharmacologically distinguishable types of  $\text{Na}^+\text{-H}^+$  exchangers, NHE-1 in the maternal-facing (brush border) membrane and NHE-2 in the fetal-facing (basal) membrane. *Biochem. J.* **284**: 33-38
16. Rajendran, V.M. and Binder, H.J. (1990) Characterization of  $\text{Na}^+\text{/H}^+$  exchanger in apical membrane vesicles of rat colon. *J. Biol. Chem.* **265**: 8408-8414
17. Wakabayashi, S., Sardet, C., Fafournoux, P., Counillon, L., Meloche, S., Pages, G. and Pouyssegur, J. (1992) Structure function of the growth factor-activatable  $\text{Na}^+\text{/H}^+$  exchanger (NHE1). *Rev. Physiol. Biochem. Pharmacol.* **119**: 157-186
18. Grinstein, S., Cohen, S., Goetz, J.D. and Rothstein, A. (1985) Osmotic and phorbol ester-induced activation of  $\text{Na/H}$  exchange: possible role of protein phosphorylation in lymphocyte volume regulation. *J. Cell. Biol.* **101**: 269-276
19. Grinstein, S., Elder, B. and Furuya, W. (1985) Phorbol ester induced changes of cytoplasmic pH in neutrophils. role of exocytosis in  $\text{Na}^+\text{-H}^+$  exchange. *Am. J. Physiol.* **248**: C379-C386
20. Owen, M.E. (1985) Effect of TPA on ion fluxes and DNA synthesis in vascular smooth muscle cells. *J. Cell. Biol.* **101**: 454-459
21. Vigne, P., Frelin, C. and Lazdunski, M. (1985) The  $\text{Na/H}$  exchange system is activated by serum and phorbol esters in proliferating myoblasts but not in differentiated myotubes. Properties of the activation process. *J. Biol. Chem.* **260**: 8008-8013
22. Cassel, D., Whiteley, B., Zhuang, Y.X. and Glaser, L. (1985) Mitogen-independent activation of  $\text{Na}^+\text{-H}^+$  exchange in human epidermoid carcinoma A431 cells: regulation by medium osmolarity. *J. Cell. Physiol.* **122**: 178-186
23. Balkovetz, D.F., Miyamoto, Y., Tiruppathi, C., Mahesh, V.B., Liebach, F.H. and Ganapathy, V. (1987) Inhibition of brush-border membrane  $\text{Na}^+\text{-H}^+$  exchanger by loperamide. *J. Pharmacol. Exp. Ther.* **243**: 150-154



24. Caverzasio, J., Rizzoli, R. and Bonjour, J.A. (1986) Sodium-dependent phosphate transport inhibited by parathyroid hormone and cyclic AMP-stimulation in an opossum kidney cell line. *J. Biol. Chem.* **261**: 3233-3237
25. Helmle-Kolb, C., Montrose, M.H., Stange, G. and Murer, H. (1990) Regulation of  $\text{Na}^+/\text{H}^+$  exchange in opossum kidney cells by parathyroid hormone, cyclic AMP and phorbol esters. *Pflügers Arch.* **415**: 461-470
26. Pollock, A.S., Warnock, D.G. and Strewler, G.J. (1986) Parathyroid hormone inhibition of Na/H exchanger activity in a cultured renal cell line. *Am. J. Physiol.* **250**: F217-F225
27. Sardet, C., Franchi, A. and Pouyssegur, J. (1989) Molecular cloning, primary structure, and expression of the human growth factor-activatable Na/H antiporter. *Cell* **56**: 271-280
28. Pouyssegur, J. (1985) The growth factor-activatable  $\text{Na}^+/\text{H}^+$  exchanger system: a genetic approach. *Trends Biochem. Sci.* **11**: 453-455
29. Pouyssegur, J., Sardet, C., Franchi, A., L'Allemain, G. and Paris, S. (1984) A specific mutation abolishing  $\text{Na}^+/\text{H}^+$  antiport activity in hamster fibroblasts precludes growth at neutral and acidic pH. *Proc. Natl. Acad. Sci. USA* **81**: 4833-4837
30. Franchi, A., Perucca Lostanlen, D. and Pouyssegur, J. (1986) Functional expression of a transfected  $\text{Na}^+/\text{H}^+$  antiporter human gene in antiporter-deficient mouse L cells. *Proc. Natl. Acad. Sci. USA* **83**: 9388-9392
31. Takaichi, K., Wang, D., Balkovetz, D.F. and Warnock, D.G. (1992) Cloning, sequencing, and expression of  $\text{Na}^+/\text{H}^+$  antiporter cDNAs from human tissues. *Am. J. Physiol.* **262**: C1069-C1076
32. Fliegel, L., Dyck, J.R.B., Wang, H. and Haworth, R.S. (1993) Cloning and analysis of the human myocardial  $\text{Na}^+/\text{H}^+$  exchanger. *Mol. Cell. Biochem.* **125**: 137-143
33. Orlowski, J., Kandasamy, R.A. and Shull, G.E. (1992) Molecular cloning of putative members of the Na/H exchanger gene family. cDNA cloning, deduced amino acid sequence, and mRNA tissue expression of the rat Na/H exchanger NHE-1 and two structurally related proteins. *J. Biol. Chem.* **267**: 9331-9339
34. Tse, C.-M., Ma, A.I., Yang, V.W., Watson, A.J.M., Levine, S., Montrose, M.H., Potter, J., Sardet, C., Pouyssegur, J. and Donowitz, M. (1991) Molecular cloning and expression of a cDNA encoding the rabbit ileal villus basolateral membrane  $\text{Na}^+/\text{H}^+$  exchanger. *EMBO J.* **10**: 1957-1967

35. Hildebrandt, F., Pizzonia, J.H., Reilly, R.F., Reboucas, N.A., Sardet, C., Pouyssegur, J., Slayman, C.W., Aronson, P.S. and Igarashi, P. (1991) Cloning, sequence and tissue distribution of a rabbit renal  $\text{Na}^+/\text{H}^+$  exchanger transcript. *Biochim. Biophys. Acta.* **1129**: 105-108
36. Reilly, R.F., Hildebrandt, F., Biemesderfer, D., Sardet, C., Pouyssegur, J., Aronson, P.S., Slayman, C.W. and Igarashi, P. (1991) cDNA Cloning and immunolocalization of a  $\text{Na}^+/\text{H}^+$  exchanger in LLC-PK<sub>1</sub> renal epithelial cells. *Am. J. Physiol.* **261**: F1088-F1094
37. Counillon, L. and Pouyssegur, J. (1993) Nucleotide sequence of the Chinese hamster  $\text{Na}^+/\text{H}^+$  exchanger NHE1. *Biochim. Biophys. Acta* **1172**: 343-345
38. Borgese, F., Sardet, C., Cappadoro, M., Pouyssegur, J. and Montais, R. (1992) Cloning and expression of a cAMP-activated  $\text{Na}^+/\text{H}^+$  exchanger: Evidence that the cytoplasmic domain mediates hormonal regulation. *Proc. Natl. Acad. Sci. USA* **89**: 6765-6769
39. Marra, M.A., Prasad, S.S. and Baillie, D.L. (1993) Molecular analysis of two genes between Let-653 and Let-56 in the Unc-22(IV) region of *Caenorhabditis elegans*. *Mol. Gen. Genet.* **236**: 289-298
40. Jia, Z.P., McCullough, N., Martel, R., Hemmingsen, S.K. and Young, P.G. (1992) Gene amplification at a locus encoding a putative  $\text{Na}^+/\text{H}^+$  antiporter confers sodium and lithium tolerance in fission yeast. *EMBO J.* **11**: 1631-1640
41. Azarani, A., Goltzman, D. and Orłowski, J. (1995) Parathyroid hormone and parathyroid hormone-related peptide inhibit the apical  $\text{Na}^+/\text{H}^+$  exchanger NHE-3 isoform in renal cells (OK) via a dual signaling cascade involving protein kinase A and C. *J. Biol. Chem.* **270**: 20004-20010
42. Krapf, R., Solioz, M. and Fehlmann, C. (1991) Na/H antiporter mRNA expression in single nephron segments of rat kidney cortex. *J. Clin. Invest.* **88**: 783-788
43. Bookstein, C., DePaoli, A., Xie, Y., Niu, P., Musch, M.W., Rao, M.C. and Chang, E.B. (1994)  $\text{Na}^+/\text{H}^+$  exchangers, NHE-1 and NHE-3, of rat intestine. Expression and localization. *J. Clin. Invest.* **93**: 106-113
44. Watson, A.M., Levine, S., Donowitz, M. and Montrose, M.H. (1991) Kinetics and regulation of a polarized Na/H exchanger from Caco-2 cell, a human intestinal cell line. *Am. J. Physiol.* **261**: G229-G238
45. Biemesderfer, D., Reilly, R.F., Exner, M., Igarashi, P. and Aronson, P. (1992) Immunocytochemical characterization of Na-H exchanger isoform NHE1 in rabbit kidney. *Am. J. Physiol.* **263**: F833-F840

46. Orlowski, J. and Shull, G.E. (1996) Characteristics of the plasma membrane  $\text{Na}^+/\text{H}^+$  exchanger gene family. In *The  $\text{Na}^+/\text{H}^+$  Exchanger* (ed. L. Fliegel), pp. 123-148. Molecular Biology Intelligence Unit, R. G. Landes Company, Biomedical Publishers, Austin, Texas
47. Wang, Z., Orlowski, J. and Shull, G.E. (1993) Primary structure and functional expression of a novel gastrointestinal isoform of the rat Na/H exchanger. *J. Biol. Chem.* **268**: 11925-11928
48. Tse, C.-M., Levine, S., Yun, C.H.C., Montrose, M.H., Little, P.L., Pouyssegur, J. and Donowitz, M. (1993) Cloning and expression of a rabbit cDNA encoding a serum-activated ethylisopropylamiloride-resistant epithelial  $\text{Na}^+/\text{H}^+$  exchanger isoform (NHE-2). *J. Biol. Chem.* **268**: 11917-11924
49. Collins, J.F., Honda, T., Bulus, N.M., Conary, J., DuBois, R. and Ghishan, F.K. (1993) Molecular cloning, sequencing, tissue distribution, and functional expression of a  $\text{Na}^+/\text{H}^+$  exchanger (NHE2). *Proc. Natl. Acad. Sci. USA* **90**: 3938-3942
50. Mount, S.M. (1982) A catalogue of splice junction sequences. *Nucleic Acids Res.* **10**: 459-472
51. Soleimani, M., Singh, G., Bizal, G.L., Gullans, S.R. and McAteer, J.A. (1994)  $\text{Na}^+/\text{H}^+$  exchanger isoforms NHE2 and NHE1 in inner medullary collecting duct cells. *J. Biol. Chem.* **269**: 27973-27978
52. Mrkic, B., Tse, C.-M., Forgo, J., Helmle-Kolb, C., Donowitz, M. and Murer, H. (1993) Identification of PTH-responsive Na/H exchanger isoforms in a rabbit proximal tubule cell line (RKPC-2). *Pflügers Arch.* **424**: 377-384
53. Kapus, A., Grinstein, S., Wasan, S., Kandasamy, R. and Orlowski, J. (1994) Functional characterization of three isoforms of the  $\text{Na}^+/\text{H}^+$  exchanger stably expressed in Chinese hamster ovary cells: ATP dependence, osmotic sensitivity, and role in cell proliferation. *J. Biol. Chem.* **269**: 23544-23552
54. Tse, C.-M., Brant, S.R., Walker, S.M., Pouyssegur, J. and Donowitz, M. (1992) Cloning and sequencing of a rabbit cDNA encoding an intestinal and kidney-specific  $\text{Na}^+/\text{H}^+$  exchanger isoform (NHE-3). *J. Biol. Chem.* **267**: 9340-9346
55. Amemiya, M., Yamaji, Y., Cano, A., Moe, O.W. and Alpern, R.J. (1995) Acid incubation increases NHE-3 mRNA abundance in OKP cells. *Am. J. Physiol.* **269**: C126-C133
56. Brant, S., Yun, C.H.C., Donowitz, M. and Tse, C.-M. (1995) Molecular cloning, functional analysis and unique tissue distribution of a human, amiloride-resistant  $\text{Na}^+/\text{H}^+$  exchanger isoform, NHE-3. *Am. J. Physiol.* **269**: C198-C206

57. Biemesderfer, D., Pizzonia, J., Exner, M., Reilly, R.F., Igarashi, P. and Aronson, P. (1993) NHE3: A Na/H exchanger isoform of the renal brush border. *Am J. Physiol.* **265**: F736-F742
58. Soleimani, M., Bookstein, C., Bizal, G.L., Musch, M.W., Hattabaugh, Y.J., Rao, M.C. and Chang, E.B. (1994) Localization of the Na<sup>+</sup>/H<sup>+</sup> exchanger isoform NHE-3 in rabbit and canine kidney. *Biochim. Biophys. Acta* **1195**: 89-95
59. Ives, H.E., Yee, V.J. and Warnock, D.G. (1983) Asymmetric distribution of the Na<sup>+</sup>/H<sup>+</sup> antiporter in the renal proximal tubule epithelial cell. *J. Biol. Chem.* **258**: 13513-13516
60. Bookstein, C., Musch, M.W., DePaoli, A., Xie, Y., Villereal, M., Rao, M.C. and Chang, E.B. (1994) A unique sodium-hydrogen exchange isoform (NHE4) of the inner medulla of the rat kidney is induced by hyperosmolarity. *J. Biol. Chem.* **269**: 29704-29709
61. Klanke, C.A., Su, Y.R., Callen, D.F., Wang, Z., Meneton, P., Baird, N., Kandasamy, R.A., Orłowski, J., Otterud, B.E., Leppert, M., Shull, G.E. and Menon, A.G. (1995) Molecular cloning, physical and genetic mapping of a novel human Na<sup>+</sup>/H<sup>+</sup> exchanger (NHE5/SLC9A5) to chromosome 16q22.1. *Genomics* **25**: 615-622
62. Mattei, M.G., Sardet, C., Franchi, A. and Pouyssegur, J. (1988) The human amiloride-sensitive Na<sup>+</sup>/H<sup>+</sup> antiporter: localization to chromosome 1 by *in situ* hybridization. *Cytogenet. Cell. Genet.* **48**: 6-8
63. Szpirer, C., Szpirer, J., Riviere, M., Levan, G. and Orłowski, J. (1994) Chromosomal assignment of four genes encoding Na/H exchanger isoforms in human and rat. *Mammalian Genome* **5**: 153-159
64. Brant, S.R., Bernstein, M., Wasmuth, J.J., Taylor, E.W., McPherson, J.D., Li, X., Walker, S., Pouyssegur, J., Donowitz, M., Tse, C.-M. and Jabs, E.W. (1993) Physical and genetic mapping of a human epithelial Na<sup>+</sup>/H<sup>+</sup> exchanger (NHE3) isoform to chromosome 5p15.3. *Genomics* **15**: 668-672
65. Miller, R.T., Counillon, L., Pages, G., Lifton, R.P., Sardet, C. and Pouyssegur, J. (1991) Structure of the 5'-flanking regulatory region and gene for the human growth factor-activatable Na/H exchanger NHE-1. *J. Biol. Chem.* **266**: 10813-10819
66. Dyck, J.R.B., Silva, N.L.C.L. and Fliegel, L. (1995) Activation of the Na<sup>+</sup>/H<sup>+</sup> exchanger gene by the transcription factor AP-2. *J. Biol. Chem.* **270**: 1375-1381
67. Blaurock, M.C., Reboucas, N.A., Kusnezov, J.L. and Igarashi, P. (1995) Phylogenetically conserved sequences in the promoter of the rabbit sodium-hydrogen exchanger isoform 1 gene (NHE1/SLC9A1). *Biochim. Biophys. Acta* **1262**: 159-163

68. Dyck, J.R.B. and Fliegel, L. (1995) Specific activation of the Na<sup>+</sup>/H<sup>+</sup> exchanger gene during neuronal differentiation of embryonic carcinoma cells. *J. Biol. Chem.* **270**: 10420-10427
69. Kyte, J. and Doolittle, R.F. (1982) A simple method for displaying the hydrophobic character of a protein. *J. Mol. Biol.* **157**: 105-132
70. Engelman, D.M., Goldman, A. and Steitz, T.A. (1982) The identification of helical segments in the polypeptide chain of *Bacteriorhodopsin*. *Methods Enzymol.* **88**: 81-89
71. Sardet, C., Counillon, L., Franchi, A. and Pouyssegur, J. (1990) Growth factors induce phosphorylation of the Na/H antiporter, a glycoprotein of 110 kD. *Science* **247**: 723-726
72. Fliegel, L. and Frohlich, O. (1993) The Na<sup>+</sup>/H<sup>+</sup> exchanger: an update on structure, regulation and cardiac physiology. *Biochem. J.* **296**: 273-285
73. Fliegel, L., Haworth, R.S. and Dyck, J.R.B. (1993) Characterization of the placental brush border membrane Na<sup>+</sup>/H<sup>+</sup> exchanger. Identification of thiol-dependent transitions in apparent molecular size. *Biochem. J.* **289**: 101-107
74. Fafournoux, P., Noël, J. and Pouyssegur, J. (1994) Evidence that Na<sup>+</sup>/H<sup>+</sup> exchanger isoforms NHE1 and NHE3 exist as stable dimers in membranes with a high degree of specificity for homodimers. *J. Biol. Chem.* **269**: 2589-2596
75. Otsu, K., Kinsella, J.L., Heller, P. and Froelich, J.P. (1993) Sodium dependence of the Na<sup>+</sup>/H<sup>+</sup> exchanger in the pre-steady state. Implications for the exchange mechanism. *J. Biol. Chem.* **268**: 3184-3193
76. Beliveau, R., Demeule, M. and Potier, M. (1988) Molecular size of the Na<sup>+</sup>/H<sup>+</sup> antiport in renal brush border membranes, as estimated by radiation inactivation. *Biochem. Biophys. Res. Commun.* **152**: 484-489
77. Counillon, L., Pouyssegur, J. and Reithmeir, R.A.F. (1994) The Na<sup>+</sup>/H<sup>+</sup> exchanger NHE-1 possesses N- and O-linked glycosylation restricted to the first N-terminal extracellular domain. *Biochemistry* **33**: 10463-10469
78. Tse, C.-M., Levine, S., Yun, C.H.C., Khurana, S. and Donowitz, M. (1994) The Na<sup>+</sup>/H<sup>+</sup> exchanger-2 (NHE-2) is an O-linked but not a N-linked sialoglycoprotein. *Biochemistry* **33**: 12594-12561
79. Haworth, R.S., Frohlich, O. and Fliegel, L. (1993) Multiple carbohydrate moieties on the Na<sup>+</sup>/H<sup>+</sup> exchanger. *Biochem. J.* **289**: 637-640
80. Yusufi, A.N.K., Szczepanska-Konkel, M. and Dousa, T.P. (1988) Role of N-linked oligosaccharides in the transport activity of the Na/H antiporter in rat renal brush-border membrane. *J. Biol. Chem.* **263**: 13683-13691

81. Aronson, P.S. (1985) Kinetic properties of the plasma membrane  $\text{Na}^+$ - $\text{H}^+$  exchanger. *Ann. Rev. Physiol.* **47**: 545-560
82. Ives, H.E., Yee, V.J. and Warnock, D.G. (1983) Mixed type inhibition of the renal  $\text{Na}^+/\text{H}^+$  antiporter by  $\text{Li}^+$  and amiloride. Evidence for a modifier site. *J. Biol. Chem.* **258**: 9710-9716
83. Grinstein, S., Cohen, S. and Rothstein, A. (1984) Cytoplasmic pH regulation in thymic lymphocytes by an amiloride sensitive  $\text{Na}^+/\text{H}^+$  antiport. *J. Gen. Physiol.* **83**: 341-369
84. Gunther, R.D. and Wright, E.M. (1983)  $\text{Na}^+$ ,  $\text{Li}^+$  and  $\text{Cl}^-$  transport by brush border membranes from rabbit jejunum. *J. Membr. Biol.* **74**: 85-94
85. Kinsella, J.L. and Aronson, P.S. (1980) Properties of the  $\text{Na}^+$ - $\text{H}^+$  exchanger in renal microvillus membrane vesicles. *Am. J. Physiol.* **238**: F461-F469
86. Knickelbein, R., Aronson, P.S., Atherton, W. and Dobbins, J.W. (1983) Sodium and chloride transport across rabbit ileal brush border. I. Evidence for Na-H exchange. *Am. J. Physiol.* **245**: G504-G510
87. Cala, P.M. (1980) Volume regulation by *Amphiuma* red blood cells. The membrane potential and its implications regarding the nature of ion flux pathways. *J. Gen. Physiol.* **76**: 683-708
88. Vigne, P., Frelin, C., Cragoe, E.J. and Lazdunski, M. (1982) The amiloride sensitive Na/H exchange system in skeletal muscle cells in culture. *J. Biol. Chem.* **257**: 9394-9400
89. Kinsella, J.L. and Aronson, P.S. (1982) Determination of the coupling ratio for Na-H exchange in renal microvillus membrane vesicles. *Biochim. Biophys. Acta* **689**: 161-164
90. Taglicht, D., Padan, E. and Schuldiner, S. (1993) Proton-sodium stoichiometry of NhaA, an electrogenic antiporter from *Escherichia coli*. *J. Biol. Chem.* **268**: 5382-5387
91. Aronson, P.S. (1983) Mechanisms of active  $\text{H}^+$  secretion in the proximal tubule. *Am. J. Physiol.* **245**: F647-F659
92. Paris, S. and Pouyssegur, J. (1983) Biochemical characterization of the amiloride-sensitive  $\text{Na}^+/\text{H}^+$  antiport in Chinese hamster lung fibroblasts. *J. Biol. Chem.* **258**: 3503-3508
93. Aronson, P.S., Nee, J. and Suhm, M.A. (1982) Modifier role of internal  $\text{H}^+$  in activating  $\text{Na}^+$ - $\text{H}^+$  exchanger in renal microvillus membrane vesicles. *Nature* **299**: 161-163

94. Boron, W.F. and Boulpaep, E.L. (1983) Intracellular pH regulation in the renal proximal tubule of the salamander. Na-H exchange. *J. Gen. Physiol.* **81**: 29-52
95. Moolenaar, W.H., Tsien, R.Y., Van der Saag, P.T. and De Laat, S.W. (1983) Na<sup>+</sup>/H<sup>+</sup> exchange and cytoplasmic pH in the action of growth factors in human fibroblasts. *Nature* **304**: 645-648
96. Benos, D.J. (1982) Amiloride: a molecular probe of sodium transport in tissues and cells. *Am. J. Physiol.* **242**: C131-C145
97. Vigne, P., Frelin, C., Cragoe, E.J. and Lazdunski, M. (1984) Structure-activity relationships of amiloride and certain of its analogues in relation to the blockade of the Na<sup>+</sup>/H<sup>+</sup> exchange system. *Mol. Pharmacol.* **25**: 131-136
98. Frelin, C., Vigne, P., Barbry, P. and Lazdunski, M. (1986) Interaction of guanidium and guanidium derivatives with the Na<sup>+</sup>/H<sup>+</sup> exchange system. *Eur. J. Biochem.* **154**: 241-245
99. Pouyssegur, J., Franchi, A., L'Allemain, G., Magnaldo, I., Paris, S. and Sardet, C. (1987) Genetic approach to structure, function, and regulation of the Na<sup>+</sup>/H<sup>+</sup> antiporter. *Kidney Internat.* **32**: S144-S149
100. Kinsella, J.L. and Aronson, P.S. (1981) Amiloride inhibition of the Na<sup>+</sup>-H<sup>+</sup> exchanger in renal microvillus membrane vesicles. *Am. J. Physiol.* **241**: F374-F379
101. Mahnensmith, R.L. and Aronson, P.S. (1985) Interrelationships among quinidine, amiloride, and lithium as inhibitors of renal Na<sup>+</sup>-H<sup>+</sup> exchanger. *J. Biol. Chem.* **260**: 12586-12592
102. L'Allemain, G., Franchi, A., Cragoe, E. and Pouyssegur, J. (1984) Blockade of the Na<sup>+</sup>/H<sup>+</sup> antiport abolishes growth factor-induced DNA synthesis in fibroblasts. Structure-activity relationships in the amiloride series. *J. Biol. Chem.* **259**: 4313-4319
103. Grinstein, S. and Smith, J.D. (1987) Asymmetry of the Na<sup>+</sup>/H<sup>+</sup> antiport of dog red cell ghosts. Sidedness of inhibition by amiloride. *J. Biol. Chem.* **262**: 9088-9092
104. Counillon, L., Scholtz, W., Lang, H.J. and Pouyssegur, J. (1993) Pharmacological characterization of stably transfected Na<sup>+</sup>/H<sup>+</sup> antiporter isoforms using amiloride analogs and a new inhibitor exhibiting anti-ischemic properties. *Mol. Pharmacol.* **44**: 1041-1045
105. Scholtz, W., Albus, U., Lang, H.J., Linz, W., Martorana, P.A., Englert, H.C. and Schölkens, B.A. (1993) HOE694, a new Na/H exchange inhibitor and its effects on cardiac ischaemia. *Br. J. Pharmacol.* **109**: 562-568

106. Ganapathy, V., Balkovetz, D.F., Miyamoto, Y., Ganapathy, M.E., Mahesh, V.B., Devoe, L.D. and Liebach, F.H. (1986) Inhibition of human placental  $\text{Na}^+\text{-H}^+$  exchanger by cimetidine. *J. Pharmacol. Exp. Ther.* **239**: 192-197
107. Aronson, P.S. and Bounds, S.E. (1980) Harmaline inhibition of Na-dependent transport in renal microvillus membrane vesicles. *Am. J. Physiol.* **238**: F210-F217
108. Orlowski, J. (1993) Heterologous expression and functional properties of amiloride high affinity (NHE-1) and low affinity (NHE-3) isoforms of the rat Na/H exchanger. *J. Biol. Chem.* **268**: 16369-16377
109. Paris, S. and Pouyssegur, J. (1984) Growth factors activate the  $\text{Na}^+\text{/H}^+$  antiporter in quiescent fibroblasts by increasing its affinity for intracellular  $\text{H}^+$ . *J. Biol. Chem.* **259**: 10989-10994
110. Moolenaar, W.H., Boonstra, J., van der Saag, P.T. and de Laat, S.W. (1981) Sodium/proton exchange in mouse neuroblastoma cells. *J. Biol. Chem.* **256**: 12883-12887
111. MacKnight, A.D.C. and Leaf, A. (1977) Regulation of cellular volume. *Physiol. Rev.* **57**: 510-573
112. Grinstein, S., Rothstein, A., Sarkadi, B. and Gelfand, E.W. (1984) Responses of lymphocytes to anisotonic media: volume regulating behaviour. *Am. J. Physiol.* **246**: C204-C215
113. Hoffmann, E.K. and Simonsen, L.O. (1989) Membrane mechanisms of volume and pH regulation in vertebrate cells. *Physiol. Rev.* **69**: 315-382
114. Grinstein, S., Rothstein, A. and Cohen, S.J. (1985) Mechanism of osmotic activation of  $\text{Na}^+\text{/H}^+$  exchange in rat thymic lymphocytes. *J. Gen. Physiol.* **85**: 765-787
115. Ullrich, K.J., Radtke, H.W. and Rumrich, G. (1971) The role of bicarbonate and other buffers on isotonic fluid absorption in the proximal tubule of the rat kidney. *Pflügers Arch.* **330**: 149-161
116. Grinstein, S., Cohen, S., Goetz, J.D., Rothstein, A. and Gelfand, E.W. (1985) Characterization of the activation of Na/H exchange in lymphocytes by phorbol esters. Change in the cytoplasmic pH-dependence of the antiport. *Proc. Natl. Acad. Sci. USA* **82**: 1429-1433
117. Grinstein, S., Mack, E. and Mills, G.B. (1986) Osmotic activation of the  $\text{Na}^+\text{/H}^+$  antiport in protein kinase C-depleted lymphocytes. *Biochem. Biophys. Res. Commun.* **134**: 8-13



118. Chambard, J.C., Paris, S., L'Allemain, G. and Pouyssegur, J. (1987) Two growth factor signalling pathways in fibroblasts distinguished by pertussis toxin. *Nature* **326**: 800-803
119. L'Allemain, G., Paris, S. and Pouyssegur, J. (1984) Growth factors action and intracellular pH regulation in fibroblasts. Evidence for a major role of the  $\text{Na}^+/\text{H}^+$  antiporter. *J. Biol. Chem.* **259**: 5809-5815
120. L'Allemain, G., Seuwen, K., Velu, T. and Pouyssegur, J. (1989) Signal transduction in hamster fibroblasts over expressing the human EGF receptor. *Growth Factors* **1**: 311-321
121. Sardet, C., Fafournoux, P. and Pouyssegur, J. (1991)  $\alpha$ -Thrombin, epidermal growth factor, and okadaic acid activate the  $\text{Na}^+/\text{H}^+$  exchanger, NHE-1 by phosphorylating a set of common sites. *J. Biol. Chem.* **266**: 19166-19171
122. Winkel, G.K., Sardet, C., Pouyssegur, J. and Ives, H.E. (1993) Role of cytoplasmic domain of the  $\text{Na}^+/\text{H}^+$  exchanger in hormonal activation. *J. Biol. Chem.* **268**: 3396-3400
123. Wakabayashi, S., Bertrand, B., Shigekawa, M., Fafournoux, P. and Pouyssegur, J. (1994) Growth factor activation and "H<sup>+</sup>-sensing" of the  $\text{Na}^+/\text{H}^+$  exchanger isoform 1 (NHE1). Evidence for an additional mechanism not requiring direct phosphorylation. *J. Biol. Chem.* **269**: 5583-5587
124. Wakabayashi, S., Fafournoux, P., Sardet, C. and Pouyssegur, J. (1992) The  $\text{Na}^+/\text{H}^+$  antiporter cytoplasmic domain mediates growth factor signals and controls "H<sup>+</sup>-sensing". *Proc. Natl. Acad. Sci. USA* **89**: 2424-2428
125. Silva, N.L.C.L., Haworth, R., Singh, D. and Fliegel, L. (1995) The carboxy-terminal region of the  $\text{Na}^+/\text{H}^+$  exchanger interacts with mammalian heat shock protein. *Biochemistry* **34**: 10412-10420
126. Bertrand, B., Wakabayashi, S., Ikeda, T., Pouyssegur, J. and Shigekawa, M. (1994) The  $\text{Na}^+/\text{H}^+$  exchanger isoform 1 (NHE1) is a novel member of the calmodulin-binding proteins. Identification and characterization of calmodulin-binding sites. *J. Biol. Chem.* **269**: 13703-13709
127. Wakabayashi, S., Bertrand, B., Ikeda, T., Pouyssegur, J. and Shigekawa, M. (1994) Mutation of calmodulin-binding site renders the  $\text{Na}^+/\text{H}^+$  exchanger (NHE1) highly H<sup>+</sup>-sensitive and  $\text{Ca}^{2+}$  regulation defective. *J. Biol. Chem.* **269**: 13710-13715
128. Goss, G.G., Orlowski, J. and Grinstein, S. (1996) Coimmunoprecipitation of a 24 kDa protein with NHE-1, the ubiquitous isoform of the  $\text{Na}^+/\text{H}^+$  exchanger. *Am. J. Physiol.* **270**: C1493-C1502

129. Kong, S.K., Choy, Y.M., Fung, K.P. and Lee, C.Y. (1989) cAMP activates Na<sup>+</sup>/H<sup>+</sup> antiporter in murine macrophages. *Biochem. Biophys. Res. Commun.* **165**: 131-137
130. Moule, S.K. and McGivan, J.D. (1990) Epidermal growth factor and cyclic AMP stimulate Na<sup>+</sup>/H<sup>+</sup> exchange in isolated rat hepatocytes. *Eur. J. Biochem.* **187**: 677-682
131. Gupta, A., Schwiening, C.J. and Boron, W.F. (1994) Effects of CGRP, forskolin, PMA, and ionomycin on pH<sub>i</sub> dependence of Na-H exchange in UMR-106 cells. *Am. J. Physiol.* **266**: C1083-C1092
132. Azarani, A., Goltzman, D. and Orlowski, J. (1995) Parathyroid hormone and parathyroid hormone-related peptide activate the Na<sup>+</sup>/H<sup>+</sup> exchanger NHE-1 isoform in osteoblastic cells (UMR-106) via a cAMP-dependent pathway. *J. Biol. Chem.* **270**: 23166-23172
133. Helmle-Kolb, C., Counillon, L., Roux, D., Pouyssegur, J., Mrkic, B. and Murer, H. (1993) Na/H exchange activities in NHE1-transfected OK-cells: cell polarity and regulation. *Pflügers Arch.* **425**: 34-40
134. Levine, S.A., Montrose, M.H., Tse, C.-M. and Donowitz, M. (1993) Kinetics and regulation of three cloned mammalian Na<sup>+</sup>/H<sup>+</sup> exchangers stably expressed in a fibroblast cell line. *J. Biol. Chem.* **268**: 25527-25535
135. Borgese, F., Malapert, M., Fievet, B., Pouyssegur, J. and Motaïs, R. (1994) The cytoplasmic domain of the Na<sup>+</sup>/H<sup>+</sup> exchangers (NHEs) dictates the nature of the hormonal response: Behavior of a chimeric human NHE1/trout βNHE antiporter. *Proc. Natl. Acad. Sci. USA* **91**: 5431-5435
136. Khan, A., Dolson, G.M., Hise, M.K., Bennett, S.C. and Weinman, E.J. (1985) Parathyroid hormone and dibutyryl cAMP inhibits Na/H exchange in renal brush border membrane vesicles. *Am. J. Physiol.* **252**: F217-F218
137. Weinman, E.J., Shenolikar, S. and Khan, A.M. (1987) cAMP-associated inhibition of Na<sup>+</sup>/H<sup>+</sup> exchanger in rabbit kidney brush-border membranes. *Am. J. Physiol.* **252**: F19-F25
138. Cano, A., Preisig, P. and Alpern, R.J. (1993) Cyclic adenosine monophosphate acutely inhibits and chronically stimulates Na/H antiporter in OKP cells. *J. Clin. Invest.* **92**: 1632-1638
139. Helmle-Kolb, C., Montrose, M.H. and Murer, H. (1990) Parathyroid hormone regulation of Na<sup>+</sup>/H<sup>+</sup> exchange in opossum kidney cells: polarity and mechanisms. *Pflügers Arch.* **416**: 615-623

140. Moe, O.W., Amemiya, M. and Yamaji, Y. (1995) Activation of protein kinase A acutely inhibits and phosphorylates Na/H Exchanger NHE-3. *J. Clin. Invest.* **96**: 2187-2194
141. Kandasamy, R.A., Yu, F.H., Harris, R., Boucher, A., Hanrahan, J.W. and Orłowski, J. (1995) Plasma membrane Na<sup>+</sup>/H<sup>+</sup> exchanger isoforms (NHE-1,-2, and -3) are differentially responsive to second messenger agonists of the protein kinase A and C pathways. *J. Biol. Chem.* **270**: 29209-29216
142. Levine, S.A., Nath, S.K., Yun, C.H.C., Yip, J.W., Montrose, M., Donowitz, M. and Tse, C.-M. (1995) Separate C-terminal domains of the epithelial specific brush border Na/H exchanger isoform NHE3 are involved in stimulation and inhibition by protein kinase/growth factors. *J. Biol. Chem.* **270**: 13716-13725
143. Weinman, E.J., Steplock, D. and Shenolikar, S. (1993) cAMP-mediated inhibition of the renal brush border membrane Na<sup>+</sup>/H<sup>+</sup> exchanger requires a dissociable phosphoprotein cofactor. *J. Clin. Invest.* **92**: 1781-1786
144. Weinman, E.J., Steplock, D., Bui, G., Yuan, N. and Shenolikar, S. (1990) Regulation of renal Na<sup>+</sup>-H<sup>+</sup> exchanger by cAMP-dependent protein kinase. *Am. J. Physiol.* **258**: F1254-F1258
145. Weinman, E.J., Steplock, D., Wang, Y. and Shenolikar, S. (1995) Characterization of a protein cofactor that mediates protein kinase A regulation of the renal brush border membrane Na<sup>+</sup>-H<sup>+</sup> exchanger. *J. Clin. Invest.* **95**: 2143-2149
146. Cassel, D., Katz, M. and Rotman, M. (1986) Depletion of cellular ATP inhibits Na<sup>+</sup>/H<sup>+</sup> antiport in cultured human cells. Modulation of the regulatory effect of intracellular protons on the antiporter activity. *J. Biol. Chem.* **261**: 5460-5466
147. Burns, K.D., Homma, T. and Harris, R.C. (1991) Regulation of Na<sup>+</sup>-H<sup>+</sup> exchange by ATP depletion and calmodulin antagonism in renal epithelial cells. *Am. J. Physiol.* **261**: F607-F616
148. Little, P.J., Weissberg, P.L., Cragoe Jr., E.J. and Bobik, A. (1988) Dependence of Na<sup>+</sup>/H<sup>+</sup> antiporter in cultured rat aortic smooth muscle on calmodulin, calcium, and ATP. Evidence for the involvement of calmodulin-dependent kinases. *J. Biol. Chem.* **263**: 16780-16786
149. Grinstein, S. and Foskett, J.K. (1990) Ionic mechanisms of cell volume regulation in leukocytes. *Annu. Rev. Physiol.* **52**: 399-414
150. Soleimani, M., Bookstein, C., McAteer, J.A., Hattabaugh, Y.J., Bizal, G.L., Musch, M.W., Villereal, M., Rao, M.C., Howard, R.L. and Chang, E.B. (1994) Effects of high osmolarity on Na<sup>+</sup>-H<sup>+</sup> exchange in renal proximal tubule cells. *J. Biol. Chem.* **269**: 15613-15618

151. Watts, B.A. and Good, D.W. (1994) Apical membrane Na/H exchange in rat medullary thick ascending limb. pH<sub>i</sub> dependence and inhibition of hyperosmolality. *J. Biol. Chem.* **269**: 20250-20255
152. Grinstein, S., Woodside, M., Sardet, C., Pouyssegur, J. and Rotin, D. (1992) Activation of the Na<sup>+</sup>/H<sup>+</sup> antiporter during cell volume regulation. Evidence for a phosphorylation-independent mechanism. *J. Biol. Chem.* **267**: 23823-23828
153. Davis, B.A., Hogan, E.M. and Boron, W.F. (1992) Role of G proteins in stimulation of Na-H exchange. *Am. J. Physiol.* **262**: C533-C536
154. Voyno-Yasenetskaya, T., Conklin, B.R., Gilbert, R.L., Hooley, R., Bourne, H.R. and Barber, D.L. (1994) Gα13 stimulates Na-H exchange. *J. Biol. Chem.* **269**: 4721-4724
155. Schrode, L.D., Klein, J.D., O'Neill, W.C. and Putnam, R.W. (1995) Shrinkage-induced activation of Na/H exchange in primary rat astrocytes: role in myosin light-chain kinase. *Am. J. Physiol.* **269**: C257-C266
156. Good, D.W. (1995) Hyperosmolality inhibits bicarbonate absorption in rat medullary thick ascending limb via a protein-tyrosine kinase-dependent pathway. *J. Biol. Chem.* **270**: 9883-9889
157. Han, J., Lee, J.-D., Bibbs, L. and Ulevitch, J. (1994) A MAP kinase targeted by endotoxin and hyperosmolality in mammalian cells. *Science* **265**: 808-811
158. Galcheva-Gargova, Z., Dérjard, B., Wu, I.-H. and Davis, R.J. (1994) An osmosensing signal transduction pathway in mammalian cells. *Science* **265**: 806-808
159. Kinsella, J.L., Cujdik, T. and Sacktor, B. (1986) Kinetic studies on the stimulation of Na<sup>+</sup>-H<sup>+</sup> exchange activity in renal brush border membranes isolated from thyroid hormone-treated rats. *J. Membr. Biol.* **91**: 183-191
160. Kinsella, J.L., Cujdik, T. and Sacktor, B. (1984) Na<sup>+</sup>-H<sup>+</sup> exchange in isolated renal brush-border membrane vesicles in response to metabolic acidosis. Kinetic effects. *J. Biol. Chem.* **259**: 13224-13227
161. Yonemura, K., Cheng, L., Sacktor, B. and Kinsella, J.L. (1990) Stimulation by thyroid hormone of Na<sup>+</sup>-H<sup>+</sup> exchange activity in cultured opossum kidney cells. *Am. J. Physiol.* **258**: F333-F338
162. Freiberg, J.M., Kinsella, J. and Sacktor, B. (1982) Glucocorticoids increase the Na-H exchange and decrease the Na gradient dependent phosphate uptake systems in renal brush border membrane vesicles. *Proc. Natl. Acad. Sci. USA* **79**: 4932-4936

163. Yun, C.H.C., Gurubhagavatula, S., Levine, S.A., Montgomery, J.L.M., Cohen, M.E., Cragoe Jr., E.J., Pouyssegur, J., Tse, C.M. and Donowitz, M. (1993) Glucocorticoid stimulation of ileal Na<sup>+</sup> absorptive cell brush border Na<sup>+</sup>/H<sup>+</sup> exchange and association with an increase in message for NHE-3, an epithelial Na<sup>+</sup>/H<sup>+</sup> exchanger isoform. *J. Biol. Chem.* **268**: 206-211
164. Kandasamy, R.A. and Orłowski, J. (1996) Genomic organization and glucocorticoid transcriptional activation of the rat Na<sup>+</sup>/H<sup>+</sup> exchanger *Nhe3* gene. *J. Biol. Chem.* **271**: 10551-10559
165. Rao, G.N., Sardet, C., Pouyssegur, J. and Berk, B.C. (1992) Na<sup>+</sup>/H<sup>+</sup> antiporter gene expression increases during retinoic acid-induced granulocytic differentiation of HL60 cells. *J. Cell. Physiol.* **151**: 361-366
166. Igarashi, P., Freed, M.I., Ganz, M.B. and Reilly, R.F. (1992) Effects of chronic metabolic acidosis on Na<sup>+</sup>/H<sup>+</sup> exchangers in LLC-PK<sub>1</sub> renal epithelial cells. *Am. J. Physiol.* **263**: F83-F88
167. Moe, O.W., Miller, R.T., Horie, S., Cano, A., Presif, P.A. and Alpern, R.J. (1991) Differential regulation of Na/H antiporter by acid in renal epithelial cells and fibroblasts. *J. Clin. Invest.* **88**: 1703-1708
168. Krapf, R., Pearce, D., Lynch, C., Xi, X.-P., Reudelhuber, T., Pouyssegur, J. and Rector Jr., F.C. (1991) Expression of rat renal Na/H antiporter mRNA levels in response to respiratory and metabolic acidosis. *J. Clin. Invest.* **87**: 747-751
169. Horie, S., Moe, O., Yamaji, Y., Cano, A. and Miller, T. (1992) Role of protein kinase C and transcription factor AP-1 in the acid-induced increase in Na/H antiporter activity. *Proc. Natl. Acad. Sci. USA* **89**: 5236-5240
170. Horie, S., Moe, O., Miller, T. and Alpern, R.J. (1992) Long-term activation of protein kinase C causes chronic Na/H antiporter stimulation in cultured proximal tubule cells. *J. Clin. Invest.* **89**: 365-372
171. Yamaji, Y., Amemiya, M., Cano, A., Preisig, P.A., Miller, R.T., Moe, O.W. and Alpern, R.J. (1995) Overexpression of csk inhibits acid-induced activation of NHE-3. *Proc. Natl. Acad. Sci. USA* **92**: 6274-6278
172. Soleimani, M., Bizal, G.L., McKinney, D. and Hattabaugh, Y.J. (1992) Effect of in vitro metabolic acidosis on luminal Na<sup>+</sup>/H<sup>+</sup> exchange and basolateral Na<sup>+</sup>:HCO<sub>3</sub><sup>-</sup> cotransport in rabbit kidney proximal tubules. *J. Clin. Invest.* **90**: 211-218
173. Agarwal, N., Haggerty, J.G., Adelberg, E.A. and Slayman, C.W. (1986) Isolation and characterization of a Na-H antiporter-deficient mutant of LLC-PK<sub>1</sub> cells. *Am. J. Physiol.* **251**: C825-C830

174. Raley-Susman, K.M., Cragoe, E.J., Sapolsky, R.M. and Kopito, R.R. (1991) Regulation of intracellular pH in cultured hippocampal neurons by an amiloride-insensitive  $\text{Na}^+/\text{H}^+$  exchanger. *J. Biol. Chem.* **266**: 2739-2745
175. Thomas, J.A., Buchsbaum, R.N., Zimniak, A. and Racker, E. (1979) Intracellular pH measurements in Ehrlich ascites tumor cells utilizing spectroscopic probes generated *in situ*. *Biochemistry* **18**: 2210-2218
176. Franchi, A., Cragoe, E. and Pouyssegur, J. (1986) Isolation and properties of fibroblast mutants overexpressing an altered  $\text{Na}^+/\text{H}^+$  antiporter. *J. Biol. Chem.* **261**: 14614-14620
177. Vigne, P., Breittmayer, J.-P., Frelin, C. and Lazdunski, M. (1988) Dual control of the intracellular pH in aortic smooth muscle cells by a cAMP-sensitive  $\text{HCO}_3^-/\text{Cl}^-$  antiporter and a protein kinase C-sensitive  $\text{Na}^+/\text{H}^+$  antiporter. *J. Biol. Chem.* **263**: 18023-18029
178. Cuthbert, A.W. and Fanelli, G.M. (1978) Effects of some pyrazinecarboxamides on sodium transport in frog skin. *Br. J. Pharmacol* **63**: 139-149
179. Kleyman, T.R. and Cragoe, E. (1988) Amiloride and its analogs as tools in the study of ion transport. *J. Membr. Biol.* **105**: 1-21
180. Gerchman, Y., Olami, Y., Rimon, A., Taglicht, D., Schuldiner, S. and Pada, E. (1993) Histidine-226 is part of the pH sensor of NhaA, a  $\text{Na}^+/\text{H}^+$  antiporter in *Escherichia coli*. *Proc. Natl. Acad. Sci. USA* **90**: 1212-1216
181. Fabiato, A. and Fabiato, F. (1978) Effects of pH on the myofilaments and the sarcoplasmic reticulum of skinned cells from cardiac and skeletal muscles. *J. Physiol.* **276**: 233-255
182. Donaldson, S.K., Hermansen, L. and Bolles, L. (1978) Differential, direct effects of  $\text{H}^+$  on  $\text{Ca}^{2+}$ -activated force of skinned fibers from the soleus, cardiac and adductor magnus muscles of rabbits. *Pflügers Arch.* **376**: 55-65
183. Mrwa, U., Achtig, I. and Ruegg, J.C. (1974) Influences of calcium concentration and pH on the tension development and ATPase activity of the arterial actomyosin contractile system. *Blood Vessels* **11**: 277-286
184. Cooke, R., Franks, K., Luciani, G.B. and Pate, E. (1988) The inhibition of rabbit skeletal muscle contraction by hydrogen ions and phosphate. *J. Physiol* **395**: 77-97
185. Takaichi, K., Balkovetz, D.F., Meir, E.V. and Warnock, D.G. (1993) Cytosolic pH sensitivity of an expressed human NHE-1  $\text{Na}^+/\text{H}^+$  exchanger. *Am. J. Physiol.* **264**: C944-C950

186. Boron, W.F. (1983) Transport of  $H^+$  and ionic weak acids and bases. *J. Membr. Biol.* **72**: 1-16
187. Schwartz, M.A., Lechene, C. and Ingber, D.E. (1991) Insoluble fibronectin activates the Na/H antiporter by clustering and immobilizing integrin  $\alpha 5 \beta 1$ , independent of cell shape. *Proc. Natl. Acad. Sci. USA* **88**: 7849-7853
188. Grinstein, S., Woodside, M., Waddell, T.K., Downey, G.P., Orlowski, J., Pouyssegur, J., Wong, D.C.P. and Foscett, J.K. (1993) Focal localization of the NHE-1 isoform of the  $Na^+/H^+$  antiport: assessment of effects on intracellular pH. *EMBO J.* **12**: 5209-5218
189. Counillon, L., Franchi, A. and Pouyssegur, J. (1993) A point mutation of the  $Na^+/H^+$  exchanger gene (*NHE1*) and amplification of the mutated allele confer amiloride resistance upon chronic acidosis. *Proc. Natl. Acad. Sci. USA* **90**: 4508-4512
190. Rotin, D. and Grinstein, S. (1989) Impaired cell volume regulation in  $Na^+-H^+$  exchange deficient mutants. *Am. J. Physiol.* **257**: C1158-C1165
191. Bianchini, L., Woodside, M., Sardet, C., Pouyssegur, J., Takai, A. and Grinstein, S. (1991) Okadaic acid, a phosphatase inhibitor induces activation and phosphorylation of the  $Na^+/H^+$  antiport. *J. Biol. Chem.* **266**: 15406-15413
192. Deng, W.P. and Nickoloff, J.A. (1992) Site-directed mutagenesis of virtually any plasmid by eliminating a unique site. *Anal. Chem.* **200**: 81-88
193. Chen, C. and Okayama, H. (1987) High-efficiency transformation of mammalian cells by plasmid DNA. *Mol. Cell. Biol.* **7**: 2745-2752
194. Goss, G.G., Woodside, M., Wakabayashi, S., Pouyssegur, J., Waddell, T., Downey, G.P. and Grinstein, S. (1994) ATP dependence of NHE-1, the ubiquitous isoform of the  $Na^+/H^+$  antiporter. Analysis of phosphorylation and subcellular localization. *J. Biol. Chem.* **269**: 8741-8748
195. Yun, C.H.C., Little, P.L., Nath, S.K., Levine, S.A., Pouyssegur, J., Tse, C.M. and Donowitz, M. (1993) Leu<sup>143</sup> in the putative fourth membrane spanning domain is critical for amiloride inhibition of an epithelial  $Na^+/H^+$  exchanger isoform (NHE-2). *Biochem. Biophys. Res. Commun.* **193**: 532-539
196. Weinman, E.J. and Shenolikar, S. (1993) Regulation of the renal brush border membrane  $Na^+-H^+$  exchanger. *Annu. Rev. Physiol.* **55**: 289-304
197. Kennelly, P.J. and Krebs, E.G. (1991) Consensus sequences as substrate determinants for protein kinases and phosphatases. *J. Biol. Chem.* **266**: 15555-15558

198. Bianchini, L., Kapus, A., Lukacs, G., Wasan, S., Wakabayashi, S., Pouyssegur, J., Yu, F.H., Orlowski, J. and Grinstein, S. (1995) Responsiveness of mutants of the NHE-1 isoform of  $\text{Na}^+/\text{H}^+$  antiport to osmotic stress. *Am. J. Physiol.* **269**: C998-C1007
199. Cabado, A.G., Yu, F.H., Kapus, A., Lukacs, G., Grinstein, S. and Orlowski, J. (1996) Distinct structural domains confer cAMP sensitivity and ATP dependence to the  $\text{Na}^+/\text{H}^+$  exchanger NHE3 isoform. *J. Biol. Chem.* **271**: 3590-3599
200. Yu, F.H., Shull, G.E. and Orlowski, J. (1993) Functional properties of the rat Na/H exchanger NHE-2 isoform expressed in Na/H exchanger-deficient Chinese hamster ovary cells. *J. Biol. Chem.* **268**: 25536-25541
201. Heizmann, C.W. and Hunziker, W. (1991) Intracellular calcium-binding proteins: more sites than insights. *Trends Biochem. Sci.* **16**: 98-103
202. Lin, X. and Barber, D.L. (1996) A calcineurin homologous protein inhibits GTPase-stimulated Na-H exchange. *Proc. Natl. Acad. Sci. USA* **93**: 12631-12636
203. Klingenberg, M. (1981) Membrane protein oligomeric structure and transport function. *Nature* **290**: 449-454